HYBRIDIZATION AND MULTI-OBJECTIVE OPTIMIZATION OF PLUG-IN HYBRID ELECTRIC VEHICLES

by

Shashi Kamal Shahi

A THESIS SUBMITTED IN PARTIAL FULLFILMENT OF
THE REQUIREMENTS FOR THE DEGREE OF

MASTER OF APPLIED SCIENCE

in the school
of
Engineering Science

© Shashi Kamal Shahi 2010
SIMON FRASER UNIVERSITY
Summer 2010

All rights reserved. However, in accordance with the *Copyright Act of Canada*, this work may be reproduced, without authorization, under the conditions for *Fair Dealing*. Therefore, limited reproduction of this work for the purposes of private study, research, criticism, review and news reporting is likely to be in accordance with the law, particularly if cited appropriately.

APPROVAL

Name: Shashi Kamal Shahi

Degree: Master of Applied Science

Title of Thesis: Hybridization and Multi-Objective Optimization of Plug-in Hybrid Electric Vehicles

Examining Committee:

Chair:

Dr. Mehrdad Moallem
Associate Professor, School of Engineering Science

Dr. Gary Wang
Senior Supervisor
Associate Professor, School of Engineering Science

Dr. Edward Park
Supervisor
Associate Professor, School of Engineering Science

Dr. Siamak Arzanpour
Internal Examiner
Assistant Professor, School of Engineering Science

Date Defended/Approved: Aug 12, 10

SFU SIMON FRASER UNIVERSITY
LIBRARY

Declaration of Partial Copyright Licence

The author, whose copyright is declared on the title page of this work, has granted to Simon Fraser University the right to lend this thesis, project or extended essay to users of the Simon Fraser University Library, and to make partial or single copies only for such users or in response to a request from the library of any other university, or other educational institution, on its own behalf or for one of its users.

The author has further granted permission to Simon Fraser University to keep or make a digital copy for use in its circulating collection (currently available to the public at the "Institutional Repository" link of the SFU Library website <www.lib.sfu.ca> at: <http://ir.lib.sfu.ca/handle/1892/112>) and, without changing the content, to translate the thesis/project or extended essays, if technically possible, to any medium or format for the purpose of preservation of the digital work.

The author has further agreed that permission for multiple copying of this work for scholarly purposes may be granted by either the author or the Dean of Graduate Studies.

It is understood that copying or publication of this work for financial gain shall not be allowed without the author's written permission.

Permission for public performance, or limited permission for private scholarly use, of any multimedia materials forming part of this work, may have been granted by the author. This information may be found on the separately catalogued multimedia material and in the signed Partial Copyright Licence.

While licensing SFU to permit the above uses, the author retains copyright in the thesis, project or extended essays, including the right to change the work for subsequent purposes, including editing and publishing the work in whole or in part, and licensing other parties, as the author may desire.

The original Partial Copyright Licence attesting to these terms, and signed by this author, may be found in the original bound copy of this work, retained in the Simon Fraser University Archive.

Simon Fraser University Library
Burnaby, BC, Canada

Last revision: Spring 09

Abstract

Plug-in hybrid electric vehicles (PHEV), which share the characteristics of both a conventional HEV and an all-electric vehicle, rely on large storage batteries. Therefore, the characteristics and hybridization of the PHEV battery with the engine and electric motor play an important role in the design and potential adoption of PHEVs. In this research work, a multi-objective optimization approach is applied to compare the operational performance of Toyota Prius PHEV20 (PHEV for 20 miles of all electric range) based on fuel economy, operating cost, and green house gas emissions for 4480 combinations (20 batteries, 14 motors, and 16 engines). Powertrain System Analysis Toolkit software package automated with the Pareto Set Pursuing multi-objective optimization method is used for this purpose on two different drive cycles. It was found that 1) battery, motor, and engine work collectively in defining an optimal hybridization scheme; and 2) the optimal hybridization scheme varies with drive cycles.

Keywords: Hybridization; Toyota Prius; Plug-in hybrid electric vehicle; Performance parameters; Powertrain system analysis toolkit; Pareto set pursuing multi-objective optimization.

Acknowledgements

I am greatly indebted to my senior supervisor Dr. G. Gary Wang, for his incessant encouragement, invaluable guidance and persistent support throughout the course of this research. I thank him for involving me in this project and having confidence in my abilities to handle such an intricate research topic. Without his critical reviews and intellectual inputs, this thesis would not have been possible in the present form. I am also sincerely thankful to Dr. Mehrdad Moallem, Dr. Edward Jung Wood Park, and Dr. Siamak Arzanpour for being my committee members.

I am grateful to Prof. Liqiang An for his valuable suggestions and help during the course of this research. I would also like to thank all my friends in the Product Design and Optimization Lab, who shared their experiences from time to time. Financial support from AUTO21, a Network of Centers of Excellence of Canada, for this Project is gratefully acknowledged. Finally, I thank my father Late Prof. Dev Raj Shahi, my mother Late Mrs. Krishna Shahi and family members, who have always supported me in my life.

Contents

List of Figures

List of Tables

Chapter 1

Introduction

1.1 Background

The first demonstration electric vehicles were made in the 1830s and commercial electric vehicles were available by the end of the 19th century [1]. The first electric vehicles of the 1830s used non-rechargeable batteries. By the end of the 19th century, with mass production of rechargeable batteries, electric vehicles became fairly widely used [2]. The first electric vehicle to exceed the *mile a minute* speed (60 mph) was *La Jamais Contente* ("The Never Satisfied"), when the Belgium racing car driver, Camille Jenatzy, drove this vehicle at a new land speed record of 106 kph (65.7 mph) in 1899. The simultaneous development of gasoline-powered internal combustion engine (ICE) vehicles in the 1850s overshadowed the development of electric vehicles technology, due to substantial progress in commercial drilling and production of petroleum in the late 19th century, which ushered in the age of modern automobiles [2]. Subsequently, the electric vehicles did not enjoy the enormous success of ICE vehicles that normally have much longer ranges and are very easy to refuel.

The high specific energy (energy produced per kg of fuel used) of petroleum fuel as compared to that of batteries has been a major contributory factor to the success of ICE vehicles. The specific energy of fuels used for ICEs is around 9000 Whkg^{-1}, whereas that of a battery used in electric vehicles is only about 30 Whkg^{-1} [2]. 4.5 litres (1 gallon) of petrol that has a mass of around 4kg will drive a typical ICE vehicle for 50 km, whereas to store the same amount of useful electric energy, an electric vehicle would require a lead acid battery with a mass of about 270 kg [2]. Moreover, as the vehicle moves, the ICE vehicle has to carry less weight as the fuel is being consumed, while the electric vehicle has to carry the same weight of the battery over the entire travelling distance. A considerable amount of extra energy is required, therefore, to accelerate and decelerate the electric vehicle and to carry 270 kg of battery weight. The weight of the

battery becomes a major limiting factor of electric vehicles for long distance travels. For lead acid batteries to have the effective energy capacity of 45 litres (10 gallons) of petrol, a straggling battery weight of 2.7 tonnes would be required. Another major problem of the batteries used in electric vehicles is the time it takes to recharge them [2]. Even when adequate electrical power is available it takes several hours to re-charge a lead acid battery, whereas 45 litres of petrol can be put into a vehicle in approximately one minute. The recharge time of some of the newly developed batteries has been reduced to one-hour, but this is still considerably longer than the time it takes to fill a tank of petrol. Yet another limiting parameter with the electric vehicles is that batteries are very expensive [3]. Therefore, the battery operated electric vehicles not only have a limited range, but also are more expensive than an ICE vehicle of similar size and quality. For example, the 2.7 tonnes of lead acid batteries, which give the same effective energy storage as 45 litres of petrol would cost around CAD$14,500 at today's prices. The batteries also have limited life, typically 5 years, which means that a further large investment is needed periodically to renew the batteries [2].

However, electric vehicles have certain advantages over ICE vehicles. They produce no exhaust emissions in their immediate environment and are inherently quiet. This makes the electric vehicles ideal for environment such as warehouses, inside buildings and on golf courses, where pollution and noise is not tolerated. A popular application of battery operated electric vehicles is the mobility device for the elderly and physically handicapped people. It can be easily driven on pavements, into shops, and in many buildings. Normally a range of 4 miles is quiet sufficient but longer ranges may also allow disabled people to drive along country lanes. Today's concerns about the environment, rising price for deleting petroleum, particularly noise pollution and exhaust emissions, coupled to new developments in batteries and fuel cells has swung the balance back in favour of electric vehicles. There is a range of electric vehicles currently available in the market. In the simplest version, there are small electric bicycles, tricycles and small commuter vehicles. In the leisure market, there are electric golf buggies. A few full sized electric vehicles, which include electric cars, delivery trucks and buses, are also available. All of these vehicles have a fairly limited range and performance, but they are sufficient for the intended purpose. Wider consumer acceptance and adoption of electric vehicles, however, depends on, among other characteristics, fuel economy, operating cost, operation green house

gas (GHG) emissions, power and performance, and safety. It is, therefore, important that the principles behind the design of electric vehicles, the relevant technological and environmental issues are thoroughly understood.

On the technological side, the energy efficiency of the batteries has been considerably improved over the conventional lead-acid batteries by developing a number of new battery technologies. Nickel cadmium or nickel metal hydride batteries are now commercially available, which can carry about double the energy, and the high temperature sodium nickel chloride or Zebra battery nearly three times the energy of lead acid batteries. These are useful improvements, but still do not allow the design of electric vehicles with a long range. Some more expensive options, such as lithium polymer battery, which has a specific energy about three times that of lead acid batteries, and Zinc air batteries, which have potentially seven times the specific energy of lead acid batteries, also show considerable promise. Although, lithium batteries are expensive, these have considerably lower weight as compared to the conventional lead acid batteries. For example, to replace the 45 liters (11.56 gallons) of petrol, which would give a vehicle a range of 450 km (281.25 miles), a mass of 800 kg of lithium battery would be required as against 2.7 tonnes mass of lead acid batteries [2]. Simultaneously with the development of battery technologies, another breakthrough in the development of electric vehicles was achieved by developing a hybrid electric vehicle (HEV), which could revolutionize the impact of electric vehicles [2].

1.1.1 Hybrid Electric Vehicle Technology

An HEV is powered by a combination of electric battery and conventional ICE. The HEV uses a small petrol engine that charges a high performance battery, which in turn powers an electric motor. Engine and motor complement each other by using the electric motor to propel the vehicle at low speeds, and automatically shifting to the petrol engine at above average cruise speed. The HEV technology is a promising idea since it uses regenerative braking for braking heavy vehicles and recovers approximately 20% of the energy, which is usually lost in the brakes, by recharging the batteries. Regenerative braking is a system where the motor acts as a generator during braking the wheel and the kinetic energy of the vehicle is converted to electrical

energy, which is returned to battery storage, from where it can be reused [2]. As a result, about one-third of the energy is likely to be recovered if the efficiency of generation, control, battery storage and passing the electricity back through the motor and controller is accounted for. The HEVs use a combination of an ICE with a battery, an electric motor, and generator in the series hybrid and the parallel hybrid combinations [2] as illustrated in Figure 1-1 and Figure 1-2.

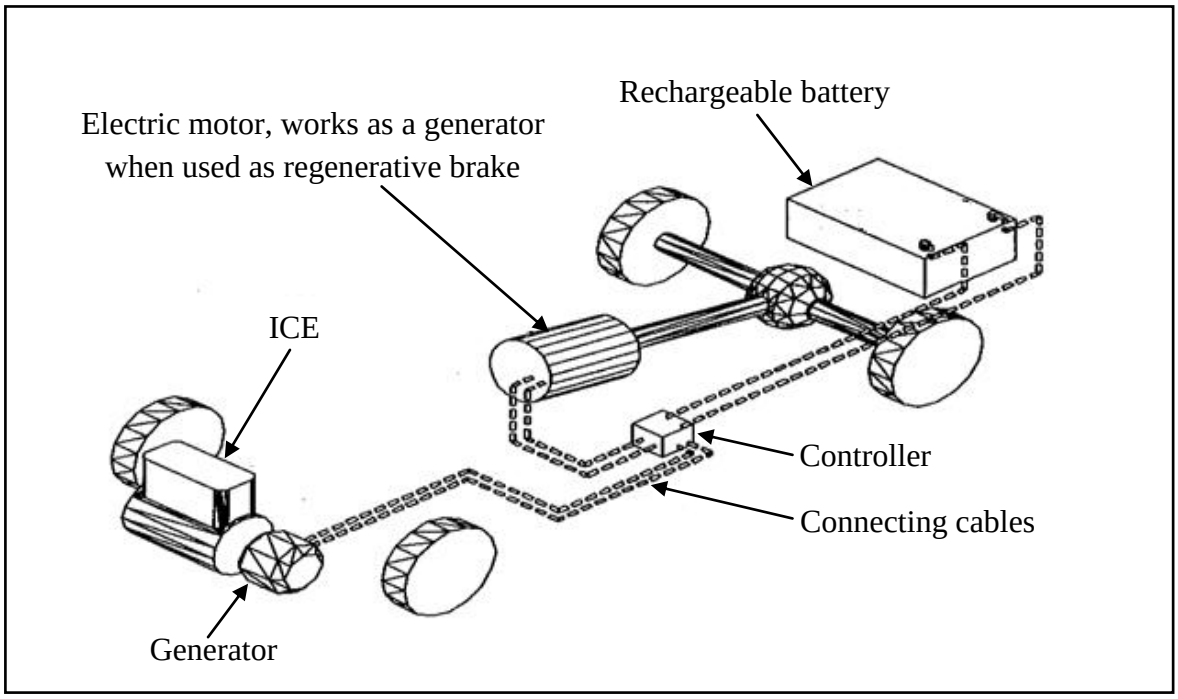

Figure 1-1. Series hybrid vehicle layout [2]

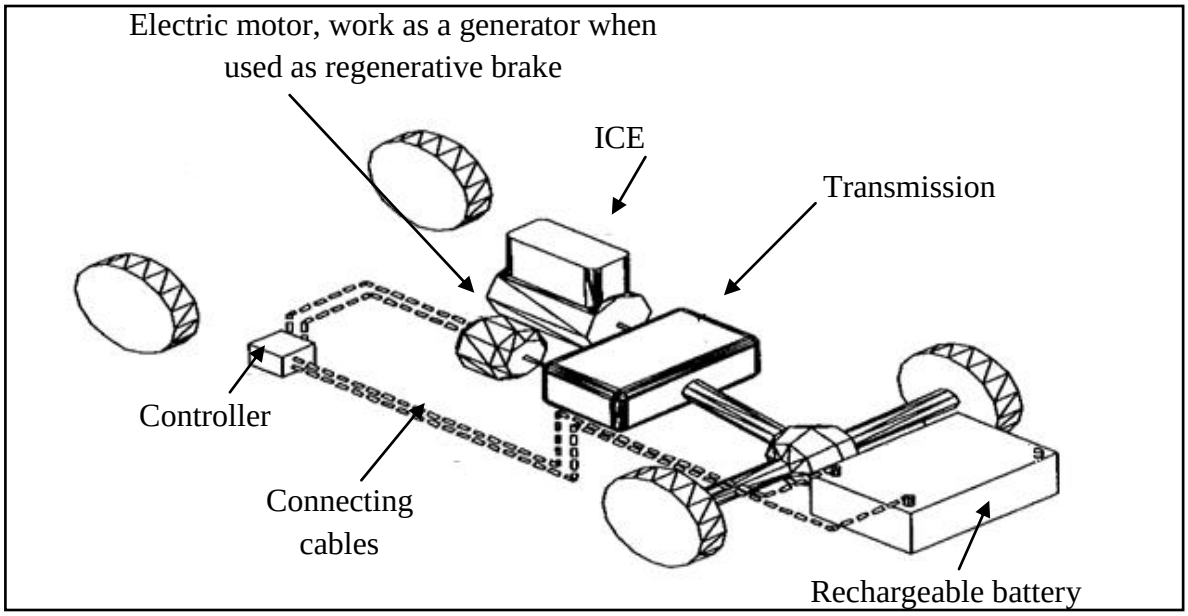

Figure 1-2. Parallel hybrid vehicle layout [2]

The series hybrid vehicle is driven by one or more electric motors, which are supplied energy either from battery or from ICE driven generator or from both. However, in either case the driving force comes entirely from the electric motor [4]. Whereas, the parallel hybrid vehicle is either driven by the ICE working directly through a transmission system to the wheels or by one or more electric motors, or by both the electric motor and the ICE at once [4]. In both series and parallel HEVs, the battery can be recharged by the ICE and generator while moving; therefore, the battery does not need to be as large as in a pure battery operated electric vehicle. Also, both types allow for regenerative braking that helps the drive motor to work as a generator and simultaneously slow down the vehicle and charge the battery [5]. The series hybrid combination is mostly used only in special applications. For example, the diesel powered railway engine is nearly always a series hybrid. Some special all-terrain vehicles are series hybrid, with a separately controlled electric motor for each wheel. The main disadvantage of the series hybrid is that all the electrical energy must pass through both the generators and the motors [2]. This adds considerably to the cost of such systems. On the other hand the parallel hybrid, with an overall efficiency of 43% as compared to only 26% of series hybrid, has scope for much wider applications. The electric motors can be much smaller and cheaper, as they do not have to convert all the energy. There are various ways in which parallel hybrid combinations can be used in vehicles. In the simplest form it can run entirely on batteries, for example, in a city where exhaust emissions are undesirable. It can also be powered solely by the ICE, for example, when travelling on highways outside the city. Alternatively, and more usefully, a parallel hybrid vehicle can use the ICE and batteries in combination, continually optimizing the efficiency of the ICE. A popular arrangement is to obtain the basic power to run the vehicle, normally around 50% of peak power requirements from the ICE, and to take additional power from the electric motor and battery, recharging the battery from the engine generator, when the battery is not needed [6]. Using modern control techniques the engine speed and torque can be controlled to minimize exhaust emissions and maximize the fuel economy. The basic principle is to keep the ICE working at high speeds in highway conditions, and shut it down in city conditions at moderate speeds. A major improvement in HEVs was achieved by using grid electricity to recharge batteries and restore these to full charge by connecting a plug to an electric power source.

1.1.2 Plug-in Hybrid Electric Vehicle Technology

A plug-in hybrid electric vehicle (PHEV) is similar to the HEV, but it has a larger battery that is charged both by the vehicle's ICE and from plugging into a standard 110 V electrical outlet for a few hours each day [7]. According to the Energy Independence and Security Act of 2007, PHEV is a either a light, medium, or heavy-duty motor vehicle or non-road vehicle that: (i) gets its motive power from a battery with a capacity of at least 4kWh, and (ii) uses an external source for recharging the battery [8]. PHEVs and HEVs both use battery-powered motors and gasoline-powered engines to get high fuel efficiency, but PHEVs can further displace fuel usage with off-board electrical energy charged at home. The result is a vehicle that can achieve far greater gas mileage than today's HEVs. The PHEV consists of an ICE, an electric battery for energy storage, an electric motor, and a controller. The battery is normally recharged from mains electricity via a plug and a battery charging unit that can either be carried onboard or fitted at the charging point. The controller known as a two-quadrant forward and backward controller, each quadrant controlling forward/backward acceleration, controls the power supplied to the motor and hence the vehicle speed. It also uses regenerative braking both to recoup energy and as a convenient form of braking. When the controller also allows for regenerative braking, it is known as four-quadrant controller, each quadrant controlling forward/backward acceleration and braking [2].

Conventional HEVs have already resulted in greater benefits to countries through less fuel consumption and increased energy security. Based on the United States Environmental Protection Agency (EPA) data, the most energy efficient existing hybrids cut gasoline consumption by around 40 % compared with similar conventional cars; PHEVs will further replace half of the remaining gasoline consumption with electricity [9]. PHEVs have achieved a fuel economy of more than 100 miles per gallon (mpg) compared to 30 to 55 mpg achieved by HEVs [2]. Thus PHEVs could reduce the consumption of fuels by at least 70 % compared with conventional cars [9]. For PHEVs with extra large batteries and motors, commuters who drive less than 20 miles a day can potentially drive exclusively with its electric motor for their daily commute [7]. In addition to reducing fuel consumption, PHEVs have the potential to also reduce total energy expenses for the owner and the electric power industry. PHEVs use grid-supplied electricity from diverse domestic energy sources such as renewable, coal and nuclear, and reduce

the nation's demand for imported oil. PHEVs can also make it easier to achieve the goal of fuel flexibility and alternative liquid fuels. Fuel flexibility is easier to incorporate in hybrid vehicles than in conventional vehicles. After PHEVs substantially reduce the liquid fuel requirement in cars, it will become much easier for alternative liquid fuels to supply the remaining liquid fuel demand [9].

A number of companies have started producing PHEV vehicles. Toyota Prius is a mid-size PHEV developed and manufactured by the Toyota Motor Corporation. The Prius is the most fuel efficient and cleanest, based on smog forming and toxic emissions, gasoline car currently sold in the U.S. according to the United States Environmental Protection Agency (EPA). The Prius first went on sale in Japan in 1997, making it the first mass-produced hybrid vehicle, and was subsequently introduced worldwide in 2001[10]. The Prius is sold in more than 40 countries and regions, with its largest markets being those of Japan and North America [11]. The modern Toyota Prius PHEV as shown in Figure 1-3 could revolutionize the impact of electric vehicles.

Figure 1-3. Toyota Prius (MY-04) [12]

While PHEVs like Toyota Prius provide a promising option, many broad energy and environmental considerations must be examined before they become widely available. For example, while a PHEV might be less costly for the consumer to drive than a gasoline-powered vehicle, it would draw power from the electrical grid when charging. Most of the electricity worldwide is generated by burning fossil fuels, such as coal. The energy costs to extract and

transport coal, as well as the environmental considerations associated with burning coal, are all part of the overall cost of using PHEV technology. These issues, however, decrease in importance as the amount of renewable energy in the electricity mix increases. There is also the question of how used batteries will be recycled, and how much that recycling will cost on a per-vehicle basis once all transport, processing, and disposal costs are considered. Significant technical barriers must also be overcome before PHEVs are available at local car dealers. These include cost, battery size and performance, durability and safety. PHEVs require additional, expensive components. Very large, heavy, and costly batteries are required to provide large vehicle range. In addition, the power electronics of PHEVs needs to be made smaller, simpler and less expensive. The safety issues surrounding the use of batteries under impact or at high temperatures need to be fully examined. Even though a vehicle is safe under normal conditions, a great deal of testing is required to determine its safety in a crash or fire. Emergency responders must also learn how to safely handle new vehicle battery technologies.

However, the most immediate needs before launching PHEVs in the market in a big way are: (i) testing their performance, range, and gradeability under different driving conditions, (ii) comparing their performance with HEVs and other vehicles, and (iii) developing an optimum hybridization of ICE, electric motor, and storage battery parameters. The PHEV performance refers to acceleration time and top speed, where the electric vehicles have a very poor reputation [13]. The range refers to the maximum distance traveled by the vehicle with a full fuel tank. Gradeability is the tractive effort available at the wheels, which should be greater than the rolling resistance encountered [13]. It is extremely important for the PHEVs to have at least as good performance and range as the current ICE vehicle, if large scale sales are to be achieved. The basic design considerations for PHEVs include vehicle architecture, drivetrain components (ICE and electric motor) selection, energy management systems, and energy storage tradeoffs [14]. In order to make an optimum use of the drivetrain component for a particular battery in a PHEV that provide optimum fuel economy, operating cost, and GHG emissions, the degree of hybridization needs to be assessed. The degree of hybridization is defined as the ratio of electric motor power to the sum of electric motor and ICE power [2]. The greater the degree of hybridization, the greater is the scope for using a smaller ICE, which operates at near its optimum efficiency for a greater proportion of the time. Accordingly, the performance of PHEVs

depends on energy management mode and the vehicle architecture. Each energy management mode calls for a different energy management control system that controls the function of the electric and combustion drivetrain within the PHEV [15].

The purpose of this research is to test the operational performance of Toyota Prius PHEV20 (PHEV version sized for 20 miles of all electric range) under different driving conditions, and develop an optimum hybridization of ICE, electric motor, and storage battery parameters based on fuel economy, operating cost, and GHG emissions. Computer based methods can be used to quickly experiment with different aspects of the vehicle, such as motor power, battery type, size, and weight and to see how the changes affect the performance and range. The data produced by the simulations can also be used for optimizing the performance of PHEVs under different driving conditions. For example, the data of motor torque and speed can be used to optimize the design of the motor and other subsystems. The U.S. Department of Energy Powertrain System Analysis Toolkit (PSAT^{TM}) vehicle simulator (Argonne National Laboratory, 2008) is used to model and examine the PHEV20 vehicle's performance. With 4480 possible combinations (including 20 batteries, 14 motors, and 16 engines), we use the Pareto Set Pursing (PSP) multi-objective optimization approach to efficiently find the optimum hybridization for Toyota Prius PHEV20. Electric grid power demand and costs associated with maintenance, manufacturing, and usage are estimated, and CO_2 emissions are calculated for fuel consumption and electricity generation. Integration of the onboard energy storage units of PHEVs with the power grid by power electronic converters and communication systems are developed, so that the energy conversion losses from the energy sources to the wheels were minimized. To take advantage of both series and parallel configurations, a split series/parallel powertrain, such as the one used in the Toyota Prius, is used. The powertrain uses a planetary gear system power split device and a separate motor and generator to allow the engine to provide torque to the wheels and/or charge the battery through the generator, depending on use conditions. Further, a PHEV can be used as range-extended or blended, depending on its energy management strategy in the charge-depleting state [16]. A range-extended PHEV functions as a pure electric vehicle in charge-depleting mode (CD-mode), using only electrical energy from the battery for propulsion and disabling any engine operation. Conversely, blended PHEVs invoke a strategy where the motor provides primary power in CD-mode and the engine is used as needed to provide additional power. Since

the performance of blended configurations can vary widely based on a broad range of control strategy parameters, for simplicity this study restricted the attention to the range-extended PHEVs that run entirely on electrical power in the CD-range and switch to operate like an HEV in the charge-sustaining mode (CS-mode).

1.1.3 Significance of Research

PHEVs are now being actively developed by many car companies, due to their significant potential in reducing fuel consumption and GHG emissions. In this work, I have developed simulation models using PSAT^{TM} software to test and compare the performance of PHEVs with other vehicles and with published performance claims of PHEV manufacturers under different driving conditions. The comparison validates the simulation models and helps in building the confidence of HEV and PHEV buyers in the market. In addition, this research will help the PHEV manufacturers in improving the performance parameters of new PHEVs under different driving conditions.

The hybridization and multi-objective optimization method for the design of PHEV's for a 20 miles of all electric range involving different combinations of battery storage, electric motor and ICE will provide the optimum fuel economy, operating costs, and GHG emissions, under different driving conditions that offers the urban commuters with a less expensive and clean driving option. The optimized hybridization of drivetrain components of the PHEVs can contribute significantly to the transportation system efficiency.

1.2 Objectives

The objectives of this research are:

(i) to test the performance of both PHEV and HEV based on the Prius platform under different driving conditions using PSAT^{TM} .

(ii) to evaluate the operational performance of PHEV20 based on fuel economy, operating cost, and operation GHG emissions through Pareto set point identification approach for 15 different types (including lithium-ion, nickel metal hydride, nickel zinc, and lead acid) of batteries.

(iii) to develop an optimization process for hybridization of ICE, electric motor, and storage battery parameters based on multi-objective optimization of fuel economy, operating cost, and operation GHG emissions using Pareto set pursuing (PSP) algorithm.

(iv) to identify optimal hybridization performances from a pool of 4480 combinations (involving 20 batteries, 14 permanent electric motors and 16 spark ignition engines), by simulating the PHEV20 vehicle on two different drive cycles: US EPA-Urban Dynamometer Driving Schedule (UDDS) and Winnipeg Weekday Drive Cycle (WWDC).

1.3 Scope of Research

The purpose of this research is to test the operational performance of Toyota Prius PHEV20 under different driving conditions, and develop an optimum hybridization of ICE, electric motor, and storage battery parameters based on fuel economy, operating cost, and GHG emissions. The scope of this research is limited to the data produced by the computer based PSAT^{TM} simulation model, which is used for optimizing the performance of Toyota Prius PHEV20 under different driving conditions using two different drive cycles: US EPA-Urban dynamometer driving schedule and Winnipeg weekday drive cycle. PSAT^{TM} vehicle simulator is used to model and examine the Toyota Prius PHEV20 vehicle's performance with 4480 different combinations (including 20 batteries, 14 motors, and 16 engines). The batteries, motors, and engines used in

this research are the most commonly available that can be used for the PHEVs, including lithium-ion, nickel metal hydride, nickel zinc, and lead acid batteries; Prius, Insight, Escape MG2, AuxilecThomson, Escape MG1, Camry MG2, UQM PowerPhase75, Honda, UQM PowerPhase100, Camry MG1 and Accord electric motors; and US04 Prius, Emission, Insight, Japan Prius, US01 Prius, Civic, Corolla, Escape Hybrid, Taurus Accord, Caravan, Explorer and Silverado gasoline engines. In addition, I use the multi-objective optimization approach to find the optimum hybridization for Toyota Prius PHEV20. To take advantage of both series and parallel powertrain configurations, a split series/parallel powertrain of Toyota Prius is used. Since the performance of blended configurations can vary widely based on a broad range of control strategy parameters, for simplicity we restricted our attention to the range-extended PHEVs that run entirely on electrical power in the CD-range and switch to operate like an HEV in the CS-mode.

Although the research only developed simulation models to test and compare the performance of Toyota Prius PHEV20 for UDDS and WWDC driving cycles, the models can be applied to other PHEVs to improve their performance parameters under different driving conditions. Since we have covered a wide range of batteries, motors, and engines, the optimized hybridization of drivetrain components of the PHEVs and moreover, the developed simulation and optimization approach, can contribute significantly to design of new PHEVs and eventually to the efficiency of the transportation system.

1.4 Thesis Outline

The focus of this research is to make the PHEVs more amenable to consumer acceptance and adoption. Therefore, three major objectives, which consumers consider as the most important, including fuel economy, operating cost, operation GHG emissions have been simultaneously optimized to find the best combination of battery and drivetrain parameters for PHEV. The multi-objective optimization approach in this research is based on using PSAT^{TM} simulations as a black box, and provides the best drivetrain combinations for UDDS and WWDC drive cycles. The thesis is organized as follows:

Chapter 2 provides a literature review on the related studies that include PHEV design studies, battery energy storage system parameter optimization, and drivetrain hybridization. PHEV design studies mostly focus on basic design considerations for vehicle architecture, energy management systems, drivetrain component function, and energy storage tradeoffs. The studies on vehicle architecture investigated the effects of weight and power on fuel consumption of HEVs, whereas the studies on energy management system emphasized that each energy management mode calls for a different energy management control system that controls the function of the electric and combustion drivetrain within the PHEV. Studies on energy storage devices indicate that batteries have been the main technical barrier for larger consumer acceptability for HEVs, both from a performance and cost perspective and highlight that optimized energy management strategies are the key to improved performance of PHEVs and characterization of the PHEV requires a detailed understanding of the energy management modes in which a particular vehicle operates.

Chapter 3 presents the PHEV modeling and simulation techniques used to model Toyota Prius PHEV20 in this study. In this chapter, first the Toyota hybrid system and Toyota Prius MY-04 vehicle model are described, second the drivetrain configurations and components used for modeling PHEV20 using PSAT^{TM} vehicle simulator are outlined, and finally the simulation set-up and simulation runs for both US Environment Protection Agency UDDS drive cycle and Winnipeg Weekday drive cycle are defined.

Chapter 4 describes the hybridization and multi-objective optimization models used for this research. The model variables, multi-objective functions, and constraints for the optimization are defined. The optimization algorithms used for battery sizing, and motor and engine sizing are outlined. The Pareto set pursuing technique used for multi-objective optimization is also described.

Chapter 5 discusses the results of the study. The performance of PHEV is compared with HEV based on the Prius platform for HWFET, UDDS and UN/ECE Normalized European driving cycle (NEDC) characterized by a city/highway driving mix conditions. Next the operational performances of PHEV20 for 15 different types of batteries are evaluated. Then the results of

hybridization and multi-objective optimization of PHEV20 using PSP are presented first for the US EPA-UDDS drive cycle and then for the Winnipeg weekday drive cycle. The results of battery sizing, and motor and engine sizing using optimization algorithms for both drive cycles are also presented. Finally the results for battery sizing, engine and motor sizing, hybridization and multi-objective optimization are compared for US EPA-UDDS and Winnipeg weekday drive cycles.

Chapter 6 concludes with both theoretical and practical contributions of the study and recommends topics for further research in the area.

Chapter 2

Literature Review

As PHEVs show promises to significantly reduce petroleum consumption and GHG emissions, earlier research in PHEV design focused on its feasibility assessment as compared to traditional HEVs and conventional vehicles. By recovering kinetic energy during braking and optimizing the engine operation to reduce fuel consumption and GHG emissions, a PHEV can outperform traditional vehicles [17]. Based on Environment Protection Agency (EPA) data, PHEVs were found to reduce the liquid fuels consumption by 70% and GHG emissions by 32% as compared with the conventional vehicles [18]. Therefore, PHEVs have the potential to reduce total energy expenses for the owner and the electric power industry. Life cycle assessment of green house gas emissions for PHEVs has also been studied [18]. Life cycle GHG emissions from PHEVs were found to reduce GHG emissions by 32% compared to conventional vehicles, but have small reductions compared to traditional hybrids. Kammen *et al*. (2008) further used the Greenhouse gases, regulated emissions, and energy use in transportation (GREET) model to provide cost-effectiveness GHG emission reductions [17]. They found that the battery prices must decline from about $1300/kWh to below $500/kWh, or U.S. gasoline prices must remain at roughly $5/gallon, for PHEVs to be cost effective as compared to the conventional vehicles. The fuel economy of PHEVs depends on many design parameters such as component sizes and control strategy parameters. Therefore, the newer front of PHEV research has focused on PHEV design, battery storage system and control strategy parameter optimization, which allows for improved real-world performance of PHEVs for consumer acceptability [19].

The operational performance of PHEVs is greatly influenced by the energy management mode and the vehicle architecture. Each energy management mode calls for a different energy management control system that controls the function of the electric and combustion drivetrain within the PHEV. The energy storage devices appear to be the main technical barrier for larger consumer acceptability both from a performance and cost perspective [20]. Technological

advancements in the energy density, power density, and lifetime of electrochemical energy storage batteries have improved the performance and lifecycle cost prospects of PHEVs. Although large batteries would be ideal for energy storage, the size affects cost, weight, and performance of the PHEV. The focus of research has, therefore, shifted to drivetrain component sizing or hybridization that optimizes the vehicle control strategy while maximizing the benefits of regenerative braking and power buffering [21]. At present there is no standard solution for optimal size or ratio of the ICE and the electric motor system for different types of batteries. It is preferable to operate the engine at low power during short trips and higher power during longer trips to maximize the efficiency of the entire system. It is believed that the fuel economy of PHEVs could be substantially improved by simultaneously optimizing the control strategy parameters and component sizing. A detailed literature review of the existing studies on PHEV designs, battery storage system optimization, and drivetrain hybridization is presented next.

2.1 PHEV Design Studies

The basic design considerations for PHEVs include vehicle architecture, energy management systems, drivetrain component function, energy storage tradeoffs, and grid connections [22]. The studies related to PHEV design mostly focused on vehicle architecture. The objective was to study the impact of architectural design and weight of PHEVs on a combination of fuel consumption and environmental benefits, because modern PHEVs are significantly more powerful and are, therefore, heavier than the first generation of HEVs. Investigating the effect of weight and power on fuel consumption in HEVs, Reynolds and Kandlikar (2007) found that heavier and more powerful HEVs are eroding the fuel consumption, and the weight penalty for fuel consumption in HEVs was significantly lower than in equivalent conventional ICE vehicles [23]. Their analysis further revealed that an HEV, which is 100 kg heavier than an identical ICE vehicle, would have a fuel consumption penalty of 0.15 liters per 100 km. Likewise, an increase in the HEV's power by 10 kW would result in a fuel consumption penalty of 0.27 liters per 100 km. Zervas and Lazarou (2008) also found that weight of the vehicle was a major parameter influencing CO_2 emissions [24]. For the same driving distance, heavier vehicles need more energy than lighter ones, because they have to move an extra weight, and thus more fuel is consumed, thereby resulting in increased CO_2 emissions. They found that significant benefits on

CO_2 emissions could be achieved if the weight of each passenger car does not exceed an upper limit.

In PHEV design studies, the performance of PHEVs has also been found to be dependent on energy management mode along with the vehicle architecture [25]. Each energy management mode calls for a different energy management control system that controls the function of the electric and combustion drivetrain within the PHEV [26]. PHEVs can operate in four energy management modes: charge-sustaining (CS), charge-depleting (CD), electric vehicle (EV), and engine only [27]. Conventional HEVs operate in CS mode for most of the time, as the battery state-of-charge (SOC) is controlled to remain within a narrow operating band in this mode. Since the battery SOC does not change with time, the liquid fuel is the net source of energy for the vehicle in the CS mode [26]. In CD mode, the battery SOC decreases during vehicle operation. The engine may be on or off, but some of the energy propelling the vehicle is provided by the electrochemical energy storage system, causing the SOC to decrease with time [27]. In EV mode, the operation of the fuel engine is prohibited. The PHEV drives as an electric vehicle, because the electrochemical energy storage system is the only sources of tractive energy, the SOC decreases with time. Further in EV mode, the operation of the electric system is very limited, as the electric traction system does not provide enough tractive power to the vehicle. Switching between energy management modes can be manually selected by the driver or automatically controlled as a function of SOC of the battery, vehicle speed, engine speed, engine torque, environment temperature, battery temperature, and air conditioning need. For instance, when the vehicle is in CS mode, the vehicle must control the SOC of the battery by regenerating energy from the combustion drivetrain, using the electric drivetrain to generate electricity. When the vehicle is in EV mode, the combustion drivetrain will be completely shut off and the electric drivetrain will perform the functions of accelerating and braking the vehicle [28]. Bradley and Frank (2007) presented the basic design considerations for PHEVs including vehicle architecture, energy management systems, drivetrain component function, and energy storage tradeoffs [27]. They found that in modern PHEVs, the performance difference between an EV mode, CD mode and CS mode is nearly imperceptible to the driver. The component performance and system design requirements of PHEVs are demanding because they exhibit similar performance requirements in each energy management mode [29]. Component design and

synthesis of the PHEV powertrain are, therefore, dependent on the specified performance requirement of the vehicle and the energy management mode.

The performance of PHEVs is also rated by all electric range (AER), which is the distance the vehicle can travel without the ICE turning on starting with SOC of 100% and finishing with the smallest possible SOC that the battery pack can sustain without being damaged [30]. HEVs with high AER have been found to have significantly better energy economy as compared to their fuel only counterparts [31]. Graham (2001) compared the benefits and impacts of HEV performance on energy economy, fuel-cycle emissions, costs, and consumer acceptance through various components sizing, packaging, and optimizing control algorithms [31]. HEVs that offer the best combination of environmental and efficiency benefits while meeting the driving needs and economic constraints of automobile owners were examined. In order to test the capacity and performance of PHEVs over full-charge, Duoba *et al*. (2007) tested procedures for benchmarking the PHEVs, by giving a full-charge test to the PHEV to find the capacity and to characterize the vehicle's operation [32]. The driving statistics that are useful in processing the full-charge test and in combining depleting with sustaining operation were developed [32].

One of the unique advantages of PHEVs is their capability to integrate the transportation and electric power generation sectors in order to improve the efficiency, fuel economy, and reliability of both systems. The fuel and electrical energy consumption for different drive cycles and operating modes have also been studied [22]. The frequency of engine operation that affects engine temperature was found to have great influence on fuel economy. The cost of PHEVs has also been found to be related to energy consumption and emissions [19]. The cost of two simulated PHEVs with energy consumption and emissions for two different powertrain configurations (series and parallel), four different driving cycles (CAFE, FTP75, NEDC and JC08), different driving distances, and user behaviors regarding battery recharging were evaluated. Other fuel economy reporting methods include cost and benefit analysis, the application of real-world driving data to quantify the impacts of travel behavior on the potential benefits of PHEVs and the optimization of energy management strategies, focusing on petroleum displacement [33]. Staunton *et al*. (2006) further evaluated the electrical and mechanical characteristics of the HEVs by conducting a full range of design characterization studies [34].

These include a design review, a packaging and fabrication assessment, bench-top electrical tests, back-electromotive force and locked rotor tests, loss tests, thermal tests at elevated temperatures, and most recently full-design-range performance testing in a controlled laboratory environment. Ferdowsi (2007) studied the integration of the onboard energy storage units of PHEVs with the power grid by power electronic converters and communication systems [35]. The powertrain configurations of PHEVs were designed in such a way that the energy conversion losses from the energy sources to the wheels were minimized.

Model-based design tool have been developed for testing the performance of PHEVs for different architecture selection, component sizing, and control algorithms via prototyping and testing [26]. Studies have looked into prototyping and testing each design combination to choose the right parameters [22]. Mendes *et al*. (2007) developed a model-based design tool for testing the performance of PHEVs and prototypes [36]. They utilized an auto-generated control code to seamlessly connect the simulations to the real-world implementation and found that their design tool gives accurate insight into architecture selection, component sizing, and control algorithms. This allows a PHEV to use electric energy to displace petroleum as a transportation fuel, with benefits in terms of increased transportation energy efficiency, reduced carbon emissions, reduced criteria emissions, reduced fueling cost, improved consumer acceptance and improved transportation energy sector sustainability. All these studies in PHEV design focused on prototyping and testing hundreds of design parameters for improving the performance of PHEVs. However, multiple testing procedures have been found to be very cumbersome and expensive. Therefore, the emphasis of research shifted to design optimization, where an objective function is minimized or maximized subject to some constraints on the design variables in order to get a better design [37].

The optimization algorithm tries to maximize the objective function by searching the multidimensional parameter space for various combinations of the design variables and selects the best combination. However, analytical optimization algorithms cannot be directly used for design optimization of PHEVs, as it would involve the derivation of an equation having hundreds of parameters [38]. Therefore, simulation-based optimization algorithms that work together in a loop with a computer simulation model to reach optimal solution have been

suggested [39]. One such simulation-based optimization algorithm is power train system analysis toolkit (PSAT^{TM}), developed by Argonne National Laboratory in collaboration with Ford, General Motors, Chrysler, and the US Department of Energy [40]. It is a state-of-the-art flexible and reusable simulation package that meets most of the requirements of automotive engineering throughout the development process, from modeling to control.

Simulation-based optimization algorithms have been used in HEV design studies to find optimal component sizes and appropriate control strategies for achieving maximum fuel economy. Hubbard and Youcef-Toumi (1997) modeled and simulated the drivetrain of an HEV and used dynamic models for developing control algorithms [41]. They used bond graphs to develop models capable of describing both transient and steady-state operation of each of the key drivetrain components as transmission, vehicle chassis, three-phase AC induction motor, lead-acid battery, and ICE [41]. Tate and Boyd (1998) developed a nonlinear convex optimization model for finding optimal ICE operation in a pure series HEV over a fixed drive cycle subject to a number of practical constraints including: nonlinear fuel/power maps, minimum and maximum battery charge, battery efficiency, nonlinear vehicle dynamics and losses, drive train efficiency, and engine slew rate limits [42]. They emphasized that this optimal solution was the lower limit of fuel consumption that any control law could achieve for the given drive cycle and vehicle. Fontaras *et al.* (2008) studied the fuel economy and GHG emissions measurements of two HEVs, Toyota Prius II and Honda Civic IMA, using the New European Driving Cycle (NEDC) and real-world simulation driving cycles (Artemis) [43]. They found that in most cases both vehicles present improved energy efficiency and reduced GHG emissions compared to conventional cars. The fuel economy benefit of the two HEVs peaked under urban driving conditions where fuel reductions of 60% and 40% were observed, respectively. However, over higher speeds the difference in fuel economy was lower. There is a variety of configurations, control strategies, and design variable choices that can be made using computer-based modeling and simulation techniques [39]. Alternative powertrains have been explored for automotive applications aiming at improving fuel economy and reducing GHG emissions. Fellini *et al.* (2007) studied the modularity, flexibility, and rigor of a design environment for alternative powertrains and applied these concepts to a hybrid diesel-electric powertrain [44]. They found that modularity allows a system to be built by combining different components, flexibility allows different levels of

conformity and different existing codes to be used, and rigor is based on mathematical methods of decision making.

A number of studies have established that the optimized performance of PHEV depends on the control strategy parameters. Rousseau et al. (2008) studied the control strategy parameter optimization of PHEVs, using a pre-transmission parallel PHEV model with 10 miles AER using PSAT^{TM} [45]. A non-derivative based algorithm, DIRECT, was used to optimize the main parameters of a pre-defined control strategy algorithm. Different sets of parameters were generated and their impact on distance and driving cycles were analyzed. Their results demonstrated the need to have different control parameters depending on distance and drive cycle. They also emphasized the need to optimize design parameters such as electric motor size, engine size, battery type, and battery capacity to determine the least cost design that meets a fixed set of vehicle performance constraints.

Wang (2005) proposed a multi-objective optimization evolutionary algorithm based on adaptive stochastic search strategy for optimal design parameters of HEVs, performing simulations over representative drive cycles [38]. He found that the stochastic nature of the evolutionary algorithm can prevent convergence upon local sub-optima and is capable of seeking out the optimal solutions for multiple objectives in an efficient fashion. Golbuff (2006) developed a methodology for optimizing PHEV design using minimum drivetrain cost to determine the optimum designs for AER of 10, 20, and 40 miles for a base vehicle platform resembling the characteristics of a mid-sized Sedan [46]. The performance constraints used in their study were: speed of 0-60 miles per hour (mph), acceleration time from 0-30 mph in electric only operation, and acceleration time from 50 to 70 mph in hybrid operation. The resulting optimum PHEV designs were simulated for fuel economy through PSAT^{TM} and the social impact in terms of gasoline use reduction and carbon emissions reduction were quantified. They found that the lead acid battery type produced the least cost design for AER of 10, 20, and 40 miles.

Further research in control strategy parameters optimization focused on maximizing the overall efficiency of the powertrain system of any HEV. Karbowski *et al*. (2006) developed a global optimization algorithm, based on the Bellman principle, to generate the most efficient control

strategy for PHEVs [37]. The global optimization algorithm was used to optimize a parallel pre-transmission hybrid and a specific driving cycle to find out the most efficient energy operating conditions. Several driving cycles were analyzed; each of them repeated a number of times to assess the impact of driving distance, engine, electric machine, and transmission operating modes to generate a rule-based control strategy in PSAT^{TM}. The component models and controls developed in PSAT^{TM}, however, require validation because of importance and complexity involved in setting up optimized control strategies [47]. They used the control strategy improvements to validate the PHEV Hymotion Prius Model. They tested the engine and half-shaft torque sensors and compared the performance results of Hymotion L5 PHEV battery pack in its original configuration with the highly instrumented Toyota Prius in Argonne's Advanced Powertrain Research Facilities. They also assessed the impact of different control strategy options for the PHEV. Based on their analysis of the control strategy, they proposed changes to minimize the number of engine ON/OFF events and maximize the engine's efficiency throughout the drive cycle. They suggested that it is preferable to operate the engine at low power during short trips and higher power during longer trips to maximize the efficiency of the entire system. The energy consumption in PHEVs has been found to be highly linked to the size of components used in the PHEV. Karbowski *et al*. (2007) studied the impact of component size on PHEV energy consumption using global optimization [39]. They modeled several vehicles based on a parallel pre-transmission architecture with AER from 5 to 40 miles on the UDDS to illustrate various levels of available electric energy and power. The vehicles were then simulated under optimal control on multiple combinations of cycle and distance by using a global optimization algorithm, which allowed estimation of the impacts of component sizing on GHG emissions in a given electricity generation scenario.

2.2 Battery Energy Storage System Parameter Optimization

The body of research on PHEVs shows that PHEVs have significant benefits for the pollution output, energy efficiency and sustainability of the transportation energy sector. However, the energy storage devices appear to be the main technical barrier for larger consumer acceptability, both from a performance and cost perspective [48]. Optimized energy management strategies are the key to improved performance of PHEVs and characterization of the PHEV requires a detailed

understanding of the energy management modes in which a particular vehicle operates. Technological advancements in the energy density, power density, and lifetime of electrochemical energy storage batteries have improved the performance and lifecycle cost prospects of PHEVs [49]. However, battery development is constrained by inherent tradeoffs among five main battery attributes: power, energy, longevity, safety, and cost. The battery weight increases with power and its energy storing capacity. Markel and Simpson (2006) proposed efficient energy storage systems for PHEV design for reducing the demand for petroleum in the transportation sector [48]. The design options include power, energy, and operating strategy management. They found that expansion of the usable SOC window will dramatically reduce cost but will likely be limited by battery life requirements. Increasing the power capability of the battery provides the ability to run EV mode more often but increases the incremental cost. They also found that increasing the energy capacity from 20 to 40 miles of electric range capability provides an extra 15% reduction in fuel consumption but also nearly doubles the incremental cost.

PHEVs require large batteries for energy storage, which affect vehicle cost, weight, and performance. The impact of battery weight and charging patterns on the economic and environmental benefits of PHEVs has been analyzed by researchers. Shiau *et al.* (2009) constructed PHEV simulation models on PSAT^{TM} to account for the effects of additional batteries on fuel consumption, cost, and GHG emissions over a range of charging frequencies [50]. They found that small-capacity PHEVs are less expensive and release fewer GHGs than HEVs or conventional vehicles when charged frequently, every 20 miles or less, using average U.S. electricity. For moderate charging intervals of 20-100 miles, PHEVs release fewer GHGs, but HEVs are more cost effective. High fuel prices, low-cost batteries, or high carbon taxes combined with low carbon electricity generation would make small-capacity PHEVs cost-effective for a wide range of drivers. Large-capacity PHEVs sized for 40 or more miles of electric-only travel may not be as cost effective. They measured the impacts of battery weight on CD mode electrical efficiency and CS mode fuel economy and found a 10% increase in power (Wh/kg) and an 8% increase in fuel economy (gallons per mile) when moving from PHEV7 (AER 7) to PHEV60 (AER 60). The best choice of PHEV battery capacity, therefore, depends critically on the distance that the vehicle will be driven between charges. Sharer et al. (2006)

developed a process that describes the impact of AER, drive cycle, and control strategy on the requirements of energy storage systems for plug-in applications [51]. They used vehicle simulation results for PHEV battery requirements and found that the battery energy is approximately a linear function of AER. However, AER itself depends upon numerous other parameters, including vehicle class, drive cycle, and control strategy.

There have been a number of developments of advanced batteries for PHEV applications. Axsen *et al.* (2008) compared the abilities of the current state of several battery chemistries, including nickel-metal hydride (NiMH) and lithium-ion (Li-Ion), to meet PHEV goals and potential trajectories for further improvement [52]. They found that the PHEV battery goals vary according to differing assumptions of PHEV design, performance, use patterns and consumer demand. Li-ion battery designs were better suited to meet the demands of more aggressive PHEV goals than the NiMH batteries currently used for HEVs. The flexible nature of Li-ion technology, as well as concerns over safety, has prompted several alternate paths of continued technological development. High specific power of Li-ion technologies does not have a significant influence on vehicle mass. Battery pack voltage yet needs to be taken into consideration for high AER, because for high AER the capacity of the battery increases which is dependent upon the nominal voltage of the battery [51]. Rousseau *et al*. (2007) studied the impact of AER, drive cycle, and control strategy for PHEV battery requirements and evaluation of early prototypes [53]. They performed the vehicle simulations for several vehicle classes and AER by using Li-ion Johnson Control Saft VL41M battery Hardware-in-the-Loop (HIL) and compared the simulated requirements, based on Urban Dynamometer Driving Schedule (UDDS), with Toyota Prius tested on a dynamometer. The validation of the cycle life performance of advanced batteries is subjected to a PHEV duty cycle. The duty cycle is generally a combination of deep and shallow discharge behavior found respectively in battery electric vehicles and HEVs and is dependent on both vehicle requirements and the energy management strategy of the hybrid powertrain [54]. The PHEV has unique battery requirements that often require a compromise between the high energy battery systems and the high power energy storage systems used in power assisted HEVs.

Nelson *et al*. (2007) further analyzed advanced simulations for Li-ion batteries for PHEVs [55]. Three vehicles were designed, each with series powertrain and simulation test weights between 1575 and 1633 kg: HEV with a 45-kg battery, PHEV with a 10-mile electric range (PHEV10) with a 60-kg battery, and PHEV20 with a 100-kg battery. These vehicles could accelerate to 60 mph in 6.2 to 6.3 seconds and achieve fuel economies of 50 to 54 mpg on the UDDS and highway fuel economy test (HWFET) cycles. The PHEVs, therefore, show promise of having a moderate cost if these were mass produced, because there is no transmission. The engine and generator may be less expensive since they are designed to operate at only one speed, and the battery electrode materials are inexpensive. Powertrain hybridization as well as electrical energy management is imposing new requirements on electrical storage systems in vehicles including: shallow-cycle life, high dynamic charge acceptance particularly for regenerative braking and robust service life in sustained partial-state-of-charge usage [56]. They found that lead acid is expected to remain the predominant battery technology for 14V systems, whereas NiMH and Li-ion are the dominating current and potential battery technologies for higher-functionality HEVs.

The application of ultracapacitors for electric energy storage has also been explored in charge sustaining mode for HEVs and PHEVs. Burke (2007) focused on the use of Li-ion batteries and carbon/carbon ultracapacitors as the energy storage technologies most likely to be used in future vehicles [57]. He found that the energy and power density characteristics of both battery and ultracapacitor technologies are sufficient for the design of attractive HEVs and PHEVs. It was also found that in CS mode, engine powered HEVs can be designed using either batteries or ultracapacitors with fuel economy improvements of 50% and greater. Moreover, PHEVs can be designed with effective AER of 30–60 miles using Li-ion batteries that are relatively small. The effective fuel economy of the PHEVs can be very high (greater than 100 mpg) for long daily driving ranges (80–150 miles) resulting in a large fraction (greater than 75%) of energy to power the vehicle from grid electricity. Mild HEVs can also be designed using ultracapacitors having an energy storage capacity of 75–150 Wh [57]. Even hydrogen fuel cells can be used to power hybrid electric vehicles with either batteries or ultracapacitors for energy storage [58].

For maximum petroleum displacement, a PHEV is expected to operate in an EV or a CD mode over a large SOC window (60-80% of total operational SOC) [50]. At low SOC, the vehicle

operates in the CS mode, similar to the current HEVs. The SOC at which the battery operates in the CS mode is mostly determined by the impact on battery life [30]. They studied the sensitivity of vehicle fuel economy in CS mode at different SOCs for all electric range in CS mode using JCS VL41M Li-ion HIL Battery. They evaluated the vehicle AER, temperature rise, and battery performance in the CS mode at low SOCs (35 to 20%) and concluded that CS operation at low SOC for an urban driving cycle has no effect on fuel economy. Inappropriate discharge/charge patterns would also result in the loss of batteries life [59]. They developed a genetic algorithm optimization based control strategy for series HEVs in order to maximize the efficiency of the powertrain while minimizing the loss and compared with the two main control strategies, namely thermostatic (engine-on-off) and power follower control strategy. In thermostatic control strategy, the generator set is turned on when the SOC of the battery reaches its maximum value, and will be turned off when the SOC of the battery reaches its minimum value. In power follower control strategy, the electric motor and ICE operating points, power output values, and efficiency points are set during the vehicle drive cycle. They also observed that the battery life increases with the lower variation of battery SOC during the vehicle drive cycle.

Other factors considered in battery designs to improve the performance of PHEV include, battery storage capability (kWh), depletion rate of the vehicle (kWh/km), average daily kilometers driven, annual share of trips exceeding the battery depletion distance, driving cycle(s), charger location (i.e. on-board or off-board), and charging rate [60]. In addition, off the vehicle, considerations include: primary overnight charging spot (garage, carport, parking garage or lot, on street), availability of primary and secondary charging locations (i.e. dwellings, workplaces, stores, etc.), time of day electric rates, seasonal electric rate, types of streets and highways typically traversed during most probable trips depleting battery charge (i.e. city, suburban, rural and high vs. low density), cumulative trips per day from charger origin, top speeds, and peak acceleration rates required to make usual trips [28]. They estimated the potential of PHEVs ability to reduce the U.S. gasoline use. They examined the costs per kWh of PHEVs capable of charge-depleting AER vs. those charge-depleting in “blended” mode, and compared the lifetime fuel savings of alternative PHEV operating/utilization strategies to battery cost estimates. The impacts of battery energy and power have also been evaluated by using a global optimization algorithm to assess the impact of temperature with constant vehicle control strategy [53]. Kelly

et al. (2002) performed comparative study of the battery usage and thermal performance of the battery packs using chassis dynamometer testing for Honda Insight and Toyota Prius in the National Renewable Energy Laboratory [61]. Specially designed charge and discharge chassis dynamometer test cycles revealed that the Honda Insight limited battery usage to 60% of rated capacity, while the Toyota Prius limited battery usage to 40% of the rated capacity. They found that Toyota Prius uses substantially more pack energy over a given driving cycle but at the same time maintains the pack within a tight target (SOC) of 54% to 56%. The Prius battery contributes to a higher percentage of the power needed for propulsion and its thermal management is more robust, whereas Honda Insight's thermal management limits pack performance in certain conditions.

A few studies have also developed simulation packages for modeling energy management strategies for HEV configurations. For example, Butler *et al.* (1999) developed a simulation package, V-Elph 2.01, at Texas A&M University for modeling energy management strategies for HEV configurations [62]. V-Elph was written in the Matlab/Simulink graphical simulation language and was composed of models for four major types of components: electric motors, internal combustion engines, batteries, and support components. Peng and Bang (2000) developed the control strategy for the energy management of a post-transmission parallel hybrid electric vehicle equipped with a continuously variable transmission [63]. The dynamic, forward simulation of a complete compact class vehicle including driver model and computer controller were also written in Matlab / Simulink.

Based on improvements in the PHEV and battery design, the Toyota Motor Corporation, which leads the world's automakers in sales of HEVs, has entered into the PHEV market in a big way. Toyota would develop a fleet of PHEVs that run on Li-ion batteries, instead of the NiMH batteries that power the Prius and other Toyota models [64]. General Motors and Ford also have plans to manufacture and sell their own PHEVs.

2.3 Drivetrain Hybridization

There is no standard solution for the optimal size or ratio of the ICE and the electric system. The optimum choice includes complex tradeoffs between the heat engine and electric propulsion system on one hand and cost, fuel economy, and performance on the other. Each component, as well as the overall system therefore, has to be optimized to give optimal performance and durability at a low price. To allow system-level analysis and trade-off studies of HEVs, an advanced vehicle simulator model, ADVISOR, was developed at the National Renewable Energy Laboratory [65]. The vehicle simulator was used for modeling different vehicles and the sensitivity of each vehicle's fuel economy to critical vehicle parameters was analyzed. Engine and electric motor were both sized so that the vehicles could meet the performance standards for acceleration time from 0 to 60 mph and gradeability of 55 mph. Vehicle mass and control strategy were scaled to get the best vehicle performance results for a specific drive cycle. Wipke and Cuddy (1997) further found that drivetrain hybridization results in a fuel economy of 65.4 mpg for light weight conventional vehicles and 80.5 mpg for hybrid configurations by using the ADVISOR vehicle simulator on mid-sized sedan on USEPA Federal Urban (FUDS) and USEPA Highway Drive Schedules (FHDS).

The efficiency of drivetrain hybridization has also been confirmed by other research studies. Chau and Wong (2001) tried to hybridize the energy sources by optimizing the mass ratio (the ratio of total energy source mass to the whole vehicle mass) and hybridization ratio (the ratio of the high specific power energy source mass to the total energy source mass), using two energy sources, one with high specific energy and the other with high specific power [66]. The microprocessor based power flow controller was used to coordinate the two energy sources for the three modes of operation including: normal driving mode, acceleration/hill-climbing mode and braking/downhill mode. The coordination was based on the predefined control strategy, which functions to operate the whole hybrid system effectively and efficiently while fulfilling the electric vehicle tractive demand. Wipke *et al.* (2001) conducted drivetrain hybridization under the hybrid vehicle propulsion system and observed that not only was the vehicle control strategy important, but that its definition should be coupled with the component sizing process that almost doubles the fuel economy without sacrificing the performance and consumer

acceptability of HEVs [67]. They emphasized that the degree of hybridization of HEVs depends on both the vehicle control strategy and drivetrain component sizing. Wipke *et al*. (2001) further studied the degree of hybridization and optimization of the energy management strategy. Mass scaling algorithms were employed to capture the effect of component and vehicle mass variations as a function of degree of hybridization. They maximized the benefits of regenerative braking and power buffering by using local and global optimization routines to determine appropriate battery pack size and found that the vehicle control strategy has to be optimized with the component sizing process.

Different hybridization levels from mild to full hybrid electric traction systems have been examined by the researchers [26]. They analyzed the effects of drivetrain hybridization on fuel economy and dynamic performance of parallel HEVs. They found that low hybridization levels provide an acceptable fuel economy benefit at a low price, while the optimal level of hybridization ranges between 0.3 and 0.5, depending on the total vehicle power. Given the advantages of downsizing the engine size, Katrasnik (2007 Part1) tried to achieve a reduction in fuel consumption of hybrid powertrains by downsizing the internal combustion engine size with the emphasis on determining the optimum hybridization ratio [68]. He offered an analytical approach based on the energy balance in order to analyze and predict the energy conversion efficiency of hybrid powertrains. However, this approach resulted in inadequate transient response and poor drivability.

In order to keep an acceptable level of driving comfort and performance for the user, it is necessary to employ the right size and capacity of the electric system. In addition, it is necessary to consider the geometrical and mechanical characteristics of ICE to model adequately the steady state and/or dynamic operation of the downsized ICE. Therefore, the advantages of the hybrid powertrain are based on the component characteristics and an optimum powertrain configuration with respect to the applied drive cycle [27]. Zeraoulia et al. (2006) studied the selection of the most appropriate electric propulsion system for a parallel HEVs based on the performances of the four main electric propulsion systems, the dc motor, the induction motor, the permanent magnet synchronous motor, and the switched reluctance motor [69]. They found that the cage induction motor better fulfils the major requirements of the HEV electric propulsion. The U.S.

Department of Energy (DOE) conducted a full range of design characterization studies to acquire knowledge and to evaluate the electrical and mechanical characteristics of the 2004 Prius and its hybrid electric drive system [70]. This testing was undertaken by the Oak Ridge national laboratory as part of the U.S. DOE – energy efficiency and renewable energy freedom car and vehicle technologies program. They effectively mapped the electrical and thermal results for motor/inverter operation over the full range of speeds and shaft loads that these assemblies are designed for in the Prius vehicle operations. In order to preserve the performance and drivability of PHEVs under all conditions, the battery pack power should increase as the ICE size decreases [47]. However, the ICE size is generally limited by the vehicle's maximum speed and gradeability requirement [39]. A review of the automotive industry literature shows that each company has developed its own solution for the relative size of the ICE to the electric motor, called the hybridization factor. Hybridization affects the energy profile and therefore, plays an important role in consumer acceptability for different drive cycles [26]. However, there is no standard solution for the optimal size or ratio of the internal combustion engine and the electric system. The process of drivetrain hybridization optimization includes complex tradeoffs between the ICE and electric propulsion system on one hand and cost, fuel economy, and performance on the other [26].

Although, hybridization and downsizing allow for fuel economy enhancements, it is necessary to determine an optimum hybridization factor in order to take the most advantages of hybridization, since further increasing the hybridization factor beyond the optimum value could lead to lower energy conversion efficiency of the powertrain and to higher fuel consumption [27]. The hybridization of powertrain and downsizing of ICE needs an extensive analysis and parametric study of hybrid powertrain parameters for different drive cycles and electric energy storage devices as well as the results of vehicle dynamics. Katrasnik (2007 Part2) found that the drive cycle has a significant influence on the optimal combination of powertrain components [71]. The fuel economy enhancements of hybrid powertrains increases with decreasing average load of the test cycle and that the point of the best fuel economy for a particular average load of the cycle moves towards higher hybridization factor when the average load of the test cycle is decreased. It is, thus, not reasonable to increase hybridization factor beyond the optimal limit, since the energy conversion efficiency of the hybrid powertrain decreases thereafter, resulting in higher fuel

consumption. Katrasnik (2007 Part2) further found that downsizing the ICE and hybridization of the powertrain performed best for test cycles with lower average load, i.e. for light duty applications, whereas powertrains with high hybridization factor were not appropriate for heavy duty applications.

In summary, for optimal performance of PHEVs, it is necessary to employ the right size and capacity of the electric system, and at the same time adequately maintain the steady state and/or dynamic operation of the downsized ICE. The optimum capacity of electric storage devices is of crucial importance for high energy conversion efficiency and good drivability of hybrid powertrains, whereas a compromise has to be made between storage capacity and electric conversion efficiency on the one hand, and weight penalty and additional costs on the other hand. The advantages of the hybrid powertrain are based on the component characteristics and an optimum powertrain configuration with respect to the applied drive cycle. Therefore, the fuel economy of PHEVs could be substantially improved and operating costs and GHG emissions reduced by optimizing the component sizing. This work limits our focus on optimal component sizing by modeling the vehicle using a simplistic control strategy.

Chapter 3

Vehicle Modeling and Simulation

The vehicle modeling and simulation tool, PSAT^{TM}, has been used to optimize the component sizing of Toyota Prius PHEV20. First the control strategy parameters of Toyota Prius PHEV20 power split drive system were modeled using PSAT^{TM} simulation tool. Using the vehicle simulation model in PSAT^{TM} as a black box, the drivetrain hybridization of Toyota Prius PHEV20 was optimized using multi-objective optimization approach for the most efficient performance in fuel consumption, operating cost, and GHG emissions on two different drive cycles, Urban Dynamometer Driving Schedule and Winnipeg Weekday Drive Cycle. The details of Toyota hybrid system and Toyota Prius PHEV20 Model Year (MY) 2004 are explained next. The vehicle modeling and simulation on PSAT^{TM} for two different drive cycles, UDDS and WWDC, follows afterwards.

3.1 Toyota Hybrid System

Toyota Hybrid System (THS) is the innovative power train used in the current best-selling hybrid vehicle in the market, the Toyota Prius. It uses a split-type hybrid configuration which contains both series as shown in Figure 3-1 and parallel as shown in Figure 3-2 power paths to achieve the benefits of both. The THS uses a planetary gear set to connect the three power sources including engine, motor, and generator. Since both the motor and generator can operate in both charging and discharging modes, they are sometimes denoted as Motor/Generator 1 and Motor/Generator 2. We use the former naming scheme to reflect their major roles. The configuration of split-type hybrid system is shown in Figure 3-3 with both parallel and series power paths. The planetary gear set provides infinite gear ratio between the engine and the vehicle speed so that it is both a power summing device and a gear ratio device as shown in Figure 3-4.

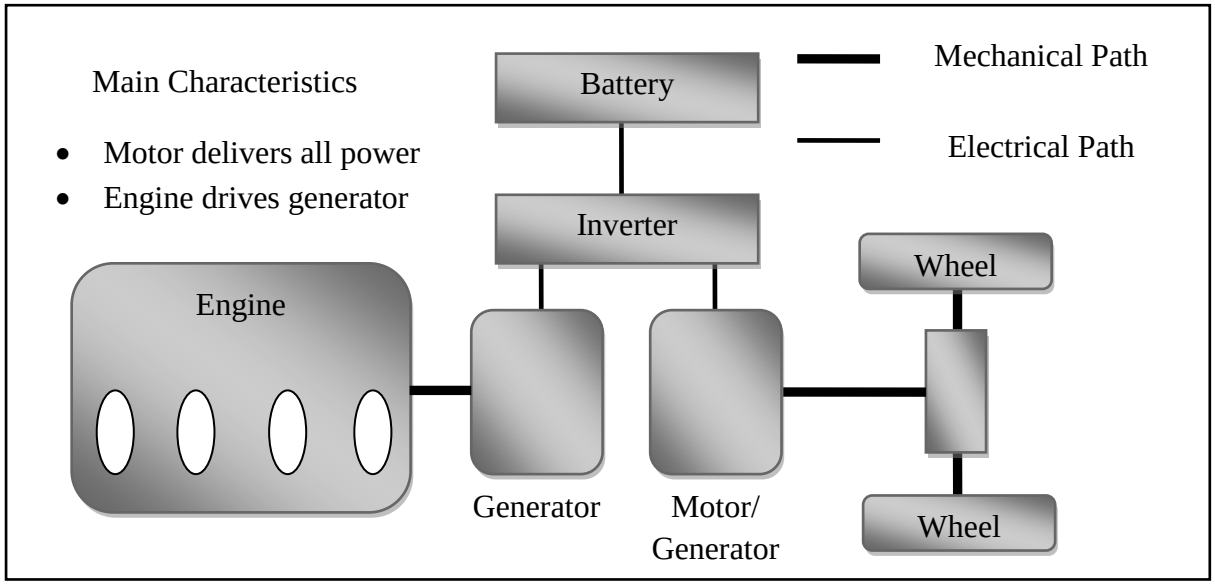

Figure 3-1. Series hybrid system [72]

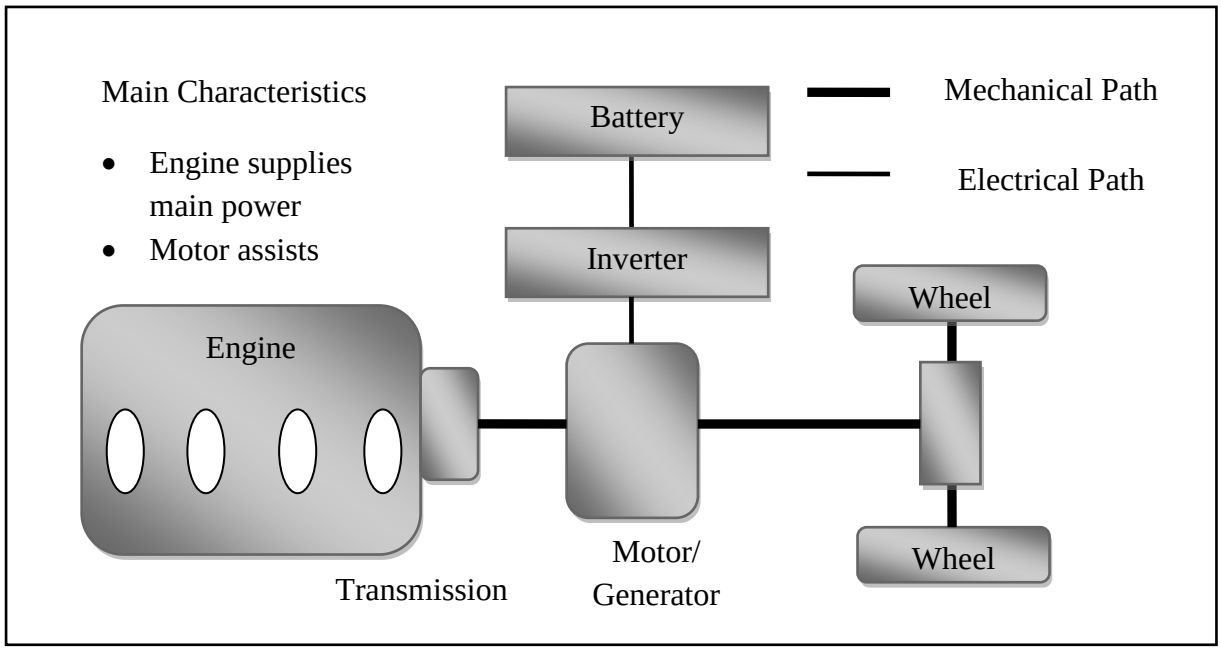

Figure 3-2. Parallel hybrid system [72]

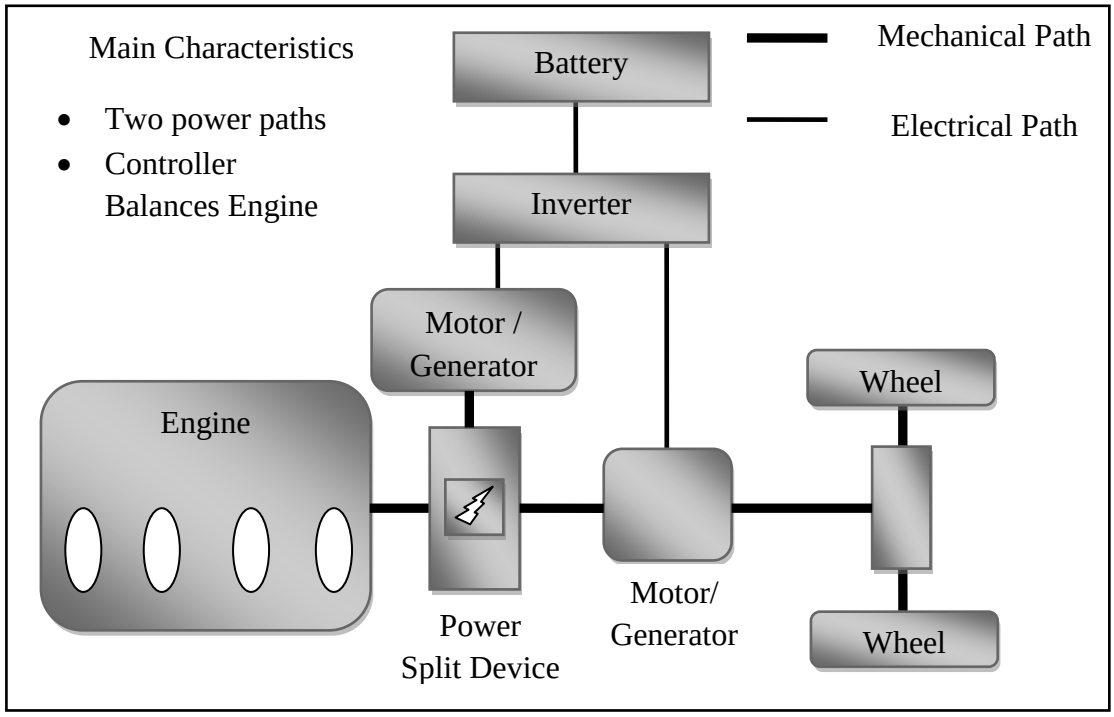

Figure 3-3. Toyota hybrid system [72]

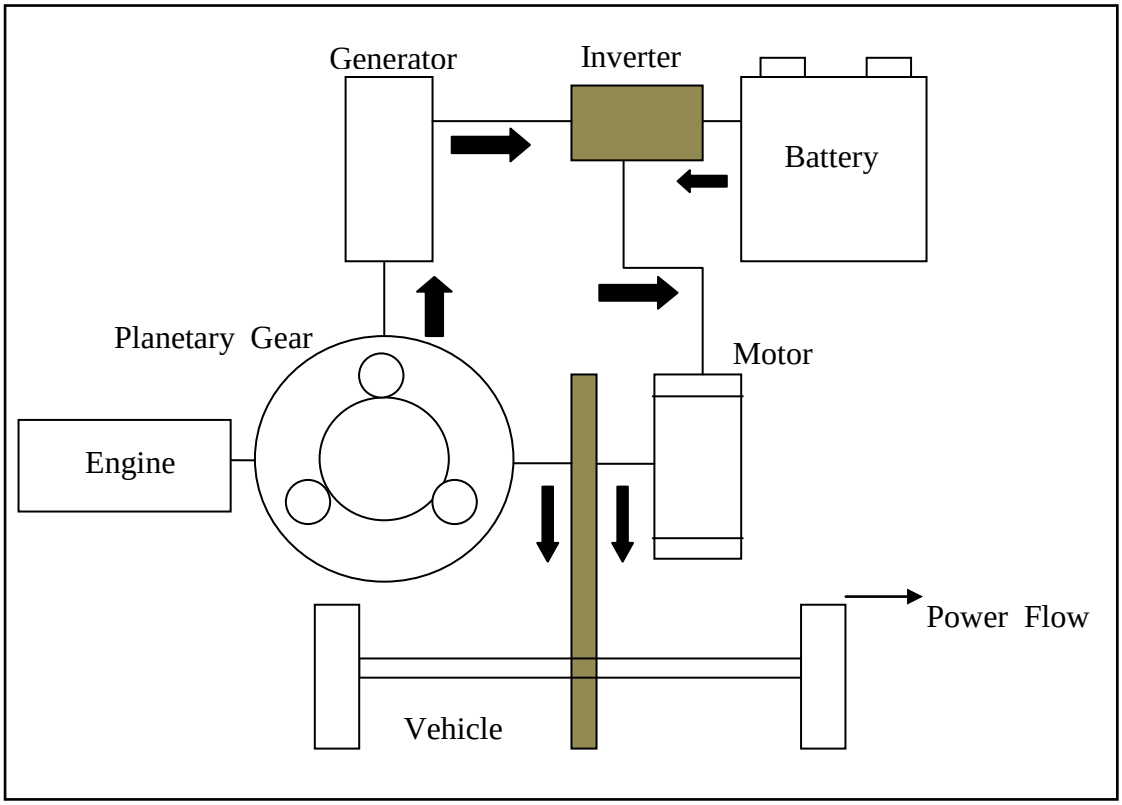

Figure 3-4. Power train configuration of the Toyota hybrid system [73]

Figure 3-5 shows the power source connection of a Toyota Hybrid System. The planetary gear has three nodes, the sun gear, the carrier gear, and the ring gear, which are connected to the generator, engine and vehicle, respectively as shown in Figure 3-6. In addition, an electric motor is also attached to the ring gear, which enables direct motor propulsion and efficient regenerative braking. The power generated by the engine is transferred to the vehicle through two paths: a mechanical path and an electrical path. The mechanical path consists of power transfer from the carrier gear directly to the ring gear, which is connected to the final drive of the vehicle. Part of the engine power transfers through the sun gear, which is then transformed to the electrical form through the generator. This power is then either pumped into the battery, or to the electric motor. The engine power going through the electrical path is less efficient than the mechanical path from an instantaneous viewpoint. However, the energy stored in the battery may be used later in a more efficient manner, which helps to improve the overall vehicle fuel economy [73].
Figure 3-7 shows the planetary gear system in the Toyota Hybrid System.

Figure 3-5. Power Source Connection of a Toyota Hybrid System [74]

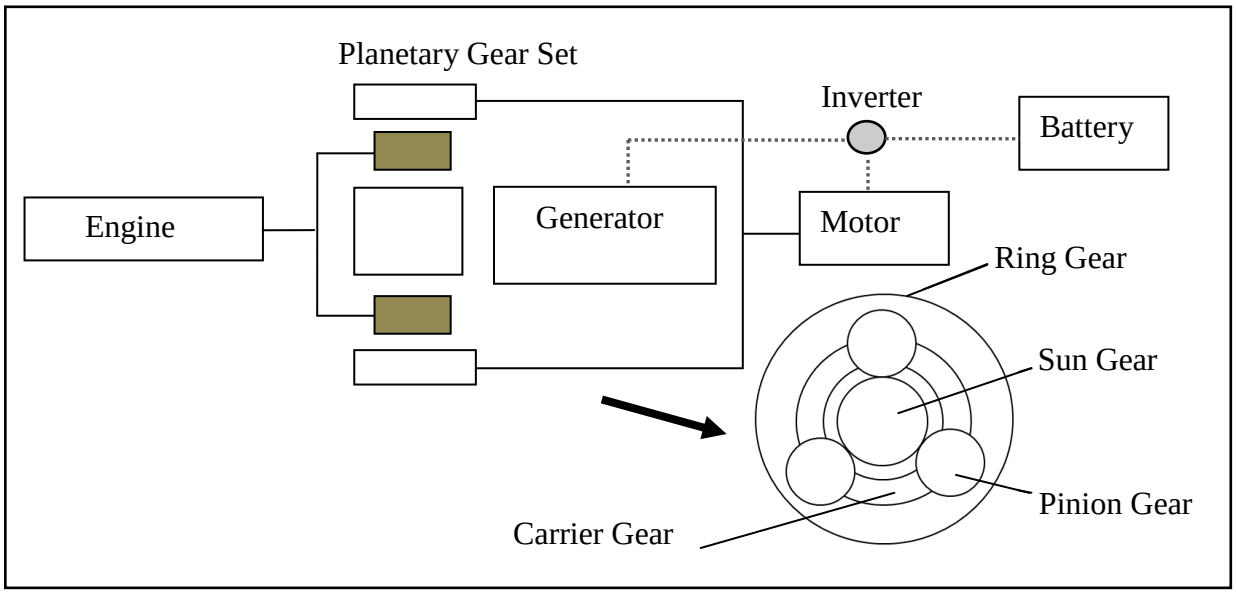

Figure 3-6. Power split (parallel / series) [73]

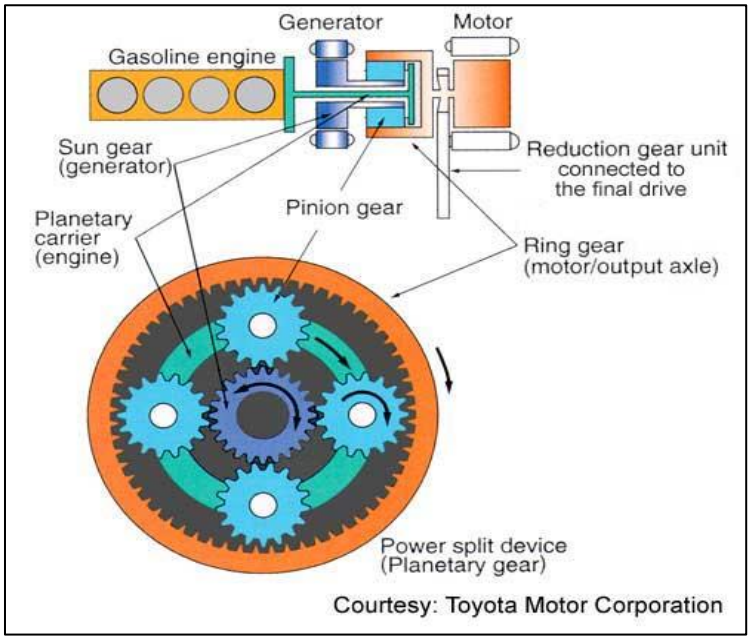

Figure 3-7. Power split (parallel / series) [72]

3.2 Toyota Prius MY-04 Vehicle Model

There are several hybrid vehicles currently on the market, and this is a sector that is set to grow rapidly in the years ahead. The Toyota Prius is the vehicle which really brought hybrid vehicles to public attention. It has enjoyed considerable sales success, and within two years of its launch in 1998 it has more than doubled the number of electric vehicles on the roads of Japan [75]. Honda also brought out its parallel hybrid Insight model in 1998, which has somewhat better fuel economy and lower emissions. However, it is only a two-seater, the luggage space is much more limited, and its market impact has not been so great. Although Toyota Prius has more fuel consumption figures, it has more luggage space than Honda hybrid Insight and five seats.

The 2004 Toyota Prius is a hybrid automobile equipped with a 1.5 litre gasoline engine, a nickel metal hydride battery and 33 kW electric motor powered by a generator. Both of these motive-power sources are capable of providing mechanical-drive power for the vehicle. The car is powered by a 16 valve four cylinder engine, which uses variable valve timing. The engine displacement is 1.5 litre with a bore of 75 mm and stroke of 84.7 mm. The engine also incorporates an aluminum double over head cam and a multi-point electronic fuel injection. This system allows the engine to maintain a high level of efficiency, so that controlled quantities of fuel are used on each combustion cycle [50]. The engine can deliver a peak-power output of 57 kilowatts (kW) at 5000 revolutions per minute (rpm) while the motor can deliver a peak-power output of 33 kW over the speed range of 1200–1540 rpm. Together, this engine-motor combination has a specified peak-power output of 82 kW at a vehicle speed of 85 kilometers per hour (km/h). In operation, the 2004 Prius exhibits superior fuel economy compared to conventionally powered automobiles [12]. The vehicle uses an electronic ignition system, which incorporates the Toyota direct ignition system. The performance details of Toyota Prius MY-04 are given in Table 3-1.

The Prius uses the gasoline engine and electric motor either in combination or separately to produce the most fuel-efficient performance. At start up or at low speeds, the Prius is powered solely by the electric motor, avoiding the use of the ICE when it is at its most polluting and least efficient operating conditions. This car uses regenerative braking and has a high overall fuel

economy of about 56.5 miles per US gallon (68 miles per UK gallon) [12]. The Prius has a top speed of 160 km/h (100 mph) and accelerates to 100 km/h (62 mph) in 13.4 seconds [12]. The Prius battery is only charged from the engine and does not use an external socket. Therefore, it is refueled with petrol only in the conventional way. In addition, it seats four people in comfort, and the luggage space is almost unaffected by the somewhat larger than normal battery. The fully automatic transmission system is a further attraction of this car that has put electric cars well into the realm of the possible for ordinary people making the variety of journeys they expect their cars to cope with [12].

Table 3-1. Performance details of the Toyota Prius MY-04 [2]

ICE size	1.5 litre, 4 cylinder, 16 valve
ICE Power	52.2kw at 4200 rpm
ICE Torque	111 N.m at 4200 rpm
Electrical motor power	33 kW
Electric Motor Torque	350 Nm at 0-400 rpm
Electrical Energy storage	NiMH battery, 288 V, 6.5 Ah
Hybrid system net power	73 kW
Fuel consumption	22/19km./L city/highway (EPA estimates)
Transmission	ECCVT (Electronically Controlled Continuously Variable Transmission)
Suspension	Independent MacPherson strut stabiliser bar and torsion beam with stabilizer bar
Steering	Rack and pinion with electro-hydraulic assist
Brakes	Front disc, rear drum, with ABS
Length	4.31 m
Width	1.69 m
Height	1.46 m
Wheelbase	2.55 m
Weight	1254 kg
Gasoline tank capacity	44.71, 11.8 US gallons
Tyres	P175/65R14 low rolling resistance

The Toyota Prius mainly has the characteristic of a parallel hybrid, in that the ICE can directly power the vehicle. However, it does have a separate motor and generator that can operate in series mode, and is not a ‘pure’ parallel hybrid. It has a fairly complex ‘power splitter’ gearbox, based on epicyclic gears that allow power from both the electric motor and the ICE, in almost any proportion, to be sent to the wheels or gearbox. Power can also be sent from the wheels to

the generator for regenerative braking. Regenerative Braking is a system where the motor acts a generator, braking the vehicle and converting the kinetic energy of the vehicle to electrical energy. It recovers about 20% of the energy, which is returned to battery storage, from where it can be reused.

Toyota Prius MY-2004 has two electrical machines, an electric motor and a generator. The motor type is a permanent magnet. This motor is able to sustain a maximum torque of 350 Nm at 0-400 rpm, which is enough to move the car at slow speeds [12]. The battery used in Toyota Prius MY-04 is a nickel-metal hydride (Ni-MH) battery, consisting of 228 cells, giving 6.5 Ah at 228 V [12]. The transmission system is an electronically controlled variable transmission, which give a better performance over the range of gears. The transmission incorporates a fairly complex system of planetary gears, called a power splitter, which directs power between the ICE, the electric motor, the generator and the wheels, in all directions. A display on the dashboard continuously indicates where the energy is going. For example, when accelerating, energy goes from both the ICE and the electric motor to the wheels; at easy steady speeds, energy goes from only the engine to the wheels and from the engine through the generator back to the battery; and when slowing, energy goes from the wheels through the generator to the battery. This display is fascinating, indeed perhaps a little too interesting to watch. The suspension uses an independent MacPherson strut with stabilizer bar at the front of the vehicle and a torsion beam with stabilizer bar at the rear. The steering column uses a rack and pinion system with electro-hydraulic power-assist and is able to achieve a turning cycle of 30.8 ft [2]. Power-assisted ventilated front discs and rear drums with standard anti-lock brake system and regenerative braking enable the vehicle to stop in a manner, which prevents skidding even when braking heavily into a corner. Traction is provided by standard P175/65R14 low rolling resistance tires on aluminum alloy wheels [2]. The car fits four people, and has a good-sized luggage space not noticeably reduced in size because of the battery, which is stored under the rear passenger seat.

3.3 Modeling and Simulation of PHEV20 using PSAT^{TM}

Toyota Prius MY-04, having an advanced powertrain configurations, is modeled by Powertrain System Analysis Toolkit software developed by the Argonne National Laboratory sponsored by the U.S. Department of Energy under the direction of Ford, General Motors, and Daimler Chrysler [40]. PSAT^{TM} is a forward-looking vehicle simulator, which models the driver as a control system that attempts to follow a target driving cycle of defined vehicle speed at every step by actuating the accelerator and brake pedals. This forward-looking model simulates vehicle fuel economy, emissions, and performance in a realistic manner, taking into account transient behavior and control system characteristics. PSAT^{TM} is a state-of-the-art flexible and reusable simulation package and can simulate an unrivaled number of predefined configurations (conventional, electric, fuel cell, series hybrid, parallel hybrid, and power split hybrid). PSAT^{TM} was designed to be a single tool that can be used to meet the requirements of automotive engineering throughout the development process, from modeling to control. It is written in MATLAB, Simulink, and StateFlow to ensure modularity and flexibility. It has a user-friendly graphical user interface written in C^{++} and provides complete Simulink models. PSAT^{TM} can be used in powertrain development to optimize a vehicle and its components with regards to the fuel consumption for any driving cycle, vehicle performance, including acceleration and grade, component sizing and transmission ratios [76]. For the PHEV modeling and simulations in our study, we used the Toyota Prius MY-04 as a baseline vehicle platform for the energy storage, motor, engine and powertrain configuration in PSAT^{TM} . Additional battery capacity was added to the drivetrain configuration in order to achieve 20 miles of all electric range; simultaneously electric motor and engine were scaled to achieve 0-60 mph within the required acceleration time specification of 10.5 +0.0/-0.5 seconds, which is approximately the acceleration performance of Toyota Prius. The PSAT^{TM} split hybrid control strategy was modified for the maximum engine efficiency so that the vehicle operates as an electric vehicle in CD-mode without engaging the engine until the battery reaches 35% of SOC, after which time the vehicle switches to CS-mode and operates like a pure Toyota Prius hybrid vehicle. PSAT^{TM} is used to model the performance of PHEV20, 20 miles of all electric range for different combinations of battery, motor and engine types for two different drive cycles: US-EPA UDDS and Winnipeg Weekday drive cycles.

3.3.1 Vehicle Modeling

Below explains the drivetrain configuration and components with split hybrid control strategy used for modeling the performance of Toyota Prius MY-04 PHEV20 vehicle model on PSAT ^{TM} for two different drive cycles, US-EPA UDDS and Winnipeg weekday drive cycle.

3.3.1.1 Drivetrain Configuration

The drivetrain configuration of Toyota Prius MY-04 PHEV20 is a link of the ICE, electric motor, transmission, wheels and axles, and battery pack. Each component has several drivetrain parameters and possible designs. Figure 3-8 shows the drivetrain configuration of split compact Toyota Prius MY-04 PHEV20 vehicle model in PSAT^{TM} .

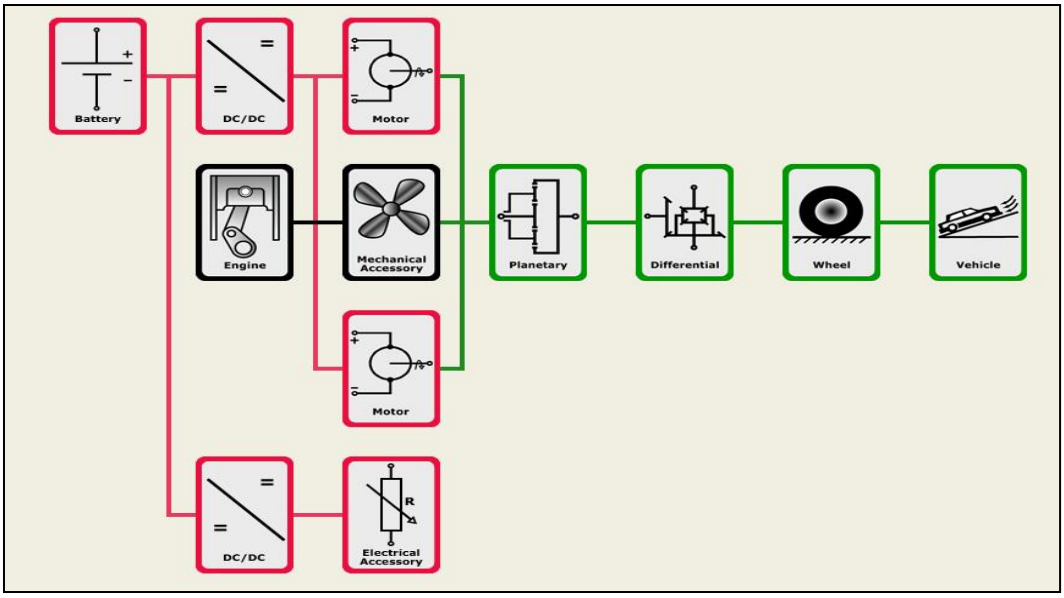

Figure 3-8. Split compact Toyota Prius MY-04 PHEV20 vehicle model in PSAT [40]

3.3.1.2 Drivetrain Components

The list of drivetrain components selected for modeling of Toyota Prius MY-04 PHEV20 vehicle include:

Driver: The driver is used to model the accelerator and brake pedals. The desired vehicle speed is compared with the current speed and a PI (Proportional-Integral) controller is used to request more or less torque to the vehicle. The control strategy maximizes the engine efficiency so that the vehicle operates as an electric vehicle in CD-mode until the battery reaches 35% of SOC, after which time the vehicle switches to CS-mode.

Motor: The electric motor transforms electrical power into mechanical power by creating a magnetic field that applies a force on current-carrying conductors. Motors that operate on this principle can be divided into two main categories: DC and AC motors. DC motors can be further divided into motors with and without brushes, whereas AC motors can be divided into two main categories: sychronous and asychronous. Figure 3-9 shows the permanent magnet and induction type electric motors.

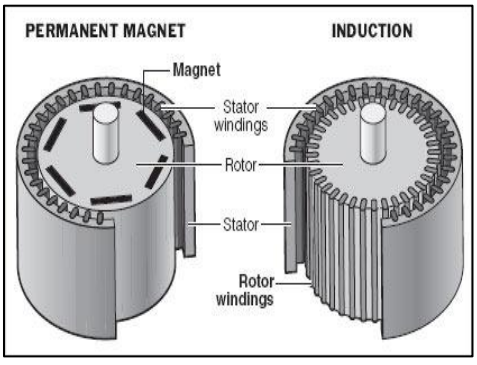

Figure 3-9. Permanent magnet and induction type electric motor [77]

14 different types of permanent magnet electric AC motors with different makes and parameters were considered for modeling and simulation of Toyota Prius MY-04 PHEV20. Various parameters of the electric motors considered for simulation are shown in Table 3-2. Figure 3-10 shows the picture of a permanent magnet electric type motor.

Table 3-2. Permanent electric motor parameters

Electric Motor Parameters	Units
motor mass	kg
minimum voltage for the motor	volts
motor inertia	kg-m
motor controller mass	kg
base speed of the motor	radian/second
max. current of the motor	ampere
max. speed of the motor	radian/second
max. torque of the motor	Newton-meter
max. power of the motor	kW

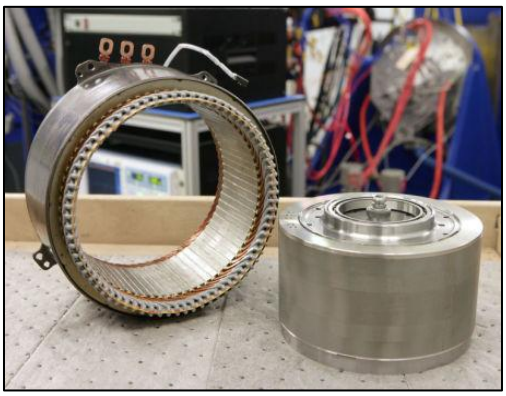

Figure 3-10. Permanent magnet electric motor [78]

Energy Storage: Several kinds of energy storage devices have been considered for hybrid vehicle applications. The primary candidates have been batteries, ultracapacitors, flywheels, and accumulators [56]. Batteries store energy electrochemically in the electron bonds between molecules, ultracapacitors store energy in the electrical field between oppositely charged surfaces, flywheels store energy in the angular momentum of a spinning mass, and accumulators store energy as the pressure of a compressed inert gas. Batteries are composed of arrays of electrically connected cells, within which an electrochemical process occurs that stores or discharges energy. A battery cell consists of three elements: the anode, cathode, and electrolyte. When the cell is connected to an external circuit, electrons disassociate from the anode and travel through the external circuit to the cathode, where they recombine with ions that have migrated through the electrolyte. Depending on the composition of the anode, cathode, and electrolyte, this process can be reversed and the battery recharged. The voltage at which this reaction takes

place also depends on the chemistry; voltage can range from 1.2 to 4 V. Cells are connected in series to produce the desired battery voltage. In a typical 12-V car battery, the anode is lead, the cathode is lead dioxide (PbO_2), and the electrolyte is sulfuric acid (H_2SO_4). The reaction in a cell occurs at 2 V.

A lot of stored energy is lost as thermal energy in the brake pads of the vehicle when the vehicle is stopped. The overall efficiency of the vehicle could be improved if this energy is recovered as regenerative braking energy and stored in the energy storage device. Accordingly, the energy storage devices should have four important characteristics: (i) Specific energy (joule/kilogram): larger specific energy means that the device can store more energy during regenerative braking. It can also be the main source of propulsion for longer periods of time; (ii) Specific power (watt/kilogram): larger specific power means that the device can absorb more regenerative braking power. Specific power also affects the amount of assistance required during acceleration and subsequently more specific power can help to reduce the engine size; (iii) Operating temperature: the energy storage device must be able to operate at low temperatures and, in the case of batteries, be able to turn the engine or fuel cell on, and (iv) Cycle life: because of the frequent acceleration and braking cycles over the lifetime of a vehicle, the energy storage device must have a high cycle life. Batteries tend to have high specific energy but low specific power. The inverse is true for ultracapacitors, which have low specific energy but high specific power.

20 different types of batteries with different makes and parameters were considered for the modeling and performance simulation of Toyota Prius MY-04 PHEV20 vehicle. These included one lithium-ion battery, one nickel cadmium battery, nine nickel metal hydride batteries, one nickel zinc battery, and nine lead acid batteries. Figure 3-11 shows the picture of a nickel metal hydride battery type. Various parameters of the batteries considered for simulation are shown in Table 3-3.

Table 3-3. Battery parameters

Battery Parameters	Units
number of modules	
number of cells in a module	
cell mass	kg
module mass	kg
battery mass	kg
cell capacity	Ah
nominal cell voltage	volts
battery capacity	kWh
cell internal resistance	ohm
state of charge of the battery	%
cell specific energy	Wh/kg
cell power density	W/kg

Figure 3-11. Nickel metal hydride battery [79]

Engine: Engines convert fuel and air through an exothermic chemical reaction, which is accompanied by the release of heat and work. The three main types of engines are reciprocating four-stroke, reciprocating two-stroke, and rotary. There are two major categories of four-stroke engines: Spark ignition and Compression ignition. In spark ignition engines, the air and fuel mixture create a homogeneous charge, which is ignited by a spark created by a large voltage at the tip of a spark plug during the combustion stroke. The timing of the ignition is controlled by

the timing of the spark. Power is controlled by controlling the engine fuel intake flow rate by using the throttle plate.

16 different types of spark ignition gasoline engines with different makes and parameters were considered for modeling and simulation of Toyota Prius MY-04 PHEV20 vehicle for this research. Figure 3-12 shows the picture of a Toyota hybrid gasoline engine. Various parameters of the gasoline engine type considered for simulation are shown in Table 3-4.

Table 3-4. Spark ignition gasoline engine parameters

Spark Ignition Gasoline Engine Parameters	Units
number of cylinders in the engine	4
mass of the engine	kg
engine idle speed	radian/second
output torque from the engine	newton-meter
max. output power of the engine	kW
engine speed	radian/second
engine fuel mass flow rate	kg/second
engine block temperature	celsius
exhaust gas temperature	celsius
engine displacement	liter
diameter of cylinder bore	meter
stroke of the cylinder	meter
engine compression ratio	
engine inertia	kg-m

Figure 3-12. Toyota hybrid gasoline engine [80]

Mechanical Accessory: The mechanical accessories in the model represent all of the belt-driven loads on the engine, except for the alternator, which is treated separately. The mechanical accessories considered in the model include the cooling fan, water pump, oil pump, and the air conditioner compressor.

Electrical Accessory: Electrical accessories, such as lamps, radiator fans, or wipers that obtain their energy from an electrical source are modeled as electrical accessories in the model.

Power converter for Electrical Accessory: The power convertor converts one form of electrical power, from the energy storage device, to another desired form and voltage for powering the electrical accessories. The V2V Constant efficiency power converter with 95% efficiency and 12V output voltage was considered in the analysis of PHEV20 model.

Gearbox: A gearbox serves the following purposes in the vehicle system: (i) produces a larger torque than the engine brake torque at the wheels of the vehicle, (ii) allows the engine to be disconnected from the drivetrain, and (iii) gives the vehicle better drivability over a greater speed range. The MY99 and MY01 Prius planetary gear sets with 30 teeth and 78 ring gears were considered in the analysis of PHEV20 model.

Final Drive Gears: Final drive gears are incorporated in the vehicle driving axles and transaxles to provide a right-angled drive from either the propeller shaft or the gearbox layshaft (this shaft, which is normally fixed to the gearbox casing, supports the various-sized driving pinions of the layshaft gear cluster) to the driven wheels. These provide a parallel drive from the gearbox layshaft to the driven wheels and to permit an additional and constant gear reduction in the transmission system. We have considered in our PHEV20 model the MY04 US Prius final drive with ratio 4.113

Wheel Axle: This wheel model includes braking losses and accounts for the braking force at each wheel and the added inertia to the drivetrain of all four wheels. We have considered in our PHEV20 model the P175/65 R14 type wheel axle used for MY04 Prius.

Vehicle: Toyota Prius MY04 vehicle is considered as PHEV20 model with body mass of 824 kg and axle base of 2.7432 meters. The various parameters of the vehicle considered for modeling and simulation are shown in the Table 3-5.

Table 3-5. Vehicle parameters

Vehicle Parameters	Value/Units
vehicle body mass	824 kg
width of the vehicle	meter
frontal area of the vehicle	meter^2
length of the vehicle	meter
height of the vehicle	meter
distance between two front axles	2.74 meter
mass of the vehicle cargo	136 kg
vehicle cg height	0.51 meter
Total vehicle mass	1630.62 kg

3.3.2 Simulation Set-Up

For testing the performance of the vehicles, it is driven in reality and a simulated driving cycle is created by developing a profile of changing speeds overtime. These test cycles correspond to realistic driving patterns in different conditions. During these tests, the vehicle speed is almost constantly changing, which makes the performance of all other parts of the system highly

variable and thereby makes the simulation computations very complex. These driving cycles (or schedules) were primarily developed to provide a realistic and practical test for measuring the emissions from the vehicle. One of the most well-known drive cycles, based on actual traffic flows in Los Angeles CA known as the United States Environmental Protection Agency Urban dynamometer driving schedule/LA-4 cycle, was used in this study [43]. We used another drive cycle known as Winnipeg weekday drive cycle based on the city driving conditions that was developed to check the performance of the hybrid vehicles on Canadian roads.

3.3.2.1 US Environment Protection Agency (EPA)-UDDS Drive Cycle

The US EPA urban dynamometer driving schedule is commonly called the LA-4 or the city test drive cycle and represents city driving conditions. It is used for light duty vehicle testing. The UDDS cycle was primarily generated to estimate vehicle emissions inventories and is affected by the restrictions of dynamometer validation tests including limited duration and acceleration/deceleration rates [81]. Table 3-6 shows the simulation statistics of US EPS UDDS drive cycle. Figure 3-13 shows the vehicle drive cycle profile between vehicle speed (meter/second) and test time (seconds).

Table 3-6. Simulations statistics of US EPA-urban dynamometer driving schedule [81]

Simulation parameters	Units	Simulation Parameters
Cycle time	sec	1369
Distance	miles	7.4504
Maximum speed	mph	56.70
Average speed	mph	19.5777
Standard deviation speed	mph	14.6959
Maximum acceleration	m/s^2	1.4752
Average acceleration	m/s^2	0.50456
Standard deviation acceleration	m/s^2	0.45096
Maximum deceleration	m/s^2	- 1.4752
Average deceleration	m/s^2	- 0.57786
Standard deviation deceleration	m/s^2	0.51905
Number of stops		17
Stop frequency	stop/mile	0.00141782
Stop duration	sec	259
Stop percent of cycle	%	18.918919

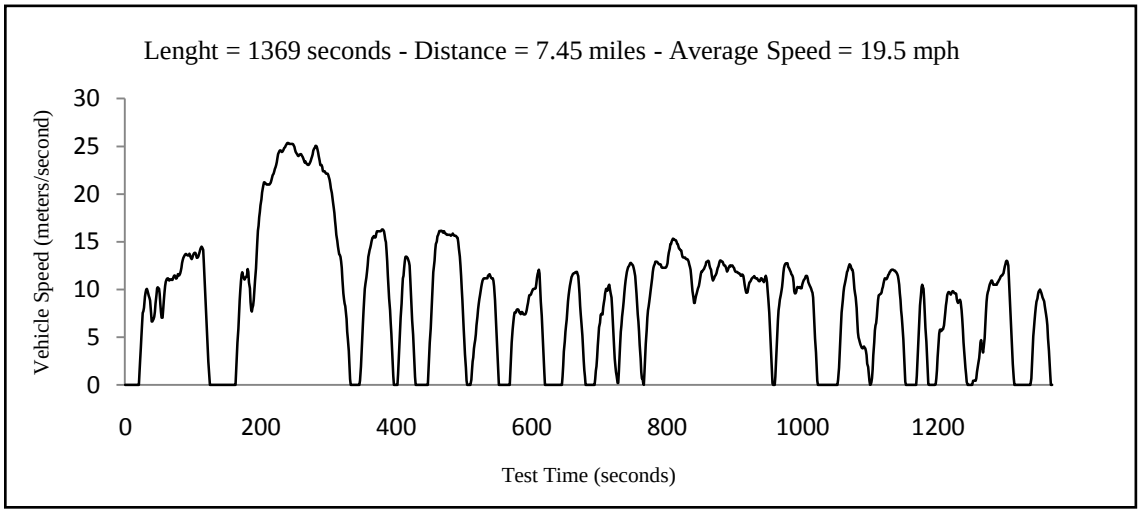

Figure 3-13. US EPA - urban dynamometer driving schedule [81]

3.3.2.2 Winnipeg Weekday Drive Cycle

The standard UDDS has been primarily developed to estimate vehicle emissions inventories and is affected by the restrictions of dynamometer validation tests including limited duration and acceleration/deceleration rates [81]. UDDS also does not provide information on parking times as opportunities for charging in case of PHEVs. The UDDS, therefore, cannot completely emulate the real-world daily power demand of a vehicle. Researchers working under the AUTO21 project at the University of Manitoba conducted an extensive literature survey and did not find any major reference on the construction of a daily vehicle usage profile for PHEVs [82]. A few studies have, however, assessed the performance of HEVs in real-world operation. For example, data collected for a fleet in the St. Louis metropolitan area was used in the simulation of energy usage in HEVs; however no single driving pattern was extracted from the collected data . Fuzzy logic pattern recognition techniques have also been used to perform driving and duty cycle analyses on data collected for a fleet of HEVs [82]. Another effort to modify standard cycles for better representing real world behavior defined a driver model in simulations using European standard cycle [82]. Driving cycle generation has also been reported based on the assumption of constant acceleration and deceleration rates and with consideration of the speed limits for road segment in representative areas [82].

Tare et al. (2010) constructed a single driving profile representing the average behavior of the fleet of 74 cars in the city of Winnipeg [82]. They used GPS-based data loggers to record one-month second-by-second time-stamped speed and location of the participant cars. Winnipeg is having a population of 0.7 million and can be regarded as a representative city of the majority of North American cities, since most of the cities, excepting a few cosmopolitan cities, in North America are having a population of less than one million people [82]. The data for constructing the daily driving profiles were collected in the month of June to avoid extreme climatic conditions and to represent general driving behavior [82]. They identified two daily driving cycles (one representing weekdays and the other weekends) among the available recorded cycles that most closely represent the average behavior of the fleet in terms of a set of characterizing parameters [82]. In addition to the parameters describing kinematics of the cycle, they also used average power demand and average breaking power to establish a more comprehensive set of performance measures for power management in hybrid vehicles. The procedure used for constructing the Winnipeg daily driving profile by Tara et al. (2010) is described next [82]. They recorded 13565driving cycles and divided these into two groups of weekday and weekend cycles. Average values of the characterizing parameters for the two groups were then calculated. Table 3-7 shows a list of the characterizing parameters (x_i) and their average values ($\bar{x}_i$) for both the weekday and weekend cycles. Characteristic parameters of each individual cycle (in both groups) were then measured against their corresponding average values and a figure of merit was calculated and assigned to the individual cycle as follows in equation 3-1.

$$\sigma = \left(\sum_{i=1}^{N} \left(\frac{x_i - \bar{x}_i}{\bar{x}_i} \right)^2 / N \right)^{1/2} \qquad \textbf{Equation 3-1}$$

where σ is the figure of merit, and N is the number of characterizing parameters (17 in this case, as listed in Table 3-7). They further defined the *candidate cycles* as cycles that have the closest set of characterizing parameters to the average values in the weekday and weekend groups [82]. The two candidate cycles did not uniformly match all the average values. The quality of candidate cycles was further enhanced using snippets of other cycles available in the data base. Snippets of driving periods bounded by two consecutive stops, also referred to as micro-trips, were extracted and classified into three traffic groups, namely congested, urban and highway. The average speeds and acceleration ranges were then used to classify micro-trips into the three

categories, as shown in Table 3-8. The micro-trips of candidate cycles were exchanged with micro-trips of the same traffic group in the data base until the best figures of merit (σ) for the candidate cycle are obtained. The average values for the enhanced candidate cycles are reported in Table 3-7.

Table 3-7. Characterizing parameters and their values [82]

	Parameter	900 Daily Driving Cycles		Enhanced Representing Cycles	
		Weekday	Weekend	Weekday	Weekend
1	Average speed of the entire driving cycle in km/h	30.9	37.2	33.0	34.8
2	Average running speed in km/h	37.7	49.8	38.9	43.1
3	Total daily distance traveled in km	35.7	37.0	37.3	38.9
4	Average acceleration of all acceleration phases in m/s^2	0.56	0.53	0.48	0.63
5	Average deceleration of all deceleration phases in m/s^2	-0.57	-0.54	-0.52	-0.63
6	Average number of change in acceleration rate (+/-) in one driving period	17	11	15	9
7	Average daily power demand in kW	6.4	7.5	5.5	8.9
8	Maximum power demand in kW	33.8	57.8	28.4	52.2
9	Total daily energy demand in Mj	13.3	19.7	13.7	18.8
10	Average daily breaking power in kW	-5.6	-6.5	-5.1	-7.5
11	Root mean square of acceleration in m/s^2	0.71	0.70	0.61	0.80
12	Average length of a driving period in km	0.44	0.90	0.48	0.97
13	Time percentage of Idling (zero velocity) in %	17.2	19.9	15.0	18.0
14	Time percentage of acceleration: acceleration>$0.1m/s^2$ in %	28.8	27.5	30.9	29.1
15	Time percentage of Cruising (acceleration [-$0.1,0.1$] m/s^2, speed>5m/s) in %	10.2	13.1	9.1	10.7
16	Time percentage of deceleration: acceleration <-$0.1m/s^2$ %	28.0	26.5	29.1	29.0
17	Time percentage of creeping (acceleration [-$0.1,0.1$] m/s^2, speed<5m/s) in %	16.0	13.0	15.9	13.2

Table 3-8. Micro-trip characteristics [82]

Traffic category	Average speed	Acceleration
Congested	Low: < 5 km/h	Mild: [-0.1,0.1] m/s^2
Urban	Moderate: [5,40] km/h	Harsh: [-3.0,3.0] m/s^2
Highway	High: > 40 km/h	Moderate: [-1.0,1.0] m/s^2

Speed-acceleration frequency distribution (SAFD) plots, which provide information about the time proportions of individual driving modes [82], were used by Tara et al. (2010) as an additional measure to demonstrate how well the final driving cycles match the collected data. A maximum 5% deviation from average daily energy demand for final driving cycles was allowed in the construction of the enhanced candidate cycles in order to ensure that the driving profiles constructed were not entirely random combinations of micro-trips. Figure 3-14 shows the enhanced weekday and weekend candidate driving cycles.

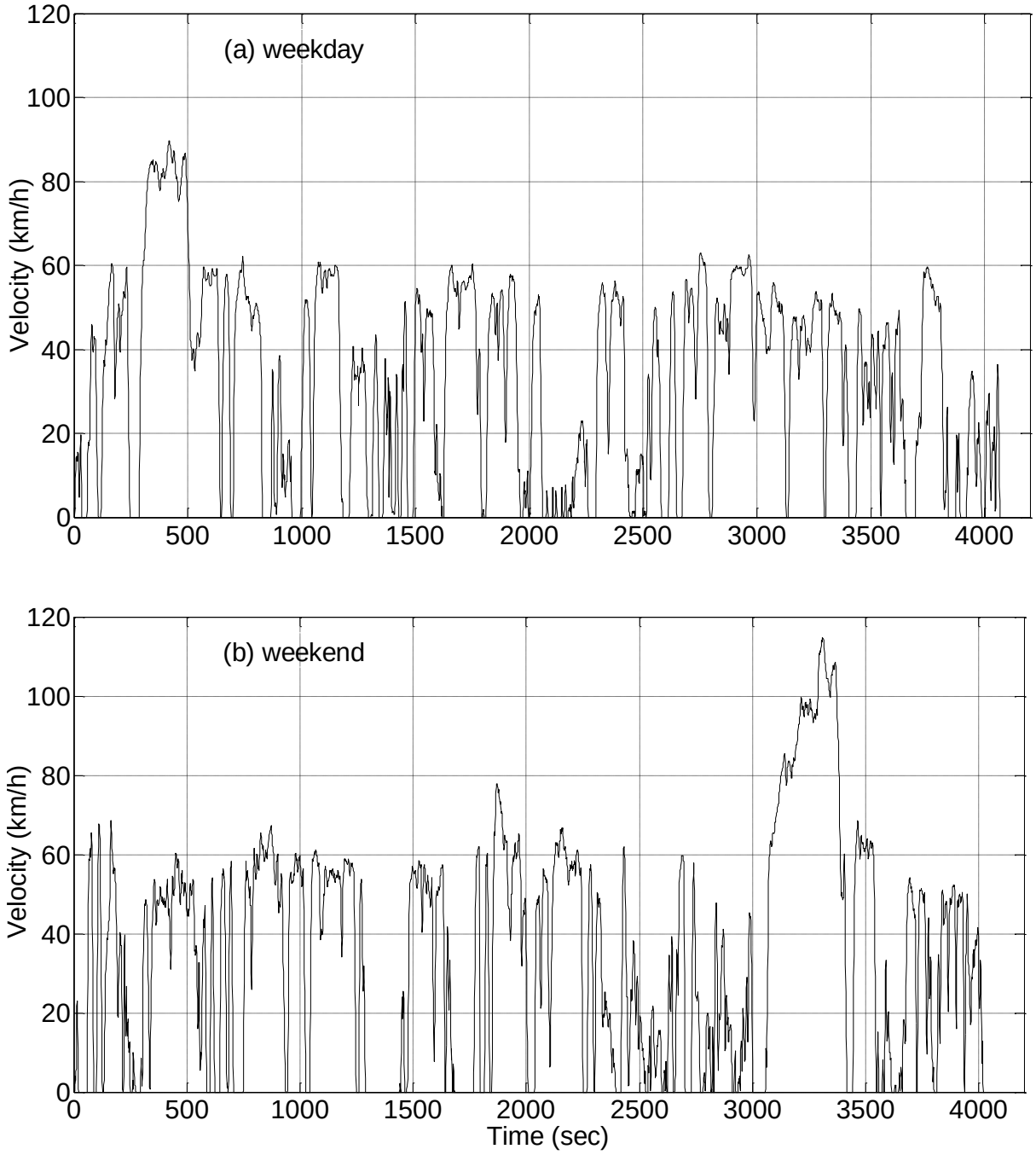

Figure 3-14. Enhanced candidate driving cycles: (a) weekday, (b) weekend [82]

Durations of the weekday and weekend cycles were found to be 4071 sec and 4023 sec, respectively. Maximum velocity in the weekend cycle was higher (114 km/hr) as compared to the weekday cycle (89.6 km/hr). The driving pattern in the weekend is slightly more aggressive

(about 20%) due to higher acceleration and deceleration rates, and higher power demand for weekends. Figure 3-15 (a) and (b) shows SAFD plot (Speed Acceleration Frequency Distribution plot) for weekday and weekend enhanced candidate driving cycles. Another difference between the two patterns is that there is about 50% higher probability of driving at moderate speeds (35-50 km/hr) in the weekday pattern as compared to the weekend pattern.

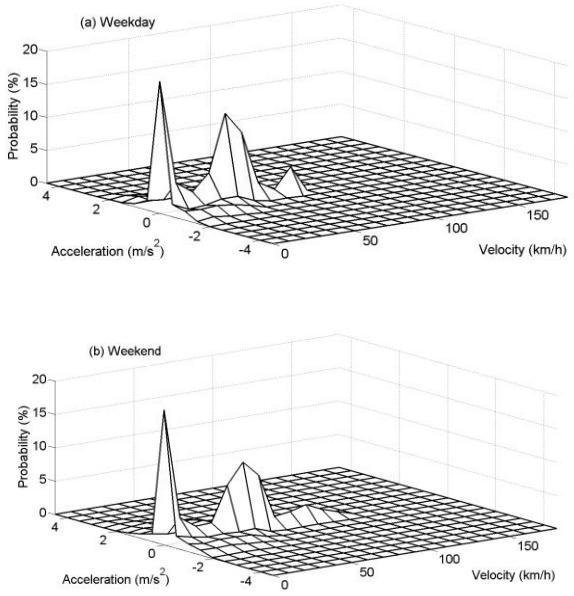

Figure 3-15. SAFD plots for the enhanced candidate driving cycles: (a) weekday, (b) weekend [82]

The probability of parking for less than three hours is plotted as a function of time for weekday and weekend drive cycles in Figure 3-16 (a) and (b) respectively. Short-duration parking most probably takes place between 12:00 PM to 6:00PM in weekdays and between 12:00 PM to 4:00PM in weekends. Tara et al. (2010) further assumed that the driver is not reluctant to plug-in during weekends and is equally charge conscious throughout the weekdays [82]. Based on the information obtained about parking times and duration of parking events, several short and long parking events as well as overnight parking periods were included in the driving cycles.

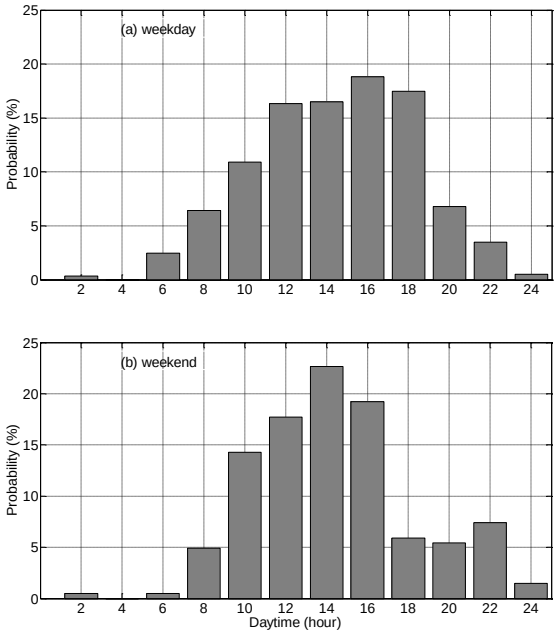

Figure 3-16. Probability of short duration parking (less than 3 hours) for opportunity charging scenarios: (a) weekday, (b) weekend [82]

Table 3-9 shows the simulation statistics of Winnipeg Weekday drive cycle. Figure 3-17 shows the vehicle drive cycle profile between vehicle speed (meter/second) and test time (seconds).

Table 3-9. Simulations statistics of Winnipeg weekday drive cycle[82]

Simulation parameters	Units	Simulation Parameters
Cycle time	sec	3386
Distance	miles	19.61
Maximum speed	mph	61.91
Average speed	mph	20.86
Standard deviation speed	mph	16.91
Maximum acceleration	m/s^2	2.78
Average acceleration	m/s^2	0.55
Standard deviation acceleration	m/s^2	0.50
Maximum deceleration	m/s^2	- 6.48
Average deceleration	m/s^2	- 0.59
Standard deviation deceleration	m/s^2	0.57
Number of stops		33
Stop frequency	stop/mile	0.001
Stop duration	sec	595
Stop percent of cycle	%	17.57

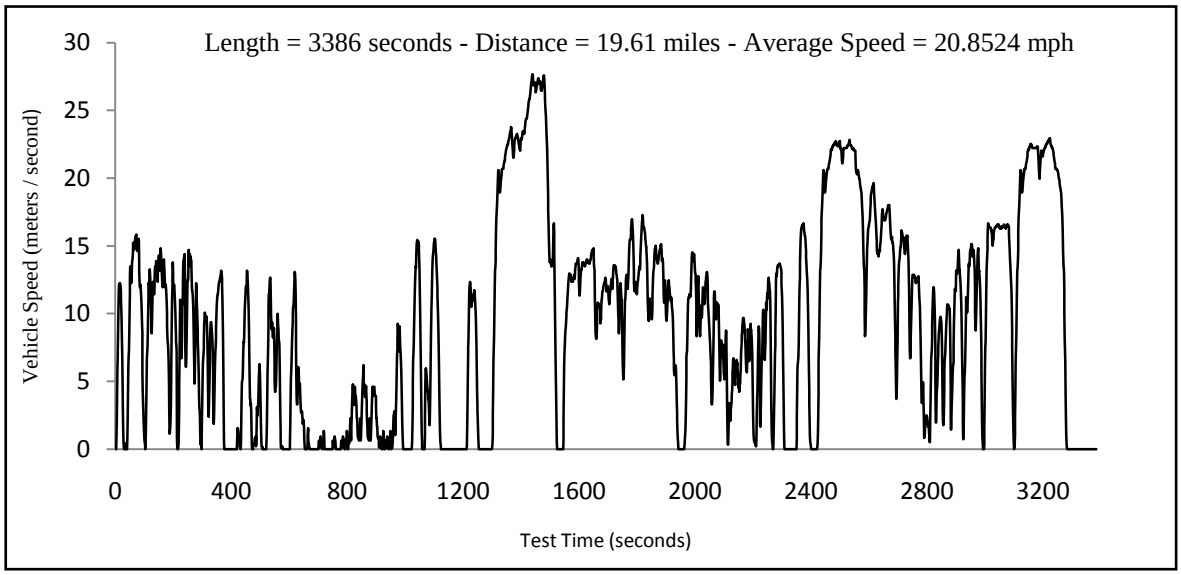

Figure 3-17. Winnipeg weekend drive cycle [82]

3.3.3 Simulation Run

Figure 3-18 shows the drivetrain simulation run screen in PSAT^{TM} . We used two drive cycles, 20 types of batteries, 14 types of electric motors, and 16 types of engines that are available in PSAT^{TM} having different design parameters for modeling the performance of Toyota Prius MY-04 PHEV20 vehicle. In US-EPA UDDS drive cycle, the sequence of the batteries, motors and engines was randomly ordered in the simulation hybridization loop. Whereas, in the Winnipeg weekday drive cycle, the sequence of batteries, motors and engines was ordered as per ascending order of battery cell specific energy, electric motor and gasoline engine desired maximum powers. Tables 3-10, 3-11 and 3-12 show the sequence of batteries, electric motors and gasoline engines orders, respectively in the US-EPA UDDS and Winnipeg drive cycle during simulation hybridization loop. The sequential ordering brings inherent relations between different choices of variables, while random ordering leads to complex relations between the input variables and the performances. Therefore, the ordering brings differences in the performance of optimization of the two drive cycles.

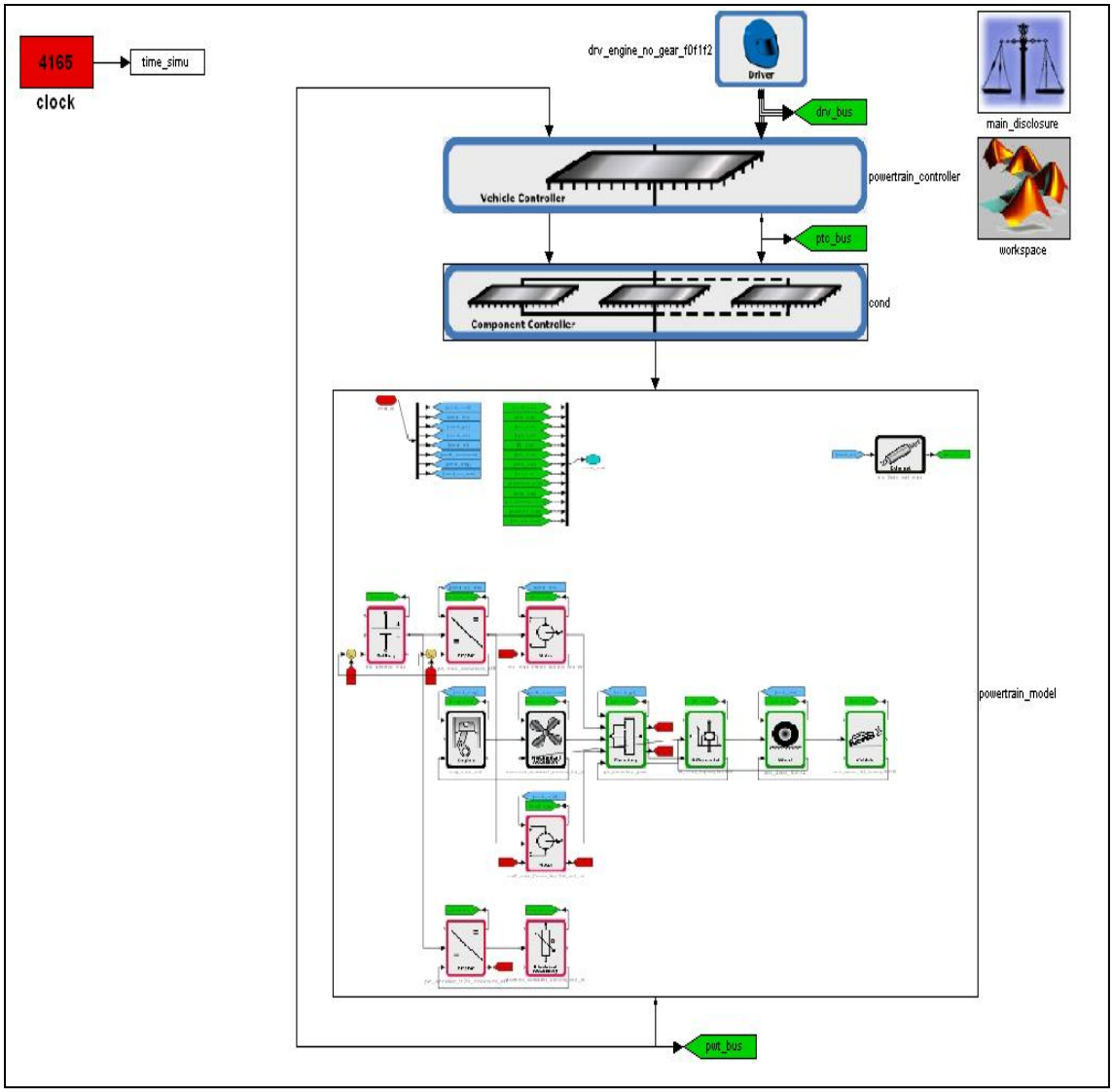

Figure 3-18. Drivetrain simulation run screen in PSAT [76]

Table 3-10. Sequence of ordering batteries in the US-EPA UDDS and Winnipeg drive cycle simulations

Battery No.	Battery Type	Cell specific energy (Wh/kg)	Battery Sequence Order No. for UDDS drive cycle	Battery Sequence Order No. for Winnipeg drive cycle
1	Lithium-ion Saft	66.96	1	16
2	NiCd	43.71	2	13
3	NiMH	9.48	3	2
4	NiMH Ovonic	56	4	15
5	NiMH Ovonic	77.14	5	19
6	NiMH Panasonic MY04 Prius	45.88	6	14
7	NiMH	31.3	7	7
8	NiMH Panasonic MY01 Prius	7.43	8	1
9	NiMH Ovonic	74.23	9	18
10	NiMH Ovonic	111.34	10	20
11	NiMH	68.47	11	17
12	NiZn Evercell	33.62	12	10
13	Lead Acid	41.6	13	12
14	Lead Acid	30.11	14	6
15	Lead Acid Hawker	31.46	15	8
16	Lead Acid	32.35	16	9
17	Lead Acid	27.28	17	3
18	Lead Acid Hawker	28.37	18	4
19	Lead Acid	28.43	19	5
20	Lead Acid	41.06	20	11

Table 3-11. Sequence of ordering electric motors in the US-EPA UDDS and Winnipeg drive cycle simulations

Motor No.	Motor Type (Permanent Magnet)	Desired max. motor power (kW)	Motor Sequence Order No. for UDDS drive cycle	Motor Sequence Order No. for Winnipeg drive cycle
1	Prius	52.35	1	8
2	Insight	10.0198	2	1
3	Prius	29.9645	3	4
4	Escape MG2	40.833	4	5
5	AuxilecThomson	44.4968	5	6
6	Escape MG1	62.82	6	10
7	Camry MG2	69.9748	7	11
8	UQM PowerPhase75	74.9652	8	12
9	Honda	48.9682	9	7
10	UQM PowerPhase100	101.492	10	13
11	Camry MG1	105.323	11	14
12	Prius	58.1085	12	9
13	Accord	15.3909	13	3
14	Prius	15.0768	14	2

Table 3-12. Sequence of ordering gasoline engines in the US-EPA UDDS and Winnipeg drive cycle simulations

Engine No.	Engine Type (Spark Ignition)	Desired max. engine power (kW)	Engine Sequence Order No. for UDDS drive cycle	Engine Sequence Order No. for Winnipeg drive cycle
1	US 04Prius	57	1	5
2	Emission	41.007	2	1
3	Insight	49.5743	3	3
4	Japan Prius	43	4	2
5	US 01Prius	52	5	4
6	Civic	85	6	6
7	Corolla	90	7	7
8	Corolla	99.54	8	9
9	Escape Hybrid	99	9	8
10	Taurus	115	10	10
11	Accord	150	11	13
12	Taurus	150	12	14
13	Caravan	132	13	12
14	Explorer	120	14	11
15	Explorer	160	15	15
16	Silverado	201	16	16

In summary, the Toyota Prius MY-04 PHEV20 vehicle is modeled using PSAT^{TM} simulator using two different simulated test driving cycles with a profile of changing speeds overtime. These test cycles correspond to realistic driving patterns in different conditions. The UDDS drive cycle is based on actual traffic flows in Los Angeles, CA; whereas the Winnipeg weekday drive cycle is based on city driving conditions and was developed to check the performance of the hybrid vehicles on Canadian roads. 4480 combinations (20 types of batteries, 14 types of electric motors, and 16 types of engines having different design parameters) available in PSAT^{TM} were used in modeling the performance of Toyota Prius MY-04 PHEV20 vehicle. A multi-objective optimization model is then used (as explained in the next Chapter) to optimize the design parameters of battery, motor and engine to find the most efficient hybridization combination.

Chapter 4

Optimization of PHEV20

4.1 Optimization Model

A multi-objective optimization model is developed to model the performance of Toyota Prius MY-04 PHEV20 model in PSAT^{TM} on two different drive cycle platforms, US-EPA UDDS and Winnipeg weekday drive cycles. The model optimizes the design parameters of battery, motor and engine for 20 miles of all electric range with a total vehicle distance travelled of 22.35 miles in city driving conditions that gives the most efficient hybridization combination of battery, motor and engine type in terms of fuel economy (miles/gallon), operating cost ($/mile) and operation GHG emissions (kg/mile) for Toyota Prius MY-04 PHEV20 model. The optimization model includes model variables, multi-objective functions and constraints, and uses PSAT^{TM} as a black box performing simulations in order to provide the best performance for the multiple objectives for a vehicle run of 22.35 miles with 20 miles of all-electric range both in CD-mode and CS-mode. A fully charged PHEV operates in CD-mode until the battery is depleted to a target SOC, 35%, and at which the vehicle switches to CS-mode, using the engine to maintain the target SOC.

In each PHEV20 battery simulation, the number of battery modules needed to reach the target AER of 20 miles was first determined in the electric only CD-mode when the battery is assumed to start with 80% SOC until reaching 35% SOC. Next, the vehicle is operated in the CS-mode to complete the full 22.35 miles. In this mode, both the battery and engine work together to support the necessary driving power. The motor and engine sizes were adjusted to achieve a 0-60 miles per hour acceleration time specification of 10.5 seconds +0.0/-0.5 seconds, which is approximately the acceleration performance of a Toyota Prius [50]. This procedure is repeated iteratively for each battery type until convergence to a vehicle profile that both AER and

acceleration specification were achieved. Finally, the electric efficiency in CD-mode (kWh/mile) and the fuel efficiency in CS-mode (miles/gallon) were measured for PHEV20. The optimization model uses *FZERO* single-variable nonlinear zero finding optimization algorithm for battery sizing and *FMINSEARCH* multidimensional unconstrained nonlinear minimization algorithm for motor and engine sizing. The optimization model includes a total of 4480 combinations of batteries, electric motors and gasoline engines with 20 types of batteries, 14 types of electric motors, and 16 types of gasoline engines.

4.1.1 Model Variables

Batteries, electric motors and gasoline engines are the main variables considered for the design of Toyota Prius MY-04 PHEV20 model in PSAT^{TM} . The detail design parameters of the variables are mentioned in section 3.3.1.1. Table 4-1 shows the list of variables that are used in the optimization model.

Table 4-1. Variables for the optimization model of PHEV20 in PSAT

No.	Variable 1 (Battery type)
1	Saft Li-ion battery, Capacity = 6Ah, Cell number = 75
2	NiCd Saft STM5-100 6-V battery, Capacity = 102Ah, Cell number = 125
3	NiMH battery, Capacity = 11Ah, Cell number = 240
4	Ovonic NiMH battery, Capacity = 28Ah, Cell number = 300
5	Ovonic P127 NiMH battery, Capacity = 45Ah, Cell number = 300
6	NiMH Panasonic battery used in the MY01 US Prius, Capacity = 6.5Ah, Cell number = 168
7	NiMH Panasonic battery used in Japan Prius, Capacity = 6.5Ah, Cell number = 240
8	NiMH Panasonic battery used in the MY01 Japan Prius, Capacity = 6.5Ah, Cell number = 240
9	Ovonic M108 NiMH battery, Capacity = 60Ah, Cell number = 300
10	Ovonic NiMH battery, Capacity = 90Ah, Cell number = 300
11	NiMH battery, Capacity = 93Ah, Cell number = 275
12	NiZn Evercell battery, Capacity = 22Ah, Cell number = 196
13	GNB 12-EVB-1180 valve-regulated lead acid battery, Capacity = 104Ah, Cell number = 150
14	Hawker Genesis lead acid battery, Capacity = 12Ah, Cell number = 150
15	Hawker Odyssey sealed lead acid battery, Capacity = 6Ah, Cell number = 72

16	Optima valve-regulated spiral-wound lead acid battery, Capacity = 18Ah, Cell number = 150
17	Hawker Genesis 12V26Ah10EP sealed valve-regulated lead acid battery, Capacity = 25Ah, Cell number = 150
18	Hawker Genesis 12V26Ah10EP sealed valve-regulated lead acid (VRLA) battery, Capacity = 26Ah, Cell number = 27
19	Johnson Controls lead acid battery, Capacity = 28Ah, Cell number = 150
20	Horizon lead acid battery, Capacity = 91Ah, Cell number = 150
	Variable 2 (Motor type) Permanent Magnet electric motor
1	MY04 Toyota Prius Mobility, Continuous power = 25kW, Peak power = 50kW
2	Honda Insight, Continuous power = 10kW, Peak power = 10kW
3	MY04 Toyota Prius, Continuous power = 15kW, Peak power = 30kW
4	MY05 Ford Escape Hybrid MG2, Continuous power = 17kW, Peak power = 33kW
5	Auxilec Thomson, Continuous Power = 32kW, Peak power = 45kW
6	MY05 Ford Escape Hybrid MG1, Continuous power = 33kW, Peak power = 65kW
7	Toyota Camry MG2, Continuos power = 35kW, Peak power = 70kW
8	UQM PowerPhase75 (Unique Mobility), Continuous power = 36kW, Peak power = 75kW
9	Honda, Continuous power = 49kW, Peak power = 49kW
10	UQM Power Phase100, Continuous power = 55kW, Peak power = 100kW
11	Toyota Camry MG1, Continuous power = 55kW, Peak power = 105kW
12	Permanent magnet electric motor with Continuous power = 58kW, Peak power = 58kW
13	Honda Accord, Continuous power = 7kW, Peak power = 14kW
14	MY99 Toyota Prius, Continuous power = 7kW, Peak power = 15kW
	Variable 3 (Engine type) Spark Ignition gasoline engine
1	1.497L 57kW MY04 USPrius gasoline engine
2	Geo 1.0L 41kW gasoline engine
3	Honda Insight 1.0L VTEC-E gasoline engine
4	1.5L 43kW Japan Prius gasoline engine
5	1.5L 52kW MY01US Prius gasoline engine
6	1.6L 85kW Civic gasoline engine
7	1.8L 90kW Corolla VVTi gasoline engine
8	1.8L 99kW Ford gasoline engine
9	2.3L 99kW MY05 Ford Escape Hybrid gasoline engine
10	3L 115kW Taurus gasoline engine
11	3L 150kW Honda Accord VTEC gasoline engine
12	3L 150kW Taurus gasoline engine
13	3.8L 132kW Caravan gasoline engine
14	4L 120kW Explorer gasoline engine
15	4L 160kW Explorer SOHC gasoline engine
16	4.8L 201kW Silverado gasoline engine

4.1.2 Model Multi-Objective Functions

Three PHEV characteristics: (i) fuel consumption (miles/gallon), (ii) operating costs ($/mile), and (iii) operational GHG emissions (kg/mile) are examined to measure the operational performance of Toyota Prius MY-04 PHEV20 vehicle configuration. Because these three performance criteria depend on the distance travelled between charges, two key quantities: the distances d_{CD} and d_{CS} travelled in CD-mode and CS-mode, respectively are needed. For a distance *d* travelled between charges in a vehicle with an AER of d_{AER}, the distances d_{CD} and d_{CS} are calculated as in equation 4-1 [50]:

$$\begin{aligned} d_{CD} &= d \quad \text{if } d \le d_{AER} \\ &= d_{AER} \quad \text{if } d > d_{AER} \end{aligned}$$

Equation 4-1

$$\begin{aligned} d_{CS} &= 0 \quad \text{if } d \le d_{AER} \\ &= d - d_{AER} \text{ if } d > d_{AER} \end{aligned}$$

In this study, the fuel economy (miles/gallon) results are obtained directly from PSAT^{TM} after simulation. The second performance represents the average consumer expense per mile associated with recharging cost and fuel expense. This average operation cost c_{OP} is calculated as in equation 4-2 [50]:

$$c_{OP} = \frac{1}{d}\left(\frac{d_{CD}}{\eta_{CD}}\frac{c_{ELEC}}{\eta_C} + \frac{d_{CS}}{\eta_{CS}}c_{GAS}\right)$$

Equation 4-2

where, η_{CD} is CD-mode vehicle electrical efficiency (miles per kWh) and η_{CS} is the fuel efficiency in CS-mode; both are also directly obtained from PSAT^{TM} simulation results; η_C is the charging efficiency; c_{ELEC} is the cost of electricity; and c_{GAS} is gasoline cost. It is assumed that c_{ELEC} = $0.11/kWh, c_{GAS} = $3.00/gallon based on the U.S. prices in 2007 [83], and η_C = 88% [84].

The third performance characteristic is calculated by including combustion and supply chain emissions associated with electricity and gasoline, which are given by v_{ELEC} = 0.730 kg CO_2-eq/kWh and v_{GAS} = 11.34 kg CO_2-eq/gallon, respectively [85]. The associated average operation GHG emissions/mile, v_{OP} is given by the following equation 4-3 [50]:

$$v_{OP} = \frac{1}{d}\left(\frac{d_{CD}}{\eta_{CD}}\frac{v_{ELEC}}{\eta_C} + \frac{d_{CS}}{\eta_{CS}}v_{GAS}\right) \qquad \textbf{Equation 4-3}$$

4.1.3 Model Constraints

The two main constraints used in the multi-objective optimization model for finding the most optimum hybridization combination of the Toyota Prius MY-04 PHEV20 vehicle were: (i) AER of 20 miles for sizing of the battery storage in CD-mode, and (ii) 0-60 miles per hour acceleration time specification of 10.5 (+0.0/-0.5) seconds for sizing the electric motor and engine in CS-mode. Both these constraints develop the battery size for 20 miles of electric range and run the Toyota Prius vehicle with required acceleration in the optimization loop. The FZERO optimization algorithm for battery sizing and FMINSERACH optimization algorithm for motor and engine sizing terminate under the defined constraints are satisfied.

4.2 Optimization for Battery Sizing

FZERO is a single-variable nonlinear zero finding optimization method that is used to find the number of battery modules for battery sizing in order to satisfy the AER of 20 miles for Toyota Prius MY-04 PHEV20 model. In our case, the single variable is the type of battery. As shown in the Figure 4-1, the input is the number of battery modules for 20 different types of batteries like Li-ion, NiCd, NiMH, NiZn, and Lead acid batteries. For each selected type of battery, PSAT^{TM} is called as black box function to calculate the simulation AER and then the FZERO function compares the difference between the simulation AER and the ideal AER (20 miles), and the process iterates and terminates on reaching the zero function value. On reaching convergence, it

gives the required battery size that is the number of battery modules for the selected battery. Equation 4-4 defines the objective function for FZERO optimization method.

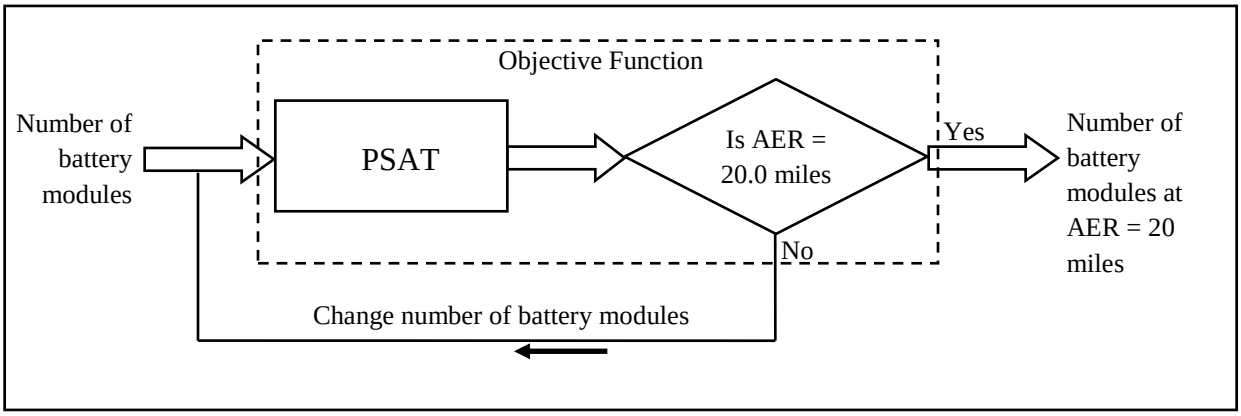

Figure 4-1. FZERO algorithm for battery sizing

Mathematically ,

$x = fzero(fun,x_0)$ tries to find a zero of function (fun) near x_0

Objective function,

$$fun = (Simulation\ AER - Ideal\ AER) \quad \textbf{Equation 4-4}$$

(without constraint)

Design Variable,

$x = number\ of\ battery\ modules$

4.3 Optimization for Motor and Engine Sizing

FMINSEARCH is a multidimensional unconstrained nonlinear minimization method that is used to size the motor and engine power to satisfy 0-60 mph acceleration time specification of 10.5 (+0.0/-0.5) seconds for Toyota Prius MY-04 PHEV20 model. In our case, the two variables considered are motor and engine powers. As shown in Figure 4-2, the input is the motor and engine power for 14 types of motors and 16 types of engines. For each combination of motor and engine powers, PSAT^{TM} is called as black box function to calculate the simulation acceleration time and then the FMINSERACH function compares the absolute difference between the simulation acceleration time and the ideal acceleration time (10.5 +0.0/-0.5 seconds), and the

process iterates and terminates on reaching the minimum function value. On reaching convergence, it gives the required motor and engine size that is the motor and engine power desired to maintain the torque and acceleration time. Equation 4-5 defines the objective function for FMINSEARCH optimization method.

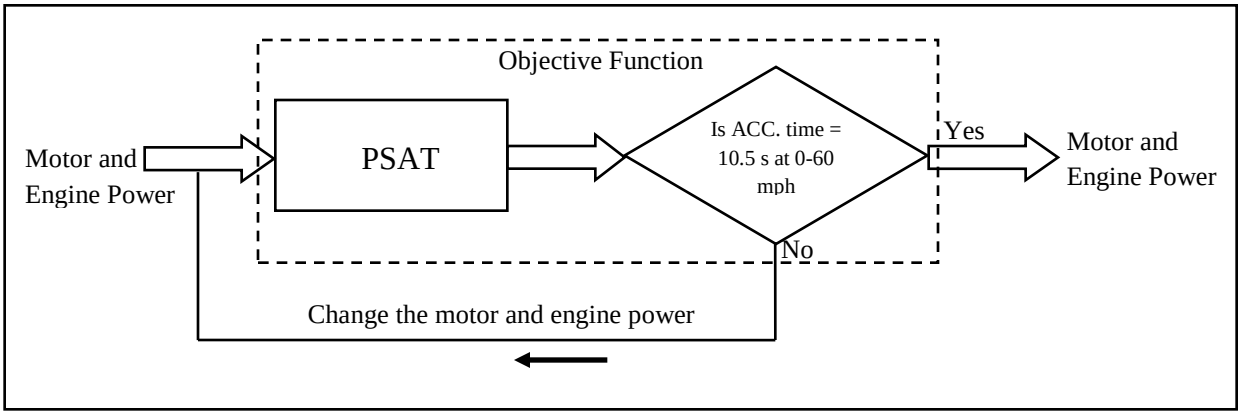

Figure 4-2. FMINSERACH algorithm for motor and engine sizing

Mathematically ,

$x = fminsearch(fun,x_0)$

starts at the point x_0 and finds a local minimum x of the function described in fun.

Objective function,

$$fun = Abs(Simulation\ ACC - Ideal\ ACC) \quad \textbf{Equation 4-5}$$

(without constraint)

Design Variables,

$vector\ x=\{x_1,x_2\}$

$x_1 = motor\ power$

$x_2 = engine\ power$

4.4 Hybridization and Multi-Objective Optimization Using PSP Method

Hybridization of the PHEV20 is done through the selection of best and most efficient combinations of the three drivetrain components: battery storage, electric motor and gasoline engine that provide maximum fuel economy (miles/gallon), and minimum operating cost

($/mile) and operation GHG emissions (kg/mile) on US-EPA UDDS and Winnipeg weekday drive cycles. For finding the most optimum hybridization from 4480 combinations (including 20 types of batteries, 14 types of electric motors, and 16 types of gasoline engines), the exhaustive search method, which selects the best combination for Toyota Prius MY-04 PHEV20, is very cumbersome and takes more than 3 hours for one complete iteration. In this way, it would take more than 13440 hours (1.53 years) to check the performance characteristic of all 4480 combinations of batteries, electric motors, and gasoline engines for Toyota Prius MY-04 PHEV20 vehicle model. Therefore, we used *Pareto Set Pursuing (PSP) multi-objective optimization approach* to select the most optimum hybridization combination from 4480 combinations for Toyota Prius MY-04 PHEV20 vehicle [86]. This method is very efficient and effective for the selection of Pareto design points, each consisting of a set of a battery, a motor, and an engine [86]. PSP has been found the most efficient method when the total of function evaluations is limited, as compared to state-of-the-art evolutionary algorithms for multi-objective design problems [88].

The Pareto set pursuing (PSP) multi-objective optimization method builds a sampling guidance function by providing efficient and uniformly distributed set of Pareto optimal points based on approximation models [86]. The formulation of the multi-objective optimization problem is taken from Shan and Wang (2005) as follows [86]:

$$\text{Minimize: } F(x) = \left\{ f_1(x), f_2(x), ..., f_i(x), ..., f_m(x) \right\} \qquad \textbf{Equation 4-6}$$

where, $\left\{ f_1(x), f_2(x), ..., f_i(x), ..., f_m(x) \right\}$ is a set of multiple objective functions, and the purpose is to find a set of points of Pareto optimality. The Pareto optimality is defined as a vector x^* if there exists no feasible vector x that decreases any objective function values without increasing at least one other objective function at the same time. Mathematically, Shan and Wang (2005) define a vector x^* as being Pareto optimum if, for any x and i,

$$\begin{aligned} & f_j(x) \le f_j(x^*), \\ & j = 1, ..., m; \ j \ne i, \\ & \Rightarrow f_i(x) \ge f_i(x^*) \end{aligned} \qquad \textbf{Equation 4-7}$$

In order to find the set of Pareto optimal points, Shan and Wang (2005) further use the concept of a fitness function [87]. The definition of the fitness function is taken from Shan and Wang (2005) as follows [86]:

$$G_i = \left[1 - \max_{j \neq i}\left(\min\left(f_{s1}^i - f_{s1}^j, f_{s2}^i - f_{s2}^j, ..., f_{sm}^i - f_{sm}^j\right)\right)\right]^l \qquad \textbf{Equation 4-8}$$

where, G_i denotes the fitness value of the i^{th} design; f_{sk}^i is scaled k^{th} objective function value of the i^{th} design, $k = 1, ..., m$; and l is called the frontier exponent, which is taken as a constant 1. First, the objectives $f_{s1}, f_{s2}, ..., f_{sm}$ in equation 4-8 are scaled to a range [0, 1]. For example for f_{s1}^i,

$$f_{s1}^i = \frac{rawf_{1,i} - rawf_{1,\min}}{rawf_{1,\max} - rawf_{1,\min}} \qquad \textbf{Equation 4-9}$$

where, $rawf_{1,i}$ denotes un-scaled value of the first objective for the i^{th} design; $rawf_{1,\max}$ denotes the maximum un-scaled value of the first objective among all designs; and $rawf_{1,\min}$ denotes the minimum un-scaled value of the first objective among all designs. If an objective function is a constant, the scaled objective function value f_{s1}^i is taken as *1* in this work. Second, the minimum in equation 4-8 over all the objectives function values $\min\left(f_{s1}^i - f_{s1}^j, f_{s2}^i - f_{s2}^j, ..., f_{sm}^i - f_{sm}^j\right)$ is calculated. Finally, the maximum in equation 4-8 over all other designs $j \neq i$ in the set $\max_{j \neq i}\left(\min\left(f_{s1}^i - f_{s1}^j, f_{s2}^i - f_{s2}^j, ..., f_{sm}^i - f_{sm}^j\right)\right)$ are calculated and the fitness function G_i is calculated.

Since all the objective function values are scaled between the interval [0, 1], the fitness function measures the relation between different points in the performance space, and for a given set of points, the following statements hold true: (i) Pareto set points should have a fitness function value in the range [1, 2]; (ii) Non-Pareto set points have a fitness value in [0, 1); and (iii) when Pareto set points are closely and evenly distributed, the fitness value of all Pareto set points tends to be 1 [86].

The PSP approximates the entire Pareto frontier directly by sampling many Pareto points for the multi-objective optimization problem of minimizing the operating costs and GHG emissions, and maximizing the fuel economy with the PSAT^{TM} black-box function. It starts with a random sample in the first iteration, but moves closer to the Pareto frontier with successive iterations. Two types of sampling guidance functions are developed in the process. The first function is for the sampling of *cheap* points from the approximation model of each objective function, and the second function is for the sampling towards the Pareto frontier [86]. Figure 4-3 shows the flowchart of the Pareto set pursuing identification approach [86]. Both FZERO and FMINSEARCH optimization algorithms help for the sizing and hybridization of three PHEV20 drivetrain components battery, motor and engine. The multi-objective optimization PSP algorithm generates the meta-model by selecting the most efficient points (combination of battery, motor and engine) and calls the PSAT^{TM} black-box to calculate the performance characteristic of the sampling points and simultaneously generates more sampling points with the mean fitness value, till it reaches to the convergence criteria. The most efficient and effective Pareto design points are generated by using the PSP algorithm. These Pareto design points give the best combination for the performance of Toyota Prius MY-04 PHEV20 vehicle based on maximum fuel economy (miles/gallon), and minimum operating cost ($/mile) and operation GHG emissions (kg/mile).

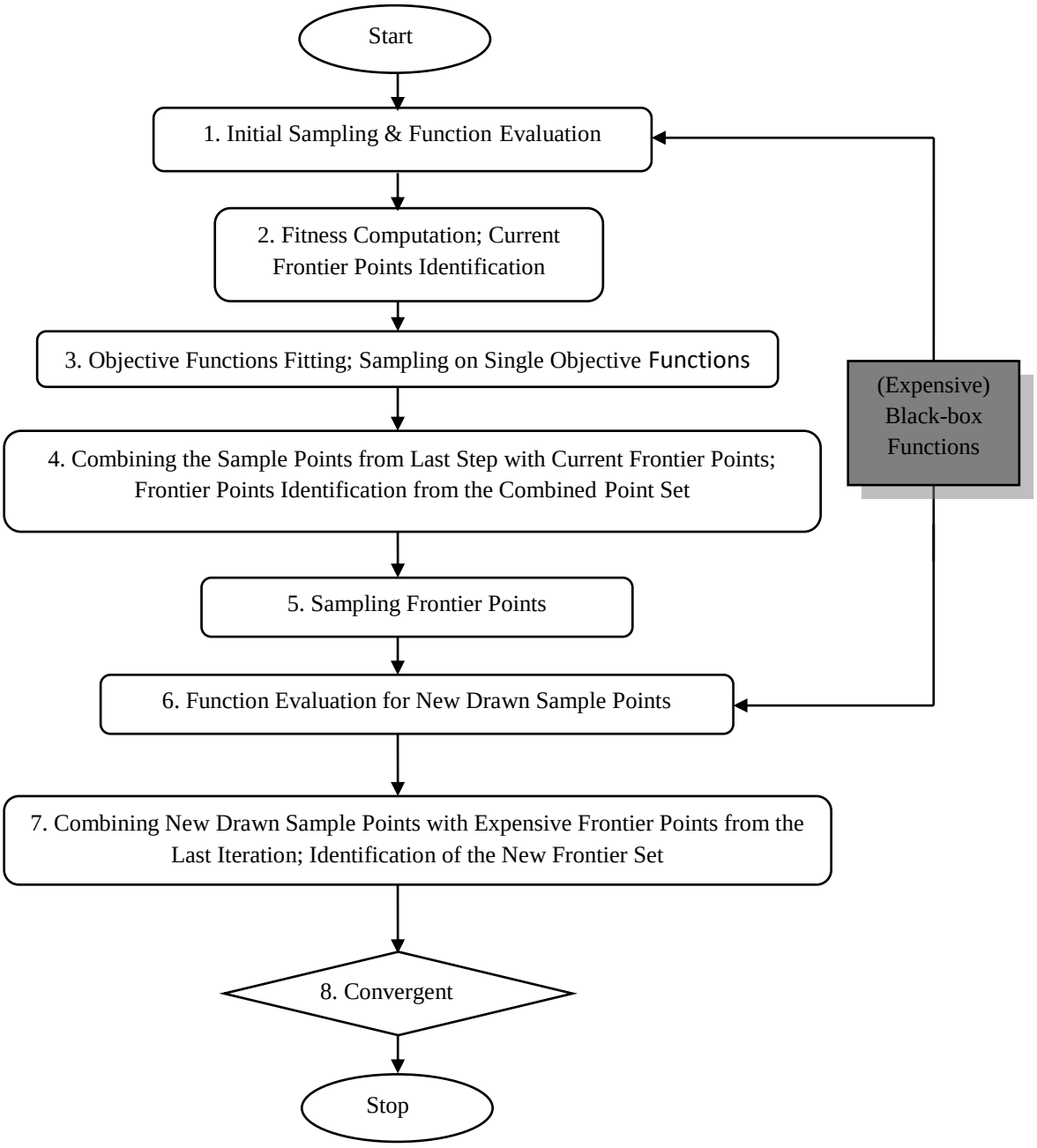

Figure 4-3. Flowchart of the Pareto set pursuing identification approach [86]

As shown in Figure 4-4, the input is the combination of battery, motor and engine. PSP algorithm selects the combination of battery, motor and engine, and FZERO and FMINSEARCH algorithms size the battery, motor and engine by calling the PSAT^{TM} as black box. PSP algorithm finds the most efficient points based on the performance characteristic value.

Mathematically, PSP multi-objective optimization algorithm with PSAT^{TM} as a black box is defined as:

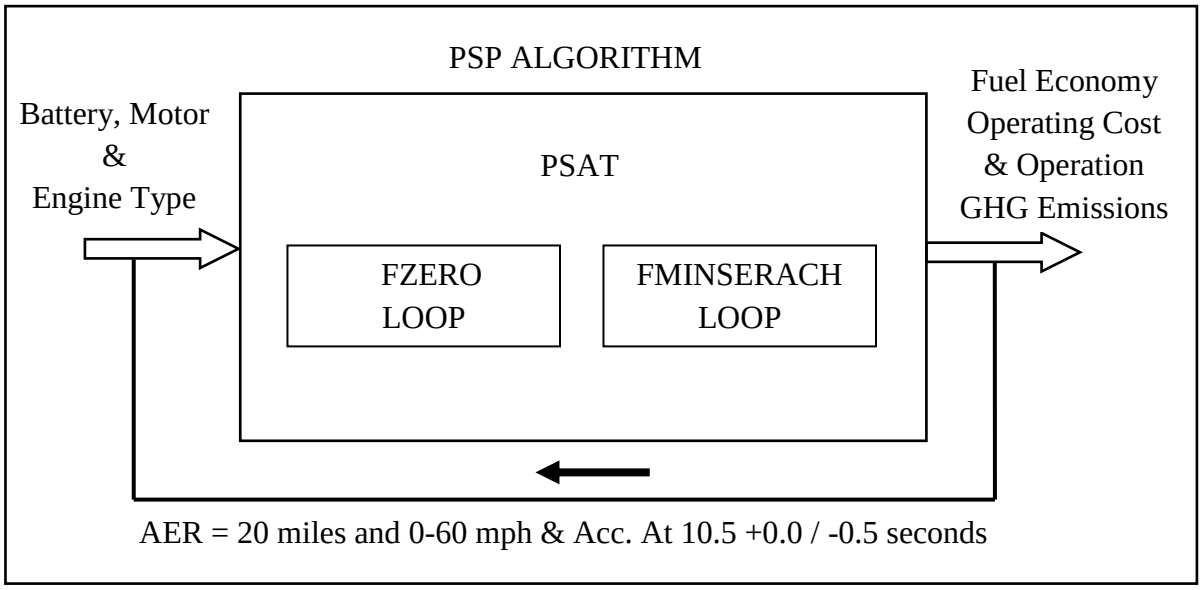

Figure 4-4. PSP multi-objective optimization algorithm with PSATTM as a black box

Mathematically ,

Objective function,

$$\text{Minimize: } F(x) = \{f_1(x), f_2(x), f_3(x)\}$$

$f_1(x)$ = *- fuel economy*

$f_2(x)$ = *operating cost,* c_{op} **Equation 4-10**

$f_3(x)$ = *operation emission,* v_{op}

Constraint,

d_{AER} = *20 miles*

Acc. time = 10.5 s for 0-60 mph

Design Variables,

vector $x=\{x_1,x_2,x_3\}$

x_1 = *battery type,* $\in [1,20]$

x_2 = *motor type,* $\in [1,14]$

x_3 = *engine type,* $\in [1,16]$

In summary, the hybridization of Toyota Prius MY-04 PHEV20 vehicle is done by selecting the best and most efficient combinations of the three drivetrain components: battery storage, electric motor and gasoline engine that provide the most optimum fuel economy (miles/gallon), operating cost ($/mile), and operation GHG emissions (kg/mile). First, the FZERO single-variable nonlinear zero finding optimization algorithm is used to find the number of battery modules for battery sizing (for 20 different types of batteries including: Li-ion, NiCd, NiMH, NiZn, and Lead acid batteries) in order to satisfy the AER of 20 miles for the vehicle. Second, the FMINSEARCH multi-dimensional unconstrained nonlinear minimization algorithm is used to size the motor (selected from 14 motors) and engine (selected from 16 gasoline engines) power of the vehicle. Finally, the *Pareto Set Pursuing (PSP) multi-objective optimization approach* is used to select the most optimum hybridization combination for Toyota Prius MY-04 PHEV20 vehicle. The results of modeling, simulation and optimization are explained in detail in the next chapter. Figure 4-5 shows the program structure for the automatic process of hybridization and multi-objective optimization of PHEV20 using US-EPA UDDS and Winnipeg weekday drive cycles.

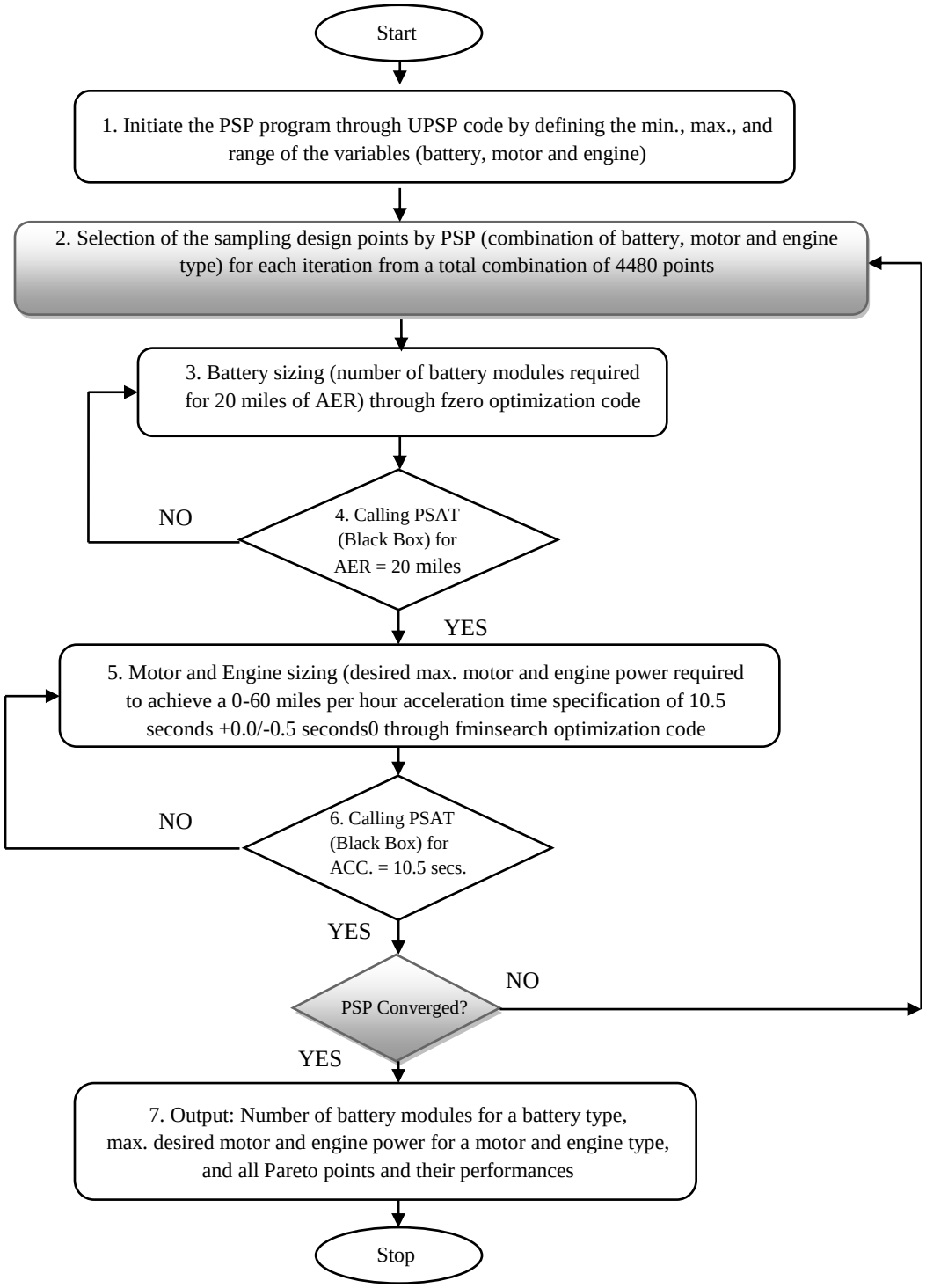

Figure 4-5. Flow chart of the program structure for the automation process

Chapter 5

Results and Discussion

5.1 Performance of PHEV over HEV Based on Prius Platform

The performance of PHEV and HEV was compared with the published data [1] by modeling and simulating the fuel economy, mass of fuel required to cover certain distance, CO_2 emission levels, wheel mechanical brake energy, and gradeability of these vehicles for highway and urban driving schedules [22]. The technical specifications of Toyota Prius HEV, used in this comparison, are given in Table 3-1.

The results of modeling and simulation, using highway fuel economy test (HWFET) driving schedule for driving conditions: speed less than 60 mph, result interval 0-764 seconds, and cycle distance of 10.26 miles are shown in Table 5-1. The results show a fuel economy saving of 26.76 %, saving in mass of fuel of 21.13% for a distance of 320 miles, reduction in CO_2 emissions of 21.11%, and saving of wheel mechanical brake energy of 97.67% for PHEV over HEV. The results of modeling and simulation, using US EPA urban dynamometer driving schedule (UDDS) test, representing city driving conditions: speed less than 60 mph, result interval 0-1369 seconds, cycle distance 7.44 miles are shown in Table 5-2. The results show a fuel economy saving of 18.02 %, saving in mass of fuel of 15.31% for a distance of 320 miles, reduction in CO_2 emissions of 15.29%, and saving of wheel mechanical brake energy of 62.5% for PHEV over HEV.

Table 5-1. Performance parameters for PHEV and HEV under highway fuel economy test driving schedule

Parameter	**PHEV**	**HEV**	**% Change**
Fuel Economy in miles/gallon	85.01	67.06	27.76%↓
Mass of Fuel needed to travel 320 miles in kg	10.67	13.53	21.13%↑
CO_2 emissions in g/mile	105.61	133.31	21.11%↑
Wheel mechanical brake energy loss in Wh	0.2293	9.86	97.67%↑

Table 5-2. Performance parameters for PHEV and HEV urban dynamometer driving schedule (UDDS) test

Parameter	**PHEV**	**HEV**	**% Change**
Fuel Economy in miles/gallon	87.21	73.89	18.02%↓
Mass of Fuel needed to travel 320 miles in kg	10.40	12.28	15.31%↑
CO_2 emissions in g/mile	102.50	121.00	15.29%↑
Wheel mechanical brake energy loss in Wh	1.59	4.24	62.50%↑

The results for gradeability for highway and city driving conditions (i.e, speed of 65 mph, result interval of 0-150 seconds, cycle distance of 2.67 miles) show gradeability of 7.99 % for HEV and 12.96% for PHEV. Therefore, a rise of 62.2% in maximum gradeability in PHEV over HEV was observed. The comparison of modeling and simulation results of fuel economy with UN/ECE Normalized European driving cycle (NEDC) characterized by a city/highway driving mix, UDDS, and HWFET are shown in Table 5-3. It can be seen for all three cycles, PHEV shows better fuel economy than HEV.

Table 5-3. Comparison of modeling and simulation results of fuel economy in miles/gallon with the published data

Vehicle	**HWFET**	**UDDS**	**NEDC**
PHEV	85.01	87.21	57.99
HEV	67.06	73.89	50.66

These results convey important information to make the hybrid electric vehicles an attractive proposition, due to increasing concerns about the environment, both in terms of overall emissions of CO_2 and also the local emission of exhaust fumes. However, the limiting factors of PHEV that have not allowed it to capture the markets have been the high cost and weight of the batteries. Although, there have been technical developments in vehicle design and improvements to rechargeable batteries, motors and controllers, there is a need to focus on researching thermal management, modeling, and systems solutions for energy storage technology. Improved power electronics is critical to hybrid efficiency and there is a need to conduct sophisticated modeling

and analysis essential to showing the economic viability of plug-ins and identifying key areas for improvement.

5.2 Operational Performance of PHEV20 for 15 Different Types of Batteries

Battery is a key component to PHEV. For a given vehicle, one needs to understand if the change of battery type will lead to different performance values and how different types of batteries influence the performances. In this work, the operational performance of PHEV20 using 15 different types of batteries (lithium-ion, nickel metal hydride, nickel zinc, and lead acid) was compared by assessing the fuel economy (miles/gallon), operating cost ($/mile), and operation GHG emissions (kg/mile) of PHEV20 using these batteries. This comparison is based on existing Toyota Prius vehicle with its own motor and engine. The key parameters of these batteries considered for evaluating the operational performance of the PHEV20 are listed in the Table 5-4.

Table 5-4. Key battery parameters used for evaluating the operational performance of PHEVs

Battery No.	Type	No. of modules	No. of cells in module	No. of cells	Cell mass (kg)	Module mass (kg)	Battery mass (kg)
	Li-ion						
1	ess_li_7_303	103	3	309	0.38	1.43	146.78
	NiMH						
2	ess_nimh_28_222_ovonic	39	6	234	0.60	4.50	175.50
3	ess_nimh_45_144_ovonic	12	12	144	0.70	10.50	126.00
4	ess_nimh_60_108_ovonic	9	12	108	0.97	14.55	130.95
5	ess_nimh_90_72_ovonic	6	12	72	0.97	14.55	87.30
6	ess_nimh_93_66	6	11	66	1.63	22.41	134.48
	NiZn						
7	ess_nizn_22_196_evercell	28	7	196	1.16	10.15	284.20
	Pb Acid						
8	ess_pb_104_36	6	6	36	5.00	37.50	225.00
9	ess_pb_12_336	57	6	342	0.79	5.93	337.73
10	ess_pb_16_228_hawker	39	6	234	1.02	7.65	298.35
11	ess_pb_18_210	35	6	210	1.11	8.33	291.55
12	ess_pb_25_144	25	6	150	1.83	13.73	343.25
13	ess_pb_26_138_hawker	24	6	144	1.83	13.73	329.52
14	ess_pb_28_144	24	6	144	1.97	14.78	354.72
15	ess_pb_91_42	7	6	42	4.43	33.23	232.61

An average vehicle mass (excluding the battery mass) of 1484 kg was considered and the battery mass includes a packing factor of 1.25. The specific energy and power density of cells for each battery are shown in Table 5-5.

Table 5-5. Specific energy and power density of cells for each battery at 88% charging efficiency

Battery No.	Cell capacity indexed at 22^0C (Ah)	Nominal cell voltage (Volts)	Battery Capacity (kWh)	Cell specific energy indexed at 22^0C (Wh/kg)	Cell power density indexed at 22^0C and 80% SOC (W/kg)
1	7	3.6	7.64	66.65	609.78
2	28	1.2	7.46	56.00	561.79
3	45	1.2	7.78	77.14	571.43
4	60	1.2	7.78	74.22	526.11
5	90	1.2	7.78	111.34	754.34
6	93	1.2	7.37	68.47	117.98
7	22	1.7	7.33	33.53	78.64
8	104	2.0	7.49	41.6	192.01
9	12	2.0	8.06	30.38	178.94
10	16	2.0	7.30	31.37	437.76
11	18	2.0	7.56	32.43	183.78
12	25	2.0	7.20	27.32	185.88
13	26	2.0	7.18	28.42	185.96
14	28	2.0	8.06	28.43	326.37
15	91	2.0	7.64	41.08	257.98

Table 5-6 presents the operational performance results of PHEV20 Toyota Prius 2004 model for 15 different types of batteries fixed at 20 miles AER capacity, obtained from PSAT^{TM} vehicle simulation software. The operational performance design points represent efficiency in CD mode (miles/kWh), efficiency in CS mode (mile/gallon), total fuel consumption (miles/gallon), operating costs ($/mile), and operational GHG emissions (kg/mile) of PHEV20.

Table 5-6. PHEV20 Operational performance simulation results of 15 batteries

Battery No.	Vehicle Wt. (ton)	etaCD (miles/kWh)	etaCS (miles/gallon)	Fuel Economy (miles/gal.)	Operation Cost ($/mile)	GHG Emissions (kg/mile)	Fitness Value
1	1.631	5.93	120.25	121.66	**0.0215**	**0.135**	**1.09**
2	1.660	5.74	120.48	120.69	0.0221	0.139	0.95
3	1.611	5.59	121.75	122.76	0.0226	0.143	0.98
4	1.615	5.53	121.41	122.23	0.0228	0.144	0.95
5	1.572	5.59	124.77	**125.51**	0.0225	0.142	**1.13**
6	1.619	4.97	116.56	117.66	0.0252	0.16	0.63
7	1.768	4.47	102.84	104.07	0.0281	0.178	0.16
8	1.710	5.41	116.99	117.87	0.0234	0.147	0.82
9	1.826	5.24	107.41	108.5	0.0243	0.153	0.58
10	1.782	5.86	116.92	118.78	0.0218	0.137	0.95
11	1.777	5.46	110.35	112.18	0.0233	0.147	0.73
12	1.828	5.27	109.39	109.43	0.0241	0.152	0.61
13	1.815	5.26	108.06	110.16	0.0242	0.152	0.60
14	1.839	5.59	111.00	112.05	0.0228	0.143	0.81
15	1.717	5.73	118.84	118.93	0.0222	0.14	0.89

Figure 5-1 shows a comparison of these operational performance design points of PHEV20 for individual batteries. The results show two batteries dominate the rest. Nickel metal hydride battery No. 5, which has a cell capacity of 90 ampere hour (Ah), provides a maximum fuel economy of 125.51 miles/gallon for PHEV20, which is about 3% more than the lithium-ion battery, about 9% more than the average of lead acid batteries, and about 17% more than the nickel zinc battery. Lithium ion battery No. 1 (cell capacity of 7Ah) has the least operation cost of 0.0215 $/mile for PHEV20, which is about 30% less than the nickel zinc battery, only 7% lower than the average of nickel metal hydride and 8% lower than the average of lead acid batteries. Lithium ion battery No. 1 also has the least operation GHG emissions of 0.135 kg/mile for PHEV20, which is about 32% less than the nickel zinc battery, and 8% less than the average of nickel metal hydride or lead acid batteries.

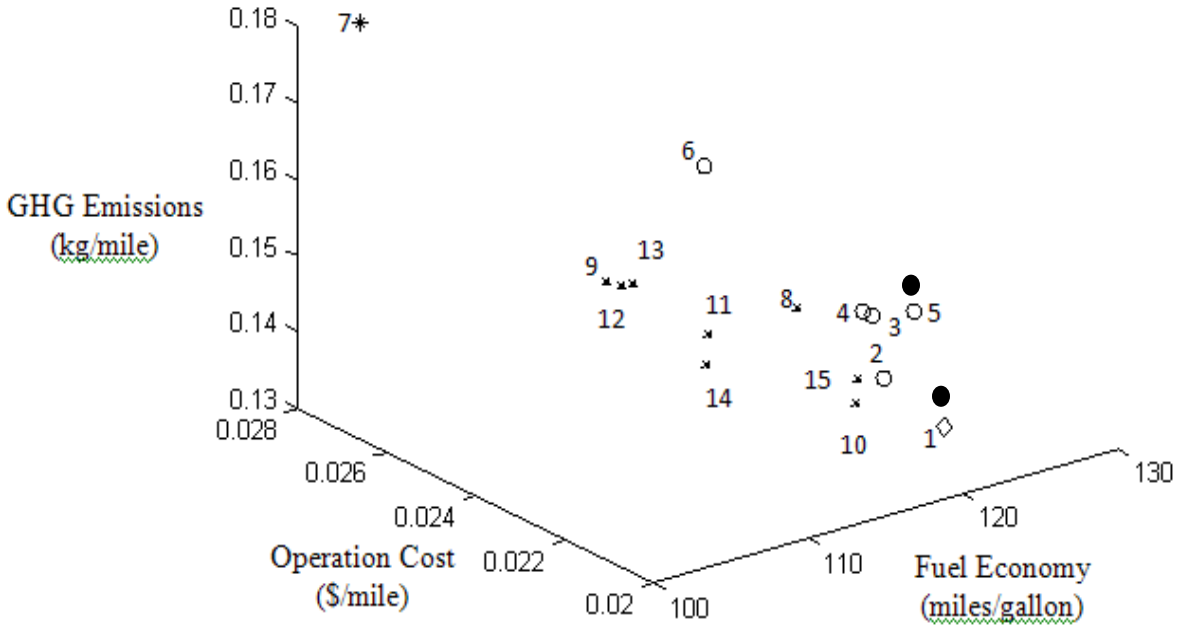

Figure 5-1. Operational performance design points of PHEV20 using 15 batteries

◊ Li-ion battery, ○ NiMH batteries, * NiZn battery, × Pb-Acid batteries
● Batteries on Pareto frontier with fitness value in the range [1, 2]

Additionally, it is found in Figure 5-2 that the performance design points of 2 batteries have a fitness value in the range [1, 2] and 7 batteries have a fitness value close to 1 (0.81-0.98). This means that the operational performance design points of 9 batteries are close to being Pareto optimal. These batteries may make competitive choices as the best two. The rest of the batteries, including Nickel Zinc battery No. 7, NiMh No. 6, and lead acid No. 9, 11, 12, and 13, are dominated design points, are not as efficient as others for the PHEV20 configuration.

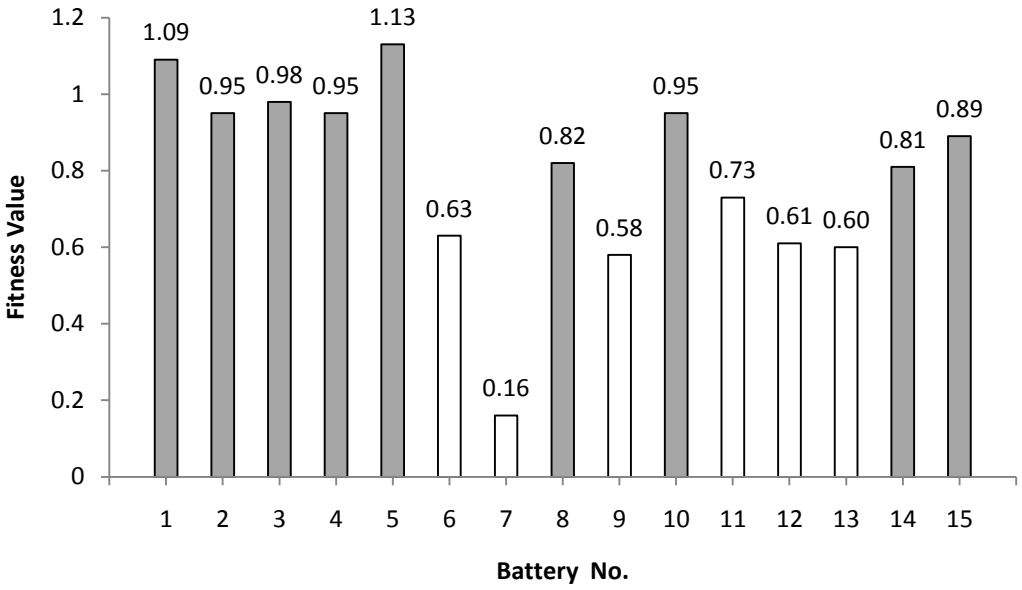

Figure 5-2. Fitness value of 15 batteries using Pareto set identification approach

Figure 5-3 shows a comparison of average performance parameters of the 9 batteries that are either Pareto optimal set design points or close to being Pareto optimal. On an average, NiMH batteries provide the highest fuel economy (mpg), with the lithium-ion battery (No.1) provides comparative fuel economy. Figure 5-3 also shows that lithium ion batteries have the lowest average operating cost and average operation GHG emissions, comparing to other types. NiMH battery (No. 2) and lead acid batteries (No. 10 and 15), however, yield comparative operating costs and GHG emissions to lithium-ion battery.

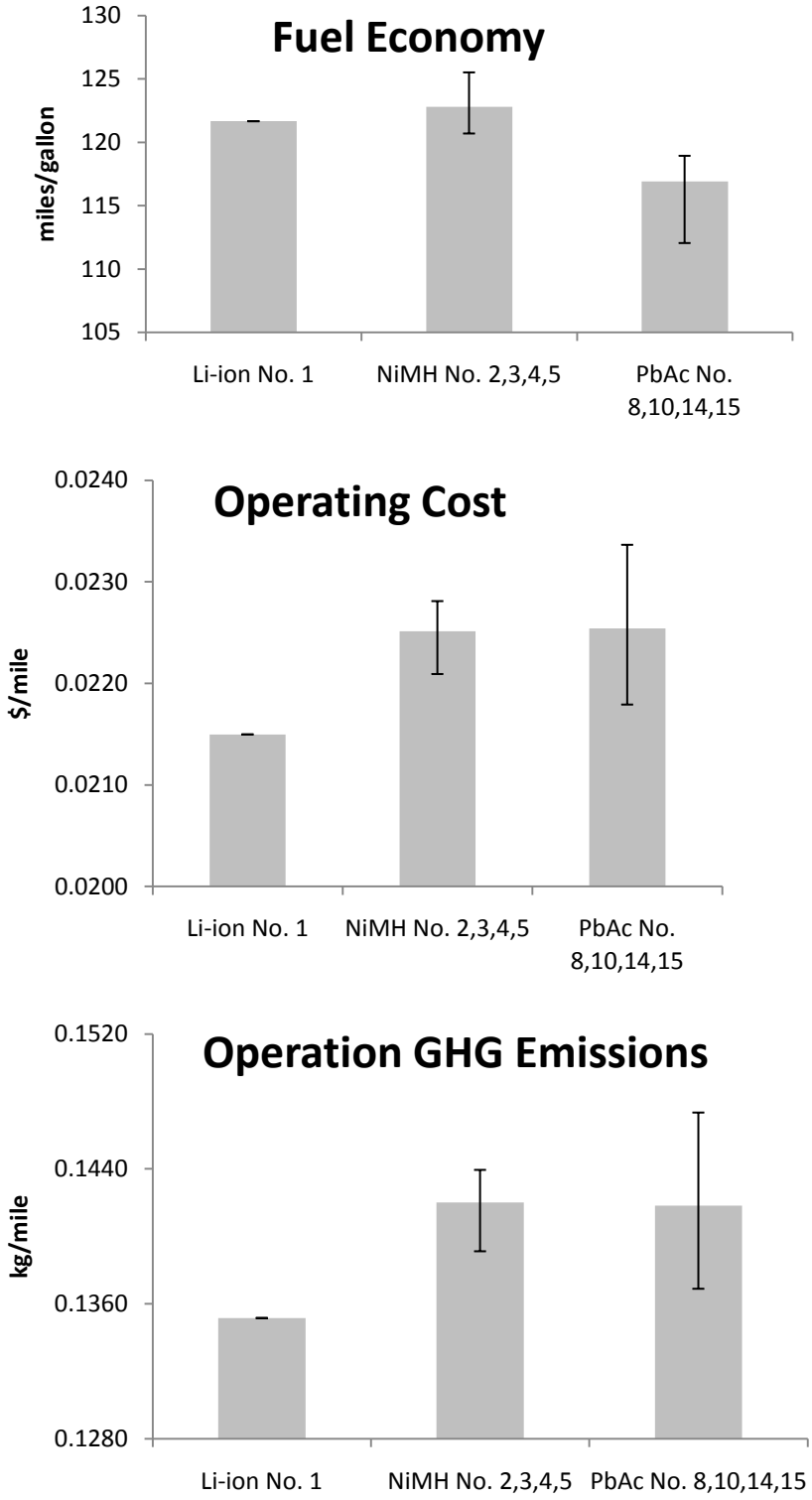

Figure 5-3. Comparison of average operational performance parameters of 9 batteries that are either Pareto optimal set design points or close to being Pareto optimal. Error bars indicate range (min.– max.) for each battery type

Given a Pareto frontier, a decision maker can pick a battery from the 9 selected batteries that are on the Pareto frontier or close to it, according to his/her own preference of the three objectives, together with other considerations that are not modeled in this study. For example, earlier studies found that lead acid batteries had the least cost for PHEV drivetrain configurations [46]. Those studies compared the design cost of a lead acid battery (about $4,845) with that of Li-ion and NiMH batteries for PHEV20, and found that lead acid battery provides 30% lower design cost as compared to NiMH battery and 70% lower design cost as compared to lithium-ion battery. This is because the battery capacity of lead acid batteries used for PHEV20 is higher as compared to Li-ion and NiMH batteries, hence their design costs are lower [46]. Li-ion batteries have higher energy density and specific energy and are benefiting from increased technological advancement, but there are concerns regarding their calendar life and safety. Internal corrosion and high environment temperatures could cause Lithium-ion batteries to explode, making these unsafe for longer use in PHEVs [52]. Li-ion and NiMH batteries are currently used in HEV designs, where batteries are selected for high power output, whereas in PHEV design, the high energy storage capacity parameter is of greater importance. For the HEV designs, the lead acid batteries may not be suitable as the discharge cycle of HEVs is much more demanding than a PHEV battery pack [32]. Moreover, it has been established that different battery chemistries do not affect the battery cost of HEVs as much as in the case of PHEVs, as PHEVs require larger battery packs for higher power and energy requirements, which substantially increases the weight and cost of the vehicle [32]. In addition, though Lithium-ion and NiMH batteries offer attractive features, they have limited charge capacity and battery life at high temperatures; their relatively more complex energy management units are also of concern [66].

5.3 Hybridization and Multi-Objective Optimization Simulation Results of PHEV20

Simulation results for hybridization and multi-objective optimization for PHEV20 are obtained by first sizing the battery capacity at 20 miles of AER and motor and engine power to satisfy 0-60 mph vehicle acceleration time specification of 10.5 (+0.0/-0.5) seconds. These simulations are done using US-EPA UDDS and Winnipeg weekday drive cycles. Table A-1 shows the sequence of selection of battery (out of 20 different batteries), Table A-2 the sequence of selection of motor (out of 14 different motors), and Table A-3 the sequence of selection of engine (out of 16 different engines) for US-EPA UDDS drive cycle. Table A-4 shows the sequence of selection of battery (out of 20 different batteries), Table A-5 the sequence of selection of motor (out of 14 different motors), and Table A-6 the sequence of selection of engine (out of 16 different engines) for Winnipeg weekday drive cycle. A total of 139 efficient hybridized sampling design points, with optimized multi-objective function values, were obtained from 57 iterations of US-EPA UDDS drive cycle and 42 iterations for Winnipeg weekday drive cycle using a convergence criterion of 1.015.

The results of mean fitness value for each iteration, number of battery modules, motor power (kW), and engine power (kW) for each sampling design point are shown in Table B-1 for US-EPA UDDS drive cycle and in Table B-4 for Winnipeg weekday drive cycle. The meta-model function used for hybridization and multi-objective optimization automatically calls PSAT^{TM} as a black box function, and finds the number of modules in the battery required to satisfy 20 miles of AER by using FZERO design optimization algorithm, and maximum desired motor and engine power (kW) required to satisfy 0-60 mph vehicle acceleration time specification of 10.5 (+0.0/-0.5) seconds by using FMINSEARCH design optimization algorithm. The results of hybridization factor values, electric efficiency (miles/kWh) of the vehicle in CD-mode, fuel efficiency (miles/gallon) of the vehicle in CS-mode, fuel economy (miles/gallon), vehicle operating cost ($/mile), and vehicle operation GHG emissions (kg/mile) for each sampling design point are shown in Table B-2 for US-EPA UDDS drive cycle and in Table B-5 for Winnipeg weekday drive cycle. The results for the number of most optimal Pareto design points, co-ordinates of the Pareto design points, and function values of the Pareto design points in terms

of fuel economy (miles/gallon), operating cost ($/mile) and operation GHG emissions (kg/mile), that converged after each iteration are shown in Table B-3 for US-EPA UDDS drive cycle and in Table B-6 for Winnipeg weekday drive cycle. Four Pareto design points (representing the most efficient hybridization combination of battery, motor, and engine) were obtained from 139 sampling design points for US-EPA UDDS drive cycle after 57 iterations, and three Pareto design points were obtained from 139 sampling design points for Winnipeg weekday drive cycle after 42 iterations for the Toyota Prius PHEV20 MY-04 vehicle. Therefore, the hybridization and multi-objective optimization model developed in this work, using PSAT^{TM} as a black box function, provides a very effective and efficient method of selecting the drivetrain components for PHEVs.

5.3.1 Simulation Results Using US-EPA UDDS Drive Cycle

The simulation results for Toyota Prius MY-04 vehicle using US-EPA UDDS drive cycle were obtained for a travel distance of 22.35 miles. Figure 5-4 shows the number of sampling design points and mean fitness value for each iteration. The ten sampling design points obtained in the first iteration define the meta-model function, which helps in selecting the sampling design points for the rest of the iterations. Metamodeling is the analysis, construction and development of the frames, rules, constraints, and theories applicable and useful for modeling a predefined class of problems within a certain domain. The number of sampling design points remain between 1 and 2 for iteration numbers 2 to 36, and then these vary between 1 and 7 for the rest of the iterations, which depends upon the non-linear function of the meta-model. The mean fitness value for each iteration varies between 1.04 and 2.00 and finally converges using convergence criteria of 1.015.The sampling design points in each iteration defines an optimized combination of battery, motor and engine under the given constraints of AER of 20 miles and maximum desired motor and engine power required to satisfy 0-60 mph vehicle acceleration time specification of 10.5 (+0.0/-0.5) seconds.

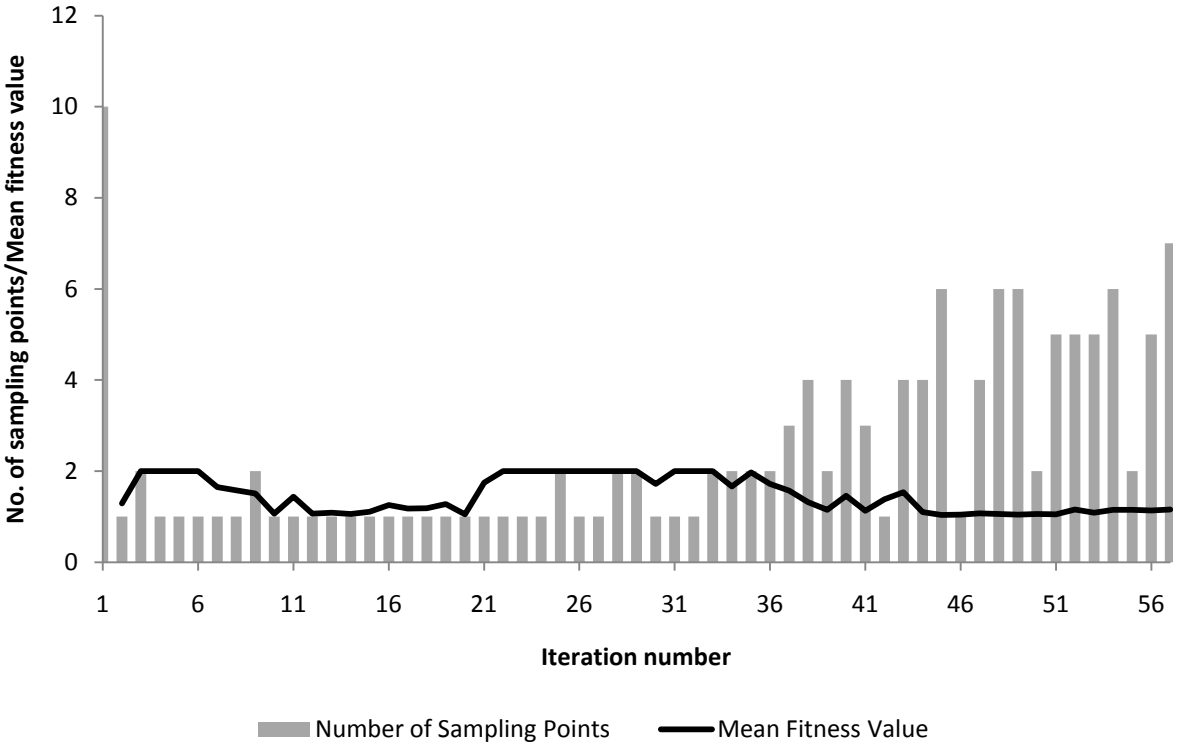

Figure 5-4. Number of sampling design points and mean fitness value for each iteration using US-EPA UDDS drive cycle

Figure 5-5 shows the amount of motor and engine power required for a defined battery capacity to satisfy 20 miles of AER in CD-mode and 10.5 seconds of vehicle acceleration time in CS-mode in each sampling design point using US-EPA UDDS drive cycle. The combinations of battery, motor and engine numbers with their sizes for each sampling design point are listed in Table B-1. The sampling design points marked with vertical lines (numbers: 1, 15, 18, 21, 31, 53, 72, 105, 114 and 128) represent Pareto design points, obtained from 139 sampling design points in 57 iterations, and show efficient combinations with optimum battery capacity, motor and engine power.

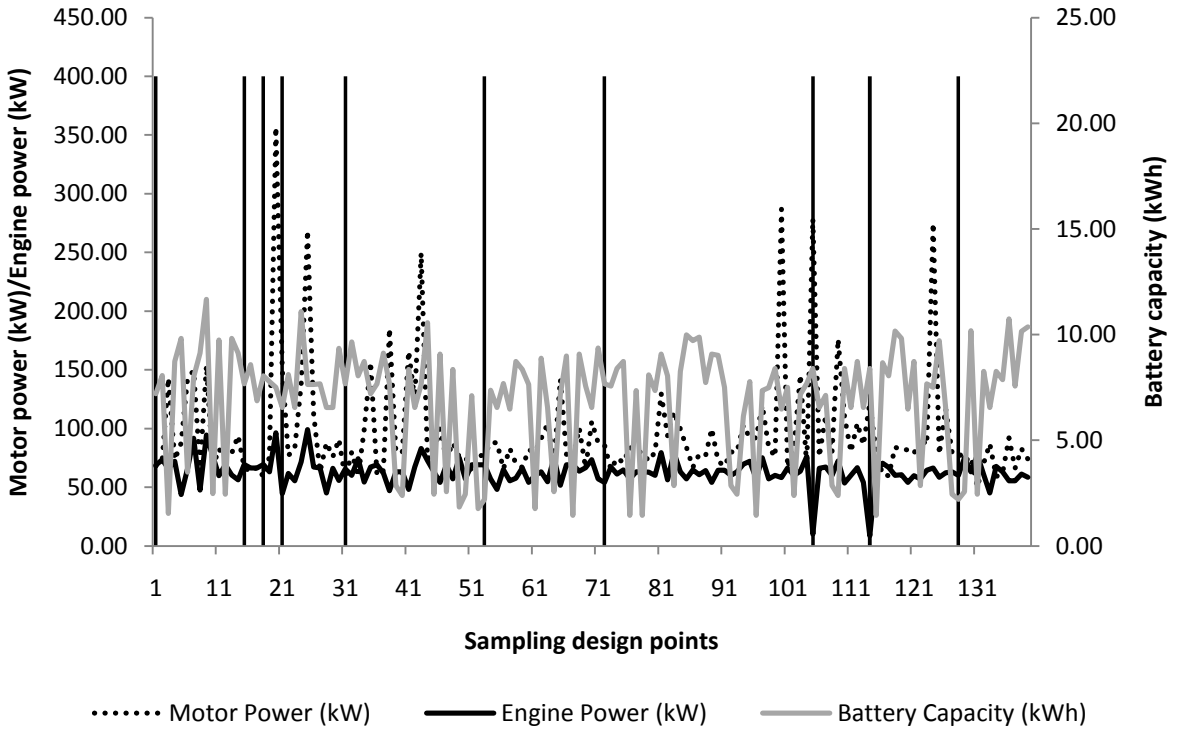

Figure 5-5. Motor and engine power (kW) with battery capacity (kWh) for each sampling design point using US-EPA UDDS drive cycle

Figure 5-6 shows the motor and engine power with hybridization factor for each sampling design point using US-EPA UDDS drive cycle. The sampling design points marked with vertical lines (numbers: 1, 15, 18, 21, 31, 53, 72, 105, 114 and 128) represent Pareto design points, obtained from 139 sampling design points in 57 iterations, and show optimum points of hybridization for Toyota Pirus PHEV20 MY-04 vehicle. The hybridization factors for each sampling design point are listed in Table B-2. The hybridization factor for the Pareto design points varies from 0.46 to 0.97. Since hybridization factor is the ratio of motor power to the total motor and engine power, a low hybridization factor indicates the selection of electric motor and gasoline engine with similar power, whereas a high hybridization factor indicates a combination of large electric motor with a small gasoline engine. For example, the Pareto design point 105 with a hybridization factor of 0.97 is made up of a combination of MY05 Ford Escape Hybrid MG2 type motor that works at a maximum desired power of 278.81kW and MY04 US Prius 1.497L gasoline engine that works at a maximum desired power of 10kW. Although, higher hybridization factor allows downsizing the gasoline engine and enhances fuel economy, further

increasing the hybridization factor beyond the optimum value, those provided by the Pareto frontier, could lead to lower energy conversion efficiency of the powertrain [26].

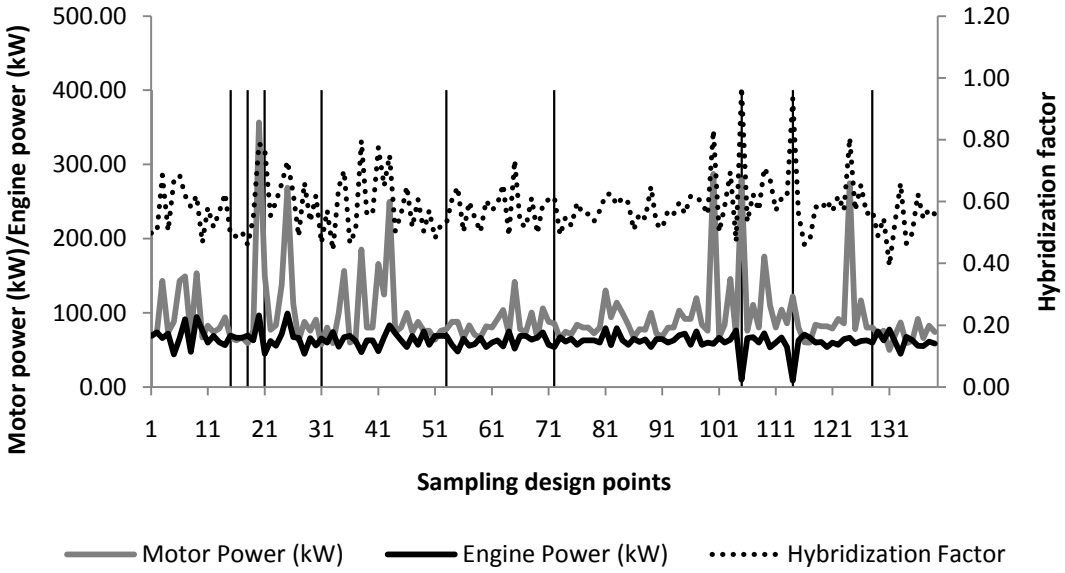

Figure 5-6. Motor and engine power (kW) with hybridization factor for each sampling design point using US-EPA UDDS drive cycle

The electrical efficiency (miles/kWh) of the vehicle in the charge depletion mode and fuel efficiency (miles/gallon) of the vehicle in the charge sustaining mode is calculated for all the 139 sampling design points using US-EPA UDDS drive cycle with battery capacity at 20 miles of AER and motor and engine power at 10.5 seconds acceleration time. The electrical efficiency (miles/kWh) of the vehicle in CD-mode depends upon the battery capacity (kWh). Figure 5-7 shows the electrical efficiency in CD-mode with battery capacity for each sampling design point. The fuel efficiency (miles/gallon) of the vehicle in CS-mode depends upon the engine power (kW). Figure 5-8 shows the fuel efficiency in CS-mode with engine power for each sampling design point. The sampling design points (numbers: 1, 15, 18, 21, 31, 53, 72, 105, 114 and 128) marked with vertical lines, define the optimum values for electrical efficiency with battery capacity and fuel efficiency with engine power, respectively in each figure. The electrical and fuel efficiency of each sampling design point are listed in the Table B-3. The electric efficiency in the CD-mode for the Pareto design points varies from 4.70 miles/kWh (battery capacity of 8.40 kWh) to 7.05 miles/kWh (battery capacity of 2.20 kWh). It seems that, the electric

efficiency of the Toyota Prius PHEV20 MY-04 vehicle is better for low battery capacities. The fuel efficiency in the CS-mode for the Pareto design points varies from 65.36 miles/gallon (engine power of 69 kW) to 193.20 miles/gallon (engine power of 8.63 kW). Therefore, the fuel efficiency of the Toyota Prius PHEV20 MY-04 vehicle is higher for smaller engines. NiMH Panasonic battery is used in Japan Prius, represented by the Pareto design point, with cell capacity of 6.5Ah gives the highest electric efficiency of 7.05 miles/kWh, whereas 1.5L 43kW Japan Prius gasoline engine, also represented by the Pareto design point, gives the highest fuel efficiency of 193.20 miles/gallon.

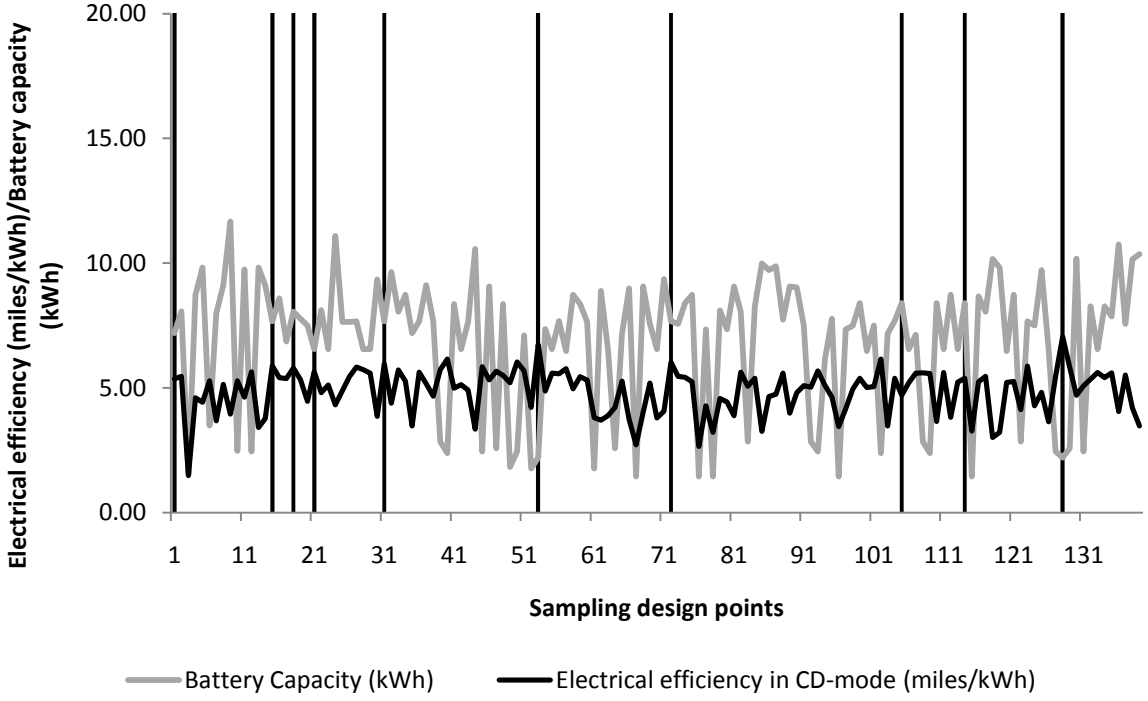

Figure 5-7. Electrical efficiency (miles/kWh) and battery capacity (kWh) in CD-mode for each sampling design point using US-EPA UDDS drive cycle

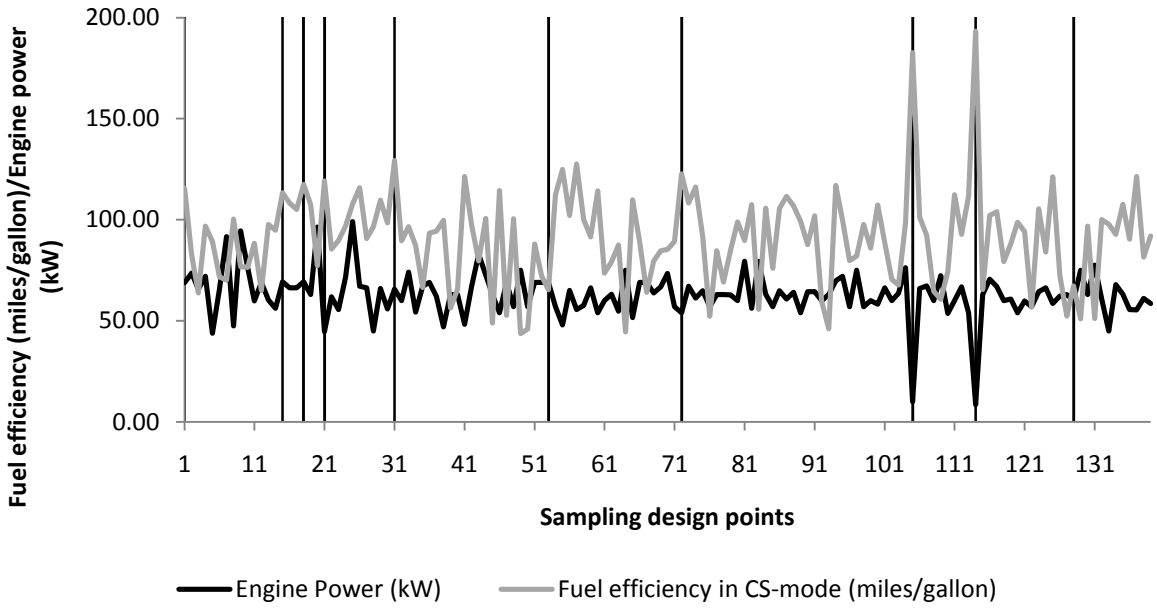

Figure 5-8. Fuel efficiency (miles/gallon) and engine power (kW) in CS-mode for each sampling design point using US-EPA UDDS drive cycle

The results of multi-objective optimization for function values of fuel efficiency (miles/gallon), operation cost ($/mile), and operation GHG emissions (kg/mile) for 139 sampling design point, obtained in 57 iterations using PSP algorithm calling PSAT^{TM} simulator as a black box function are shown in Figure 5-9. The 3D-plot also shows all the Pareto design points (numbers: 1, 15, 18, 21, 31, 53, 72, 105, 114 and 128) marked as grey dots obtained from 139 sampling design points in 57 iterations using US-EPA UDDS drive cycle. At the end of the final (57^{th}) iteration, four Pareto design points, out of a total of 139 sampling design points, were found that represent the most optimal hybridization combinations of battery, motor and engine for Toyota Prius PHEV20 MY-04, using US-EPA UDDS drive cycle. These final four Pareto design points (numbers: 31, 72, 114, and 128) with mean fitness value of 1.16, obtained in the final iteration are shown in Figure 5-10.

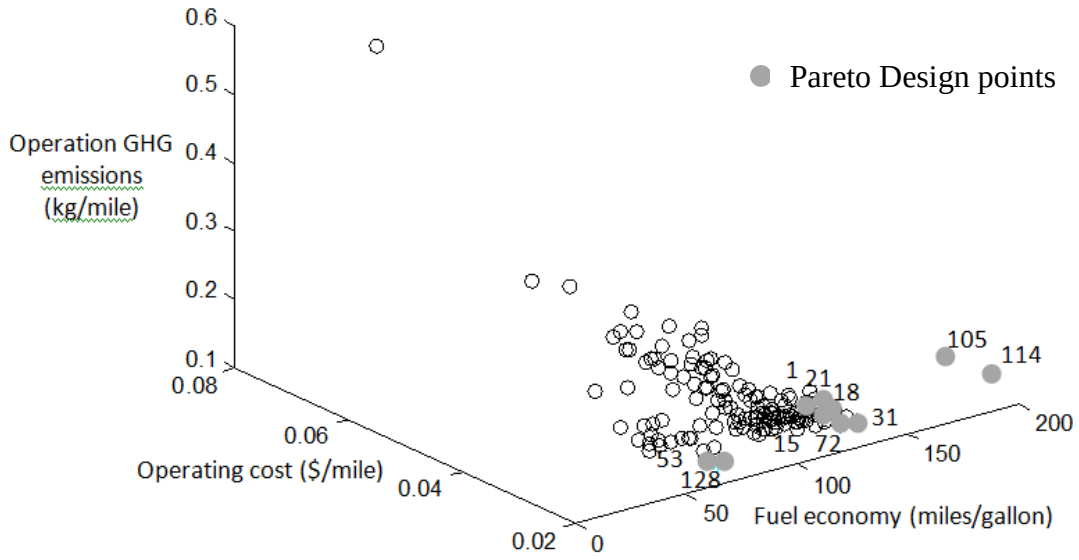

Figure 5-9. Fuel Efficiency (miles/gallon), operation cost ($/mile) and operation GHG emissions (kg/mile) for all 139 sampling design points using US-EPA UDDS drive cycle

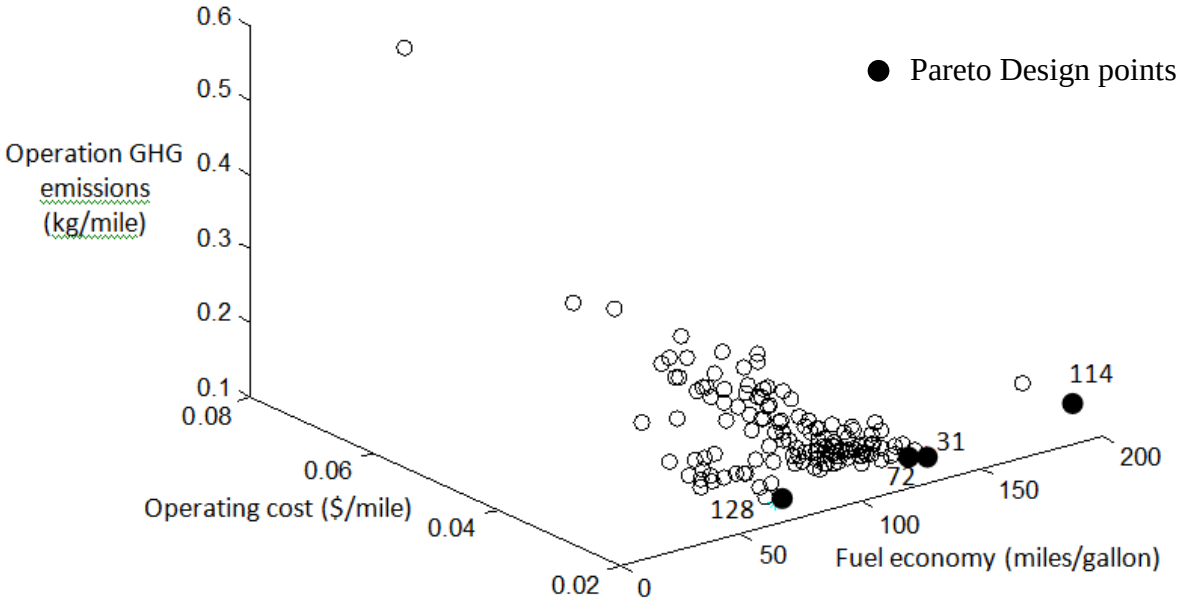

Figure 5-10. Fuel Efficiency (miles/gallon), operation cost ($/mile) and operation GHG emissions (kg/mile) including the final four Pareto design points obtained in the 57th iteration using US-EPA UDDS drive cycle

Table 5-7 shows the co-ordinates, function values, and parameters of the four most optimum hybridization combinations of battery, motor and engine represented by the Pareto design points for Toyota Prius PHEV20 MY-04. These four combinations provide the most optimum values of the objective functions: fuel efficiency (miles/gallon), operation cost ($/mile), and operation GHG emissions (kg/mile) under the given constraint. Table 5-8 provides the details of the battery, motor and engine for the Pareto design points of Toyota Prius PHEV20 MY-04 vehicle model using US-EPA UDDS drive cycle.

Table 5-7. Co-ordinates and function values of the final Pareto design points (PDP) using US-EPA UDDS drive cycle

Sampling Design Point	Co-ordinates of PDPs			Function Value of PDPs			Parameters of the PDPs		
	Battery No.	Motor No.	Engine No.	Fuel Economy (mpg)	Operation Cost ($/mile)	GHG Emissions (kg/mile)	Number of Battery Modules	Motor Power (kW)	Engine Power (kW)
114	19	8	4	193.20	0.022	0.144	25	122.00	8.63
128	7	6	5	67.21	0.021	0.123	51	80.00	60.00
31	1	1	3	129.31	0.021	0.134	101	57.20	65.63
72	1	6	1	122.73	0.021	0.133	101	86.00	54.00

Table 5-8. Battery, motor and engine types for Pareto design points using US-EPA UDDS drive cycle

Battery No.	**Battery Type**
19	Johnson Controls lead acid battery, Capacity = 28Ah, Cell number = 150
7	NiMH Panasonic battery used in Japan Prius, Capacity = 6.5Ah, Cell number = 240
1	Saft Li-ion battery, Capacity = 6Ah, Cell number = 75
1	Saft Li-ion battery, Capacity = 6Ah, Cell number = 75
Motor No.	**Motor Type**
8	UQM PowerPhase75 (Unique Mobility), Continuous power = 36kW, Peak power = 75kW
6	MY05 Ford Escape Hybrid MG1, Continuous power = 33kW, Peak power = 65kW
1	MY04 Toyota Prius Mobility, Continuous power = 25kW, Peak power = 50kW
6	MY05 Ford Escape Hybrid MG1, Continuous power = 33kW, Peak power = 65kW
Engine No.	**Engine Type**
4	1.5L 43kW Japan Prius gasoline engine
5	1.5L 52kW MY01US Prius gasoline engine
3	Honda Insight 1.0L VTEC-E gasoline engine
1	1.497L 57kW MY04 US Prius gasoline engine

5.3.2 Simulation Results Using Winnipeg Weekday Drive Cycle

The simulation results for Toyota Prius MY-04 vehicle using Winnipeg weekday drive cycle were obtained for a travel distance of 22.35 miles. Figure 5-11 shows the number of sampling design points and mean fitness value for each iteration. The ten sampling design points obtained in the first iteration define the meta-model function, which helps in selecting the sampling design points for the rest of the iterations. The number of sampling design points remain between 1 and 3 for iteration numbers 2 to 11, and then these vary between 1 and 7 for the rest of the iterations, which depends upon the non-linear function of the meta-model. The mean fitness value for each iteration varies between 1.04 and 1.59 and finally converges using convergence criteria of 1.015. The sampling design points in each iteration defines an optimized combination of battery, motor and engine under the given constraints of AER of 20 miles and maximum desired motor and engine power required to satisfy 0-60 mph vehicle acceleration time specification of 10.5 (+0.0/-0.5) seconds.

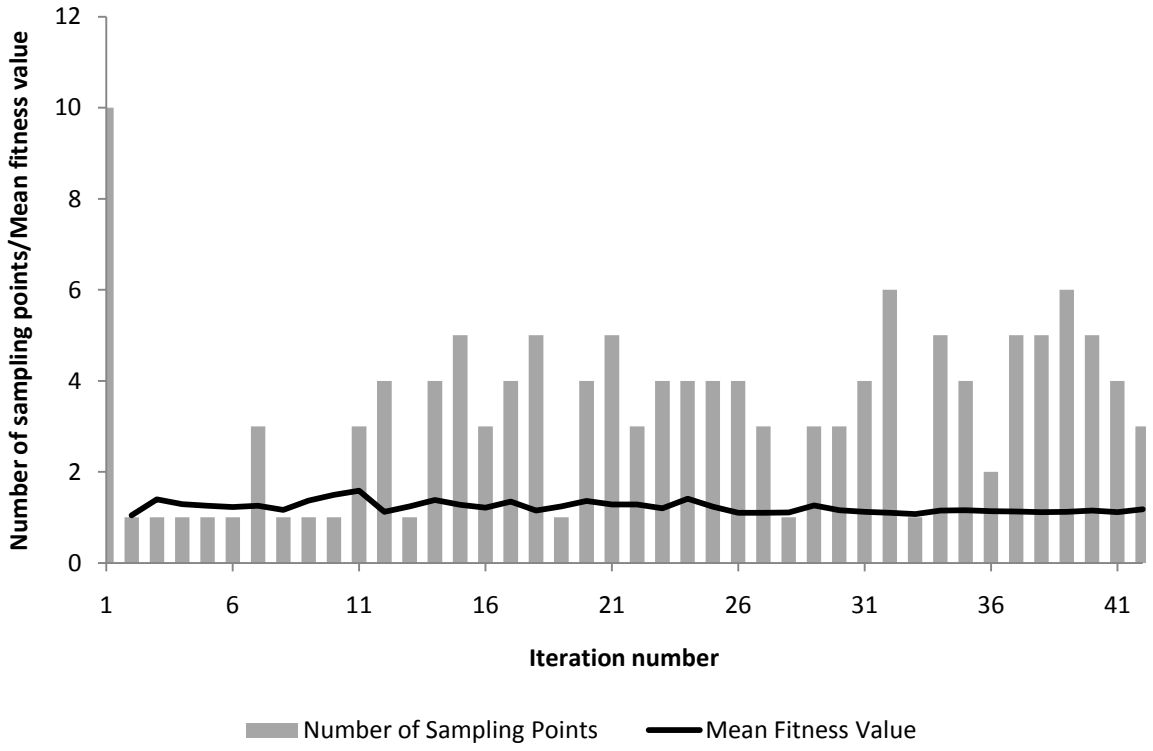

Figure 5-11. Number of sampling design points and mean fitness value for each iteration using Winnipeg weekday drive cycle

Figure 5-12 shows the amount of motor and engine power required for a defined battery capacity to satisfy 20 miles of AER in CD-mode and 10.5 seconds of vehicle acceleration time in CS-mode in each sampling design point using Winnipeg weekday drive cycle. The sampling design points marked with vertical lines (numbers: 5, 8, 10, 13, 16, 18, 30, 39, 56, and 71) represent Pareto design points, obtained from 139 sampling design points in 42 iterations, and show efficient combinations with optimum battery capacity, motor and engine power.

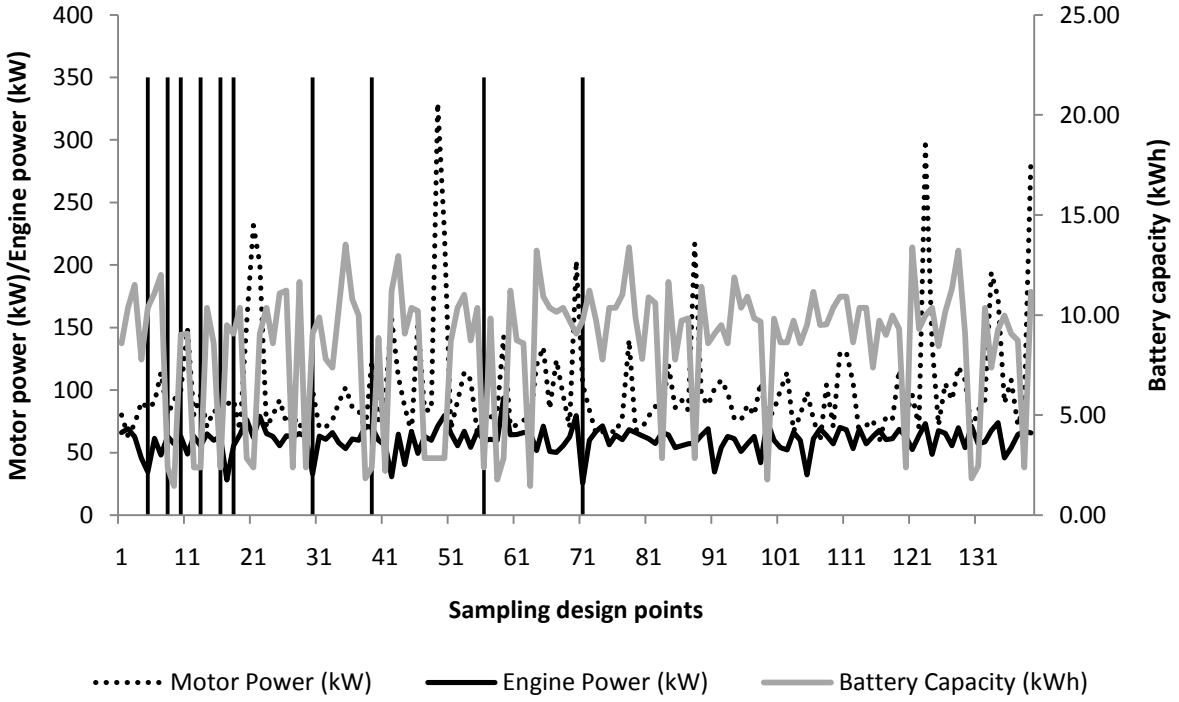

Figure 5-12. Motor and engine power (kW) with battery capacity (kWh) for each sampling design point using Winnipeg weekday drive cycle

Figure 5-13 shows the motor and engine power with hybridization factor for each sampling design point using Winnipeg weekday drive cycle. The sampling design points marked with vertical lines (numbers: 5, 8, 10, 13, 16, 18, 30, 39, 56, and 71) represent Pareto design points, obtained from 139 sampling design points in 42 iterations, and show optimum points of hybridization for Toyota Prius PHEV20 MY-04 vehicle with larger motor and smaller engine sizes. The hybridization factors for each sampling design point are listed in Table B-5. The hybridization factor for the Pareto design points varies from 0.56 to 0.84. For example, the Pareto design point 42 with a hybridization factor of 0.84 is made up of a combination of Toyota

Camry MG1 type motor that works at a maximum desired power of 157.36 kW and 1.5L 43kW Japan Prius gasoline engine that works at a maximum desired power of 30.60 kW. The highest hybridization factor obtained from the Pareto design points of Winnipeg weekday drive cycle is lower than that of US-EPA UDDS drive cycle, and uses a smaller motor and a bigger gasoline engine. Therefore, higher hybridization factor of the powertrain performs better for lower average load applications, as in Winnipeg weekday drive cycle, as compared to test cycles with heavy duty applications.

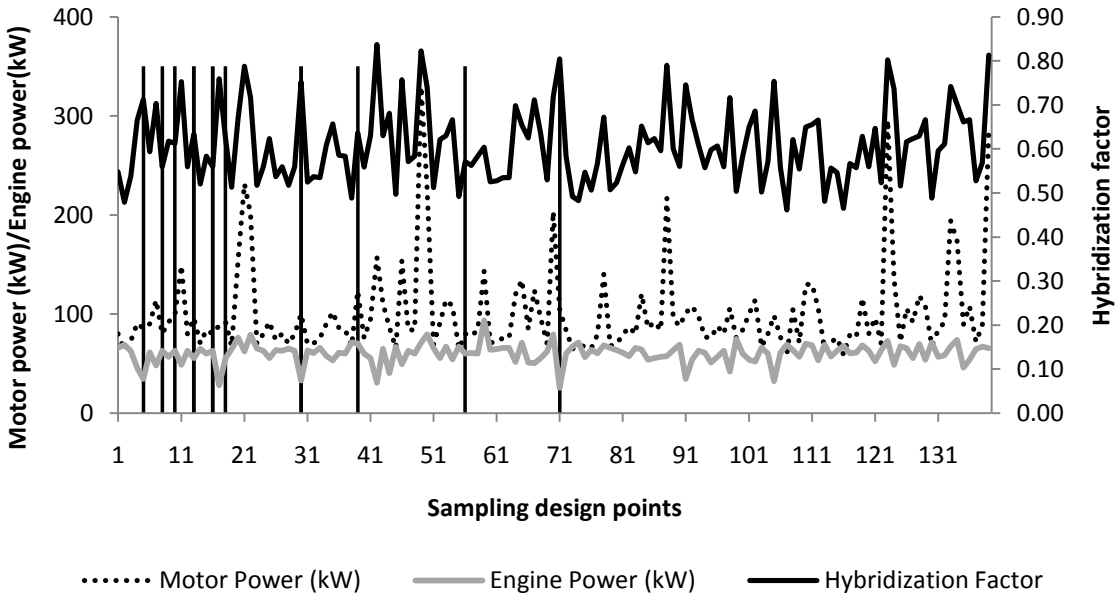

Figure 5-13. Motor and engine power (kW) with hybridization factor for each sampling design point using Winnipeg weekday drive cycle

The electrical efficiency (miles/kWh) of the vehicle in the charge depletion mode and fuel efficiency (miles/gallon) of the vehicle in the charge sustaining mode is calculated for all the 139 sampling design points using Winnipeg weekday drive cycle with battery capacity at 20 miles of AER and motor and engine power at 10.5 seconds acceleration time. The electrical efficiency (miles/kWh) of the vehicle in CD-mode depends upon the battery capacity (kWh). Figure 5-14 shows the electrical efficiency in CD-mode with battery capacity for each sampling design point. The fuel efficiency (miles/gallon) of the vehicle in CS-mode depends upon the engine power (kW). Figure 5-15 shows the fuel efficiency in CS-mode with engine power for each sampling design point. The sampling design points (numbers: 5, 8, 10, 13, 16, 18, 30, 39, 56, and 71) marked with vertical lines, define the optimum values for electrical efficiency with battery capacity and fuel efficiency with engine power, respectively in each figure. The electrical and

fuel efficiency of each sampling design point are listed in the Table B-6. The electric efficiency in the CD-mode for the Pareto design points varies from 4.14 miles/kWh (battery capacity of 10.37 kWh) to 6.38 miles/kWh (battery capacity of 2.39 kWh). It seems that, the electric efficiency of the Toyota Prius PHEV20 MY-04 vehicle is better for low battery capacities. The fuel efficiency in the CS-mode for the Pareto design points varies from 51.49 miles/gallon (engine power of 63 kW) to 109.96 miles/gallon (engine power of 25.5 kW). Therefore, the fuel efficiency of the Toyota Prius PHEV20 MY-04 vehicle is higher for smaller engines. NiMH Panasonic battery is used in the MY01 Japan Prius, represented by a Pareto design point, with cell capacity of 6.5Ah gives the highest electric efficiency of 6.38 miles/kWh, whereas 1.8L 99kW Ford gasoline engine, also represented by a Pareto design point, gives the highest fuel efficiency of 109.96 miles/gallon.

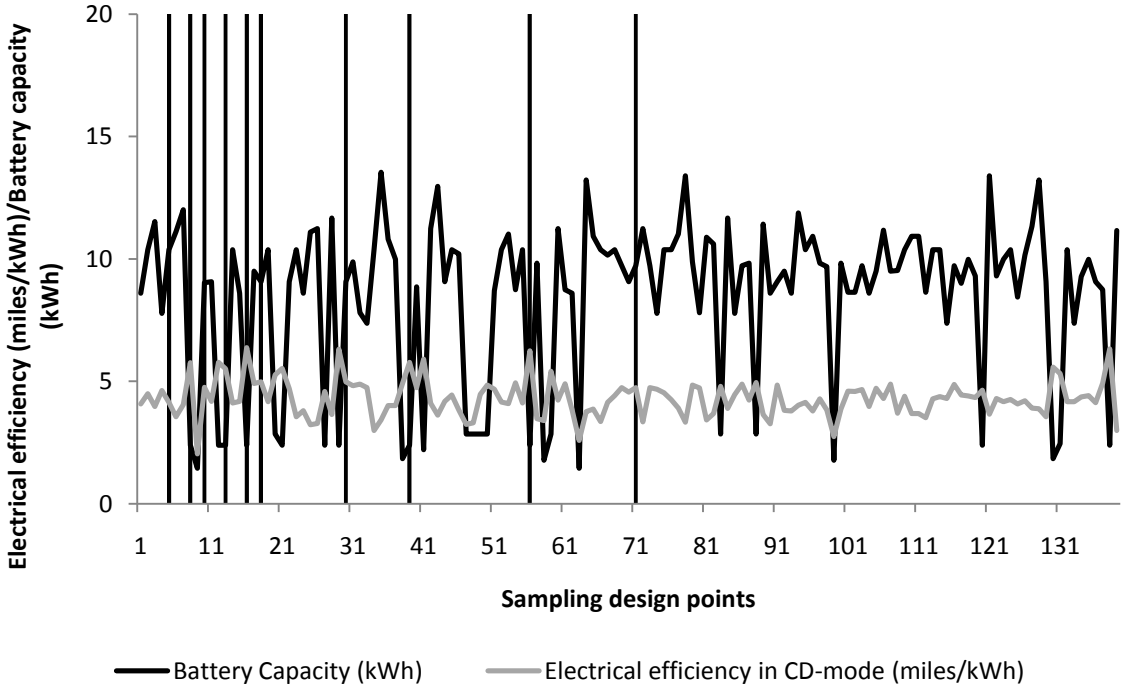

Figure 5-14. Electrical efficiency (miles/kWh) and battery capacity (kWh) in CD-mode for each sampling design point using Winnipeg weekday drive cycle

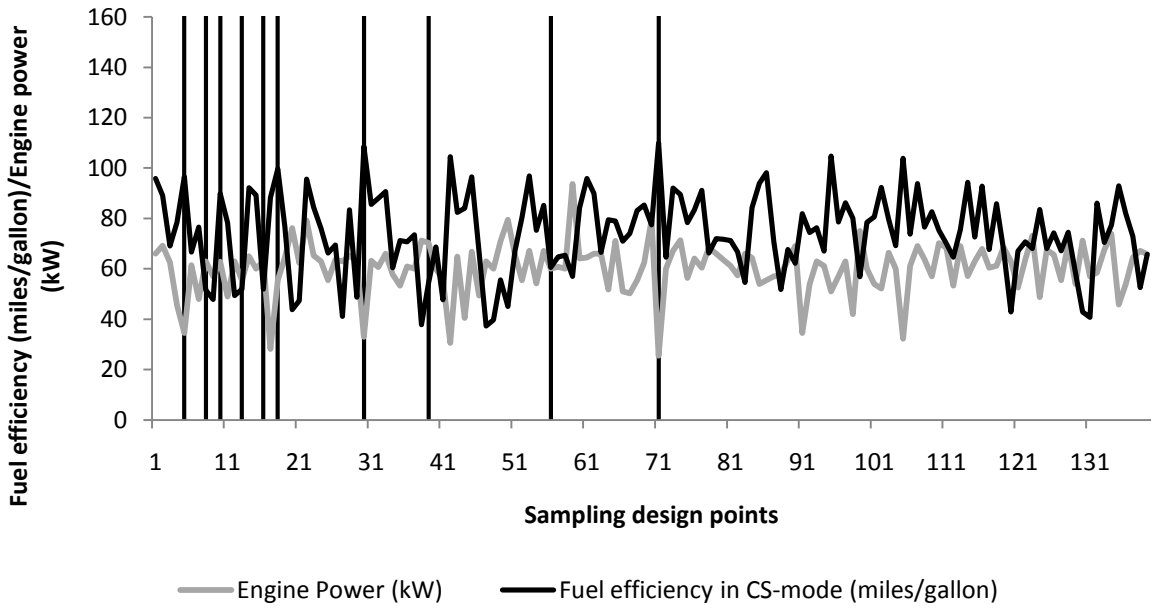

Figure 5-15. Fuel efficiency (miles/gallon) and engine power (kW) in CS-mode for each sampling design point using Winnipeg weekday drive cycle

The results of multi-objective optimization for function values of fuel efficiency (miles/gallon), operation cost ($/mile), and operation GHG emissions (kg/mile) for 139 sampling design point, obtained in 42 iterations using PSP algorithm calling PSAT^{TM} simulator as a black box function are shown in Figure 5-16. The 3D-plot also shows all the Pareto design points (numbers: 5, 8, 10, 13, 16, 18, 30, 39, 56, and 71) marked as grey dots obtained from 139 sampling design points in 57 iterations using Winnipeg weekday drive cycle. At the end of the final (42nd) iteration, three Pareto design points, out of a total of 139 sampling design points, were found that represent the most optimal hybridization combinations of battery, motor and engine for Toyota Prius PHEV20 MY-04, using Winnipeg weekday drive cycle. These final four Pareto design points (numbers: 30, 56, and 71) with mean fitness value of 1.18, obtained in the final iteration are shown in Figure 5-17.

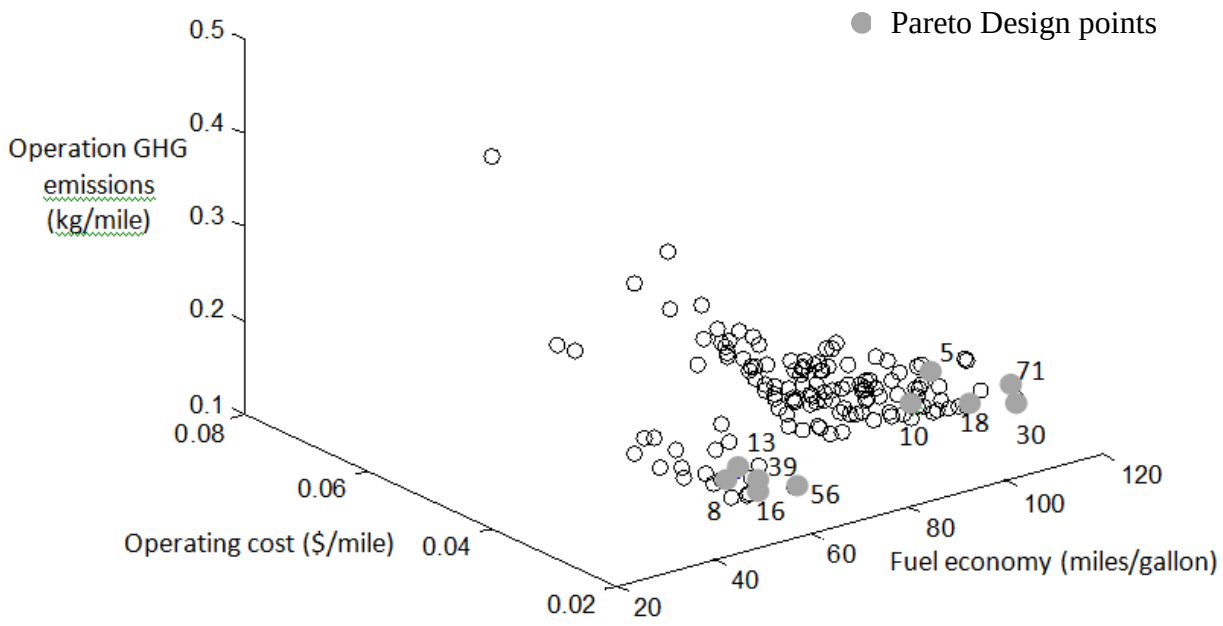

Figure 5-16. Fuel Efficiency (miles/gallon), operation cost ($/mile) and operation GHG emissions (kg/mile) for all 139 sampling design points using Winnipeg weekday drive cycle

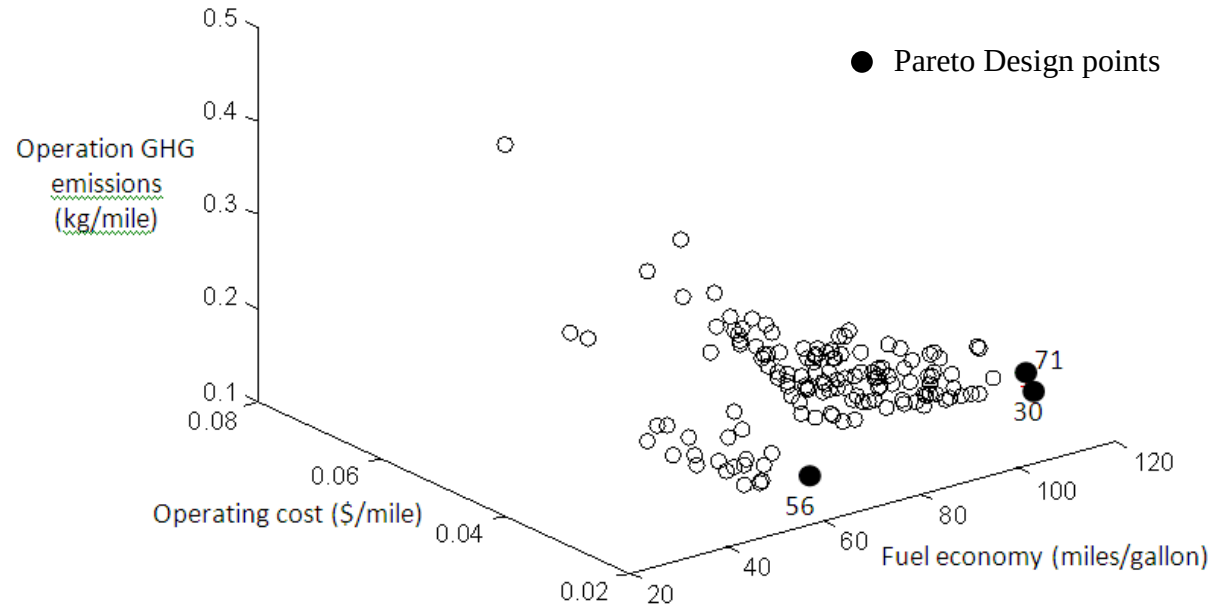

Figure 5-17. Fuel Efficiency (miles/gallon), operation cost ($/mile) and operation GHG emissions (kg/mile) including the final four Pareto design points obtained in the 42nd iteration using Winnipeg weekday drive cycle

Table 5-9 shows the co-ordinates, function values, and parameters of the three most optimum hybridization combinations of battery, motor and engine represented by the Pareto design points for Toyota Prius PHEV20 MY-04. These three combinations provide the most optimum values of the objective functions: fuel efficiency (miles/gallon), operation cost ($/mile), and operation GHG emissions (kg/mile) under the given constraint. Table 5-10 provides the details of the battery, motor and engine for the Pareto design points of Toyota Prius PHEV20 MY-04 vehicle model using Winnipeg weekday drive cycle.

Table 5-9. Co-ordinates and function values of the final Pareto design points (PDP) using Winnipeg weekday drive cycle

Sampling Design Point	Co-ordinates of PDPs			Function Value of PDPs			Parameters of the PDPs		
	Battery No.	Motor No.	Engine No.	Fuel Economy (mpg)	Operation Cost ($/mile)	GHG Emissions (kg/mile)	Number of Battery Modules	Motor Power (kW)	Engine Power (kW)
56	1	8	2	60.50	0.023	0.139	51	80.00	60.00
30	20	8	3	108.54	0.025	0.160	7	100.00	33.00
31	19	8	9	109.96	0.027	0.167	15	105.00	25.50

Table 5-10. Battery, motor and engine types for Pareto design points using Winnipeg weekday drive cycle

Battery No.	**Battery Type**
1	NiMH Panasonic battery used in the MY01 Japan Prius, Capacity = 6.5Ah, Cell number = 240
20	Ovonic NiMH battery, Capacity = 90Ah, Cell number = 300
19	Ovonic P127 NiMH battery, Capacity = 45Ah, Cell number = 300
Motor No.	**Motor Type**
8	MY04 Toyota Prius Mobility, Continuous power = 25kW, Peak power = 50kW
Engine No.	**Engine Type**
2	1.5L 43kW Japan Prius gasoline engine
3	Honda Insight 1.0L VTEC-E gasoline engine
9	1.8L 99kW Ford gasoline engine

5.3.3 Comparison of US-EPA UDDS and Winnipeg Weekday Drive Cycle Results

The simulation results of US-EPA UDDS and Winnipeg weekday drive cycles were compared to check the performance of Toyota Prius PHEV20 MY-04 vehicle model on two different

platforms. The standard UDDS was primarily developed to estimate vehicle emissions inventories and, therefore, cannot completely emulate the real-world daily power demand of a vehicle. The Winnipeg weekday drive cycle, on the other hand, is a driving profile representing the average driving behavior of a fleet of cars in a representative city of North America. The Winnipeg weekday drive cycle uses average power demand and average breaking power to establish a more comprehensive set of performance measures for power management in PHEVs.

For checking the performance of Toyota Prius PHEV20 MY-04 vehicle model, the main difference between the two drive cycles in this research work was the ordering of battery, motor, and engine for simulations. In UDDS drive cycle, the ordering of the components battery, motor and engine for simulation are selected arbitrarily as available in PSAT^{TM} while in Winnipeg weekday drive cycle the ordering of the components is done as per the ascending order of battery specific energy (Wh/kg) and motor and engine maximum desired power (kW), respectively. Figure 5-18 shows the comparison of the number of sampling design points selected in each iteration during simulation runs for both drive cycles. It is observed that the Winnipeg weekday drive cycle generates more sample points in the iterations as compared to the US-EPA UDDS drive cycle. Overall, in order to generate 139 simulation sampling design points from a total set of 4480 combinations, UDDS took 57 iterations while Winnipeg weekday drive cycle took only 42 iterations.

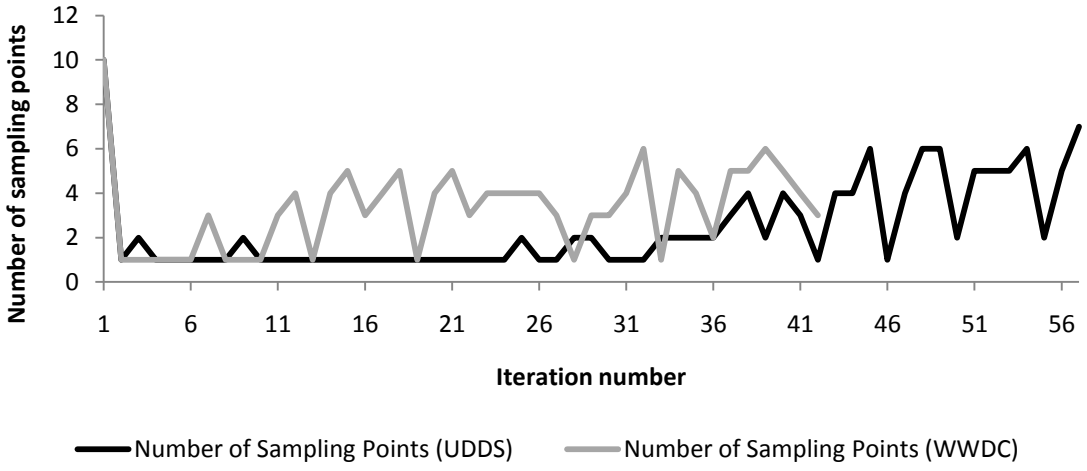

Figure 5-18. Comparison of sampling design points in each iteration of UDDS and WWDC drive cycles

Figure 5-19 shows the comparison of mean fitness value generated at each iteration during simulation runs for both drive cycles. The mean fitness value generated by the Winnipeg weekday drive cycle is closer to 1 as compared to the US-EPA UDDS drive cycle. Therefore, the Winnipeg weekday drive cycle performs better in terms of generating the sampling design points and the mean fitness value.

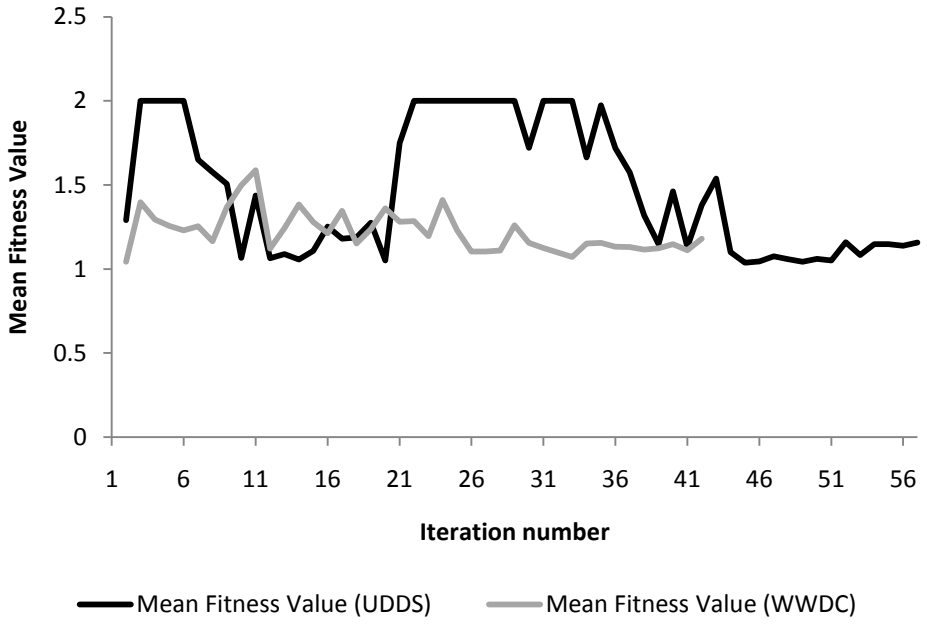

Figure 5-19. Comparison of mean fitness value at each iteration of UDDS and WWDC drive cycles

Figure 5-20 shows the comparison of generating number of Pareto design points after each iteration for both drive cycles. It is observed that the Winnipeg weekday drive cycle generates more Pareto desing points, thereby indicating its superiority in performance, as compared to the US-EPA UDDS drive cycle in each iteration. Although, at the end of 139 sampling design points, the US-EPA UDDS drive cycle generates one more Pareto design point as compared to the Winnipeg weekday drive cycle.

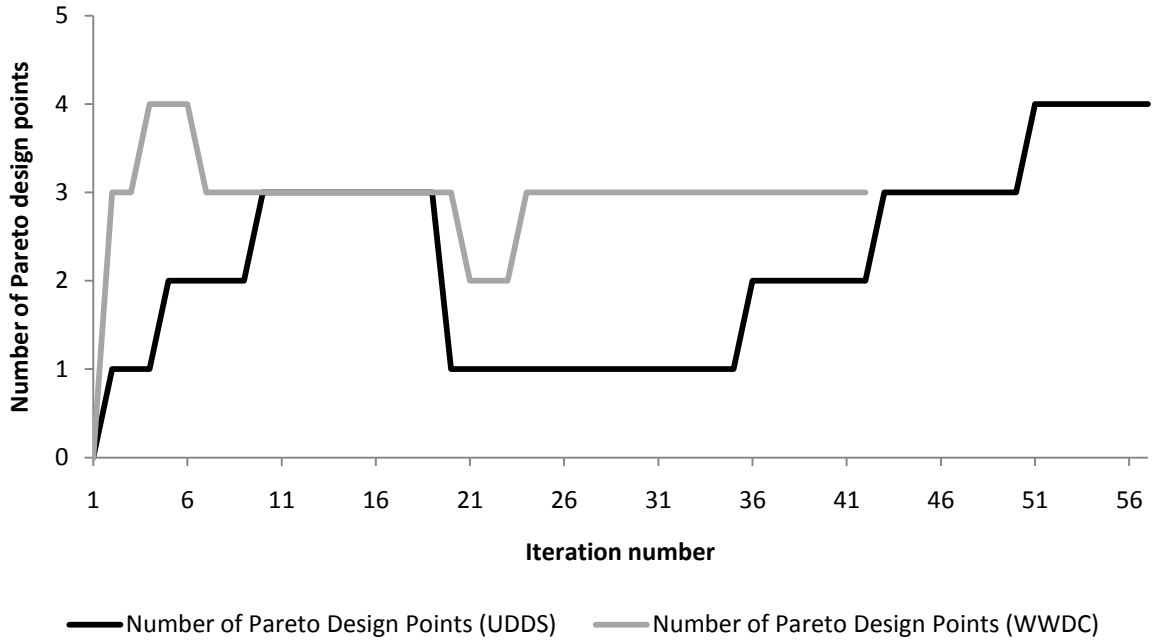

Figure 5-20. Comparison of number of Pareto design points after each iteration in UDDS and WWDC drive cycles

The history of convergence for the three objective functions: (i) fuel economy (miles/gallon), (ii) operating cost ($/mile), and (iii) operation GHG emissions ($/kg) of all the sampling design points is compared for both drive cycles. Figure 5-21, Figure 5-22, and Figure 5-23 shows the history of convergence for all the sampling design points for fuel economy (miles/gallon), operating cost ($/mile), and operation GHG emissions (kg/mile), respectively for both drive cycles. It is observed that the US-EPA UDDS drive cycle gives a better fuel economy, operating cost, and operation GHG emissions as compared the Winnipeg weekday drive cycle. On an average, the US-EPA UDDS drive cycle provides a fuel economy of 90.90 miles/gallon, whereas Winnipeg weekday drive cycle provides a fuel economy of 74.13 miles/gallon. UDDS gives an average operating cost of 0.028 $/mile, whereas Winnipeg weekday drive cycle gives 0.031 $/ mile, and UDDS gives an average operation GHG emissions of 0.174 kg/mile, whereas Winnipeg weekday drive cycle gives 0.195 kg/mile.This is because the Winnipeg weekday drive cycle represents the average driving behavior in city conditions and takes into account average power demand and breaking power. Therefore, the Winnipeg weekday drive cycle establishes a more realistic set of performance measures for all the three objective functions for PHEV's design.

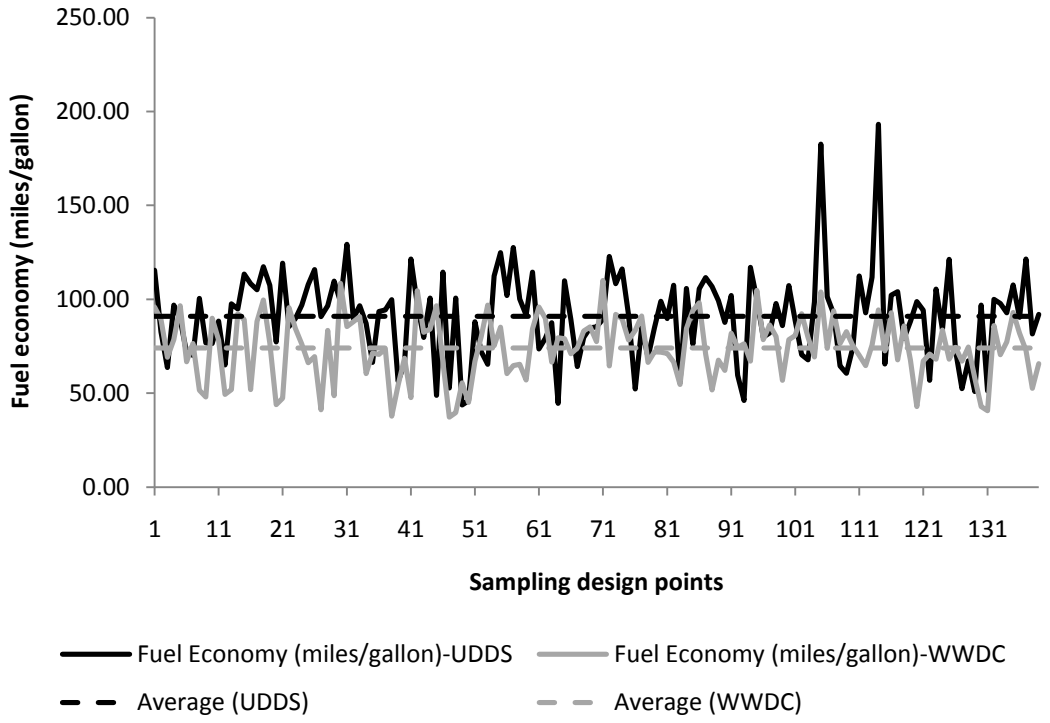

Figure 5-21. History of convergence of sampling design points with the fuel economy (miles/gallon) in UDDS and WWDC drive cycles

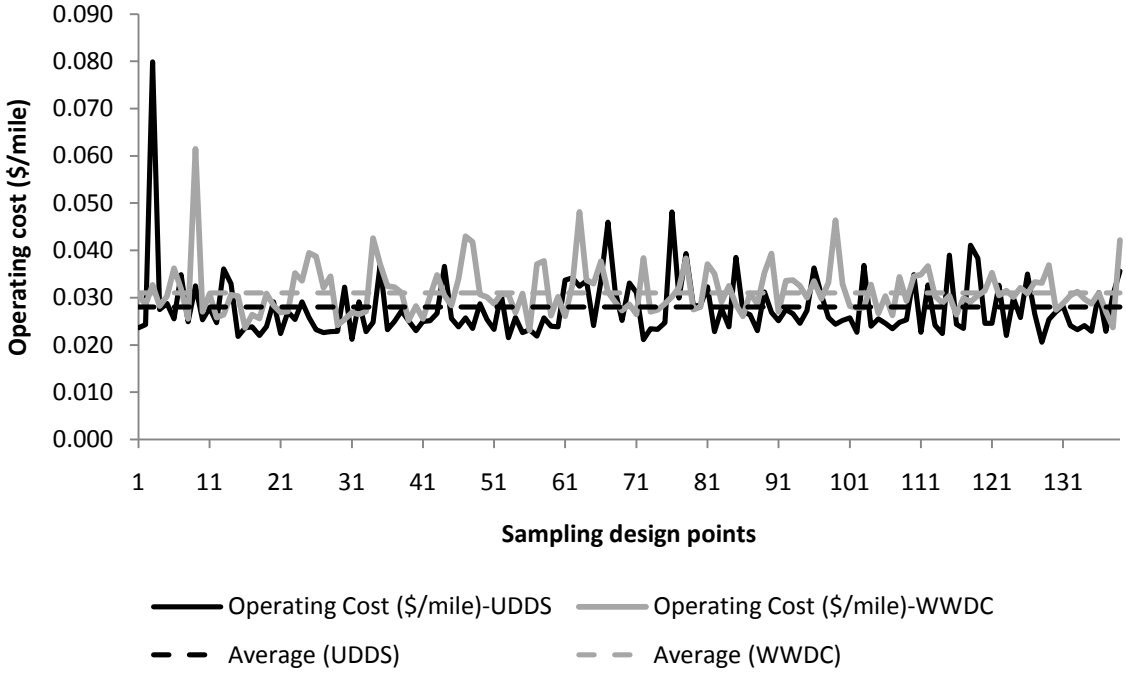

Figure 5-22. History of convergence of the sampling design points with the operating cost ($/mile) in UDDS and WWDC drive cycles

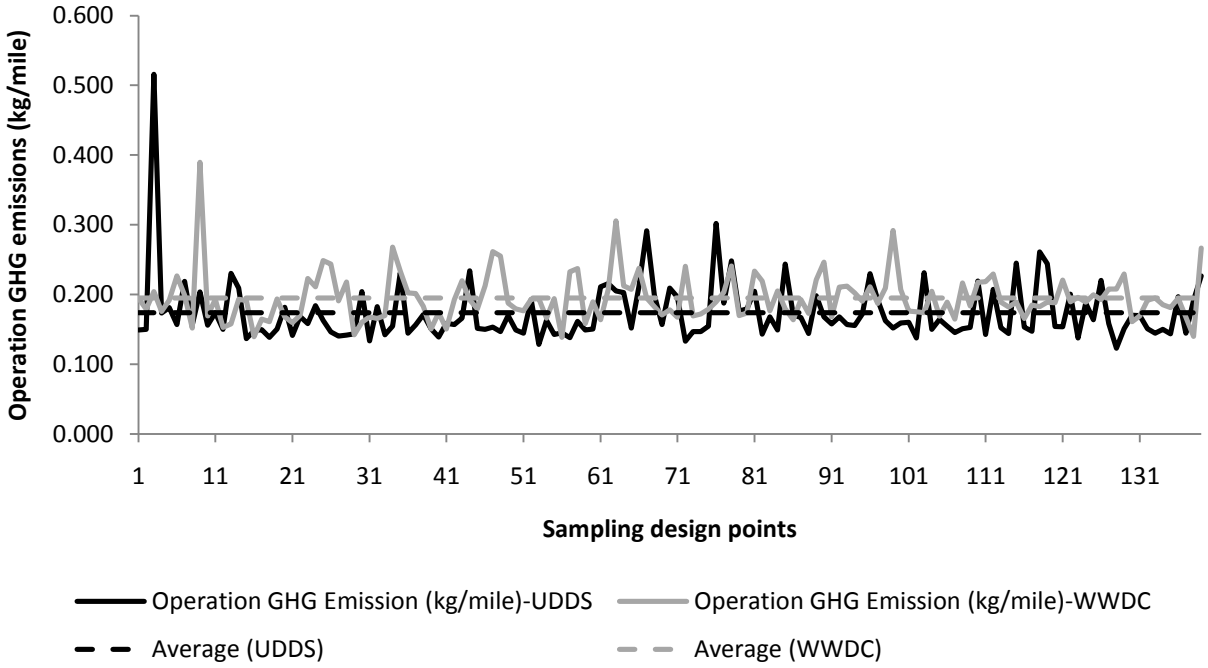

Figure 5-23. History of convergence of the sampling design points with the operation GHG emission (kg/mile) in UDDS and WWDC drive cycles

From the above results, it is clear that battery, motor, and engine work collectively in defining an optimal hybridization scheme for optimum performance of PHEVs. In addition, the optimal hybridization scheme varies with drive cycles. It is also established that the proposed simulation and optimization model is an effective and efficient method in finding the best hybridization combination for PHEVs with respect to a given drive cycle. To the best of my knowledge, it is the first time that multi-objective optimization has been applied for PHEV hybridization design and the optimization has been automated with PSAT^{TM} .

Chapter 6

Conclusions

The purpose of this research was to test the operational performance of Toyota Prius PHEV20 under different driving conditions, and develop an optimum hybridization of ICE, electric motor, and storage battery parameters based on fuel economy, operating cost, and GHG emissions. The hybridization and optimization model developed in this work calls PSAT^{TM} simulator as a black box and uses Pareto set pursuing algorithm for multi-objective optimization of fuel economy, operating cost, and operation GHG emissions. The model tests and compares the optimal hybridization performance from a pool of 4480 combinations (involving 20 batteries, 14 permanent electric motors and 16 spark ignition engines), by simulating the Toyota Prius PHEV20 MY-04 vehicle on two different drive cycles: US EPA-UDDS and Winnipeg weekday drive cycle. Since PHEVs and HEVs are now being actively developed by many car companies, due to their significant potential in reducing fuel consumption and GHG emissions, I used the simulation and optimization model to test the performance of both PHEV and HEV based on the Prius platform under different driving conditions. The simulation and optimization model was also used to evaluate the operational performance of Toyota Prius PHEV20 MY-04 vehicle for 15 different types (including lithium-ion, nickel metal hydride, nickel zinc, and lead acid) of batteries.

The modeling and simulation results indicate that there is substantial improvement in performance parameters for Toyota Prius PHEV over HEV, including fuel economy, fuel mass, CO_2 emissions, wheel mechanical brake energy loss, and maximum grade. These results convey important information to make the PHEVs an attractive proposition. The results of operational performances of Toyota Prius PHEV20 MY-04 vehicle for 15 different types of batteries, with the constraints to achieve the same required acceleration and AER of 20 miles, indicate two clear winners from the group and seven other currently available batteries offer competitive advantages if viewed from fuel economy, operation cost, and GHG emissions simultaneously. Nickel Zinc battery is not as competitive as others. Nickel metal hydride gives the highest fuel

economy, while lithium-ion yields the lowest operating costs and GHG emissions. When comparing different types of batteries, lithium-ion and nickel metal hydride batteries provide more attractive performances than others, with a few lead acid batteries giving similar performances. Finally, the results of optimum hybridization of Toyota Prius PHEV20 MY-04 vehicle under different driving conditions show that battery, motor, and engine work collectively in defining an optimal hybridization scheme for optimum performance of PHEVs. In addition, the optimal hybridization scheme varies with drive cycles.

The scope of this research is limited to the data produced by the computer based PSAT^{TM} simulation model for different drive cycles. The analysis is only valid for 4480 combinations of variables (20 batteries, 14 motors, and 16 engines) selected for this study. Since the performance of blended configurations can vary widely based on a broad range of control strategy parameters, for simplicity we restricted our attention to the range-extended PHEVs that run entirely on electrical power in the CD-range and switch to operate like an HEV in the CS-mode. Another limitation of this study is that the simulation time is very high. It takes 3 hours to obtain one design point from the simulations. High speed processors are therefore, required for conducting simulations using our model.

6.1 Contributions

The main contributions of this thesis can be categorized from theoretical and practical perspectives as below.

6.1.1 Theoretical Contributions

It is the first time that multi-objective optimization has been applied for PHEV drivetrain components hybridization design. The simulation and optimization models have been automated with PSAT^{TM} simulator as a black box. It has also been established that the proposed simulation and optimization model is an effective and efficient method in finding the best hybridization combination for PHEVs drivetrain components with respect to a given drive cycle.

6.1.2 Practical Contributions

The hybridization and multi-objective optimization model developed in this research work helps in comparing the operational performance of Toyota Prius PHEV20 under different driving conditions based on fuel economy, operating cost, and GHG emissions. The comparison helps in building the confidence of HEV and PHEV buyers in the market. Since consumer acceptance and adoption of PHEVs mainly depends on fuel economy, operating cost, operation GHG emissions, power and performance, and safety among other characteristics, this research will help the PHEV manufacturers in improving the performance parameters of new PHEVs under different driving conditions. The PHEV manufacturers can then offer the urban commuters with a less expensive and cleaner driving option. Therefore, the optimized hybridization of drivetrain components of the PHEVs can significantly contribute to the transportation system efficiency.

The proposed hybridization and multi-objective optimization model for the design of PHEVs is efficient and effective, as the whole process is fully automated by integrating the multi-objective optimization method and PSAT^{TM} simulator. The methodology can be applied to other PHEV designs at different AERs suitable for different drive cycles by controlling the control strategy of the vehicle.

6.2 Future Work

There are areas in the design of PHEVs, such as reducing the cost and weight of the batteries that could lead to potential improvement and adoption of PHEVs. Therefore, more research needs to be done for optimum design of the energy storage systems used in PHEVs. Modeling and simulations tools need to be developed to test the economic viability of such design improvements, so as to ensure that PHEVs provide a more competitive option in a global vehicle market. There are a number of other factors, which could be considered for optimization to improve the performance of PHEV that include: kWh battery storage capability, kWh/km depletion rate of the vehicle, average daily kilometers driven, annual share of trips exceeding the battery depletion distance, charger location (i.e. on-board or off-board), and charging rate. In addition, other consideration in OFF vehicle model include: primary overnight charging spot

(garage, carport, parking garage or lot, on street), availability of primary and secondary charging locations (i.e. dwellings, workplaces, stores, etc.), time of day electric rates, seasonal electric rate, types of streets and highways typically traversed during most probable trips depleting battery charge (i.e. city, suburban, rural and high vs. low density), cumulative trips per day from charger origin, top speeds and peak acceleration rates required to make usual trips would also affect the PHEV performance. Future work may also include hybridization optimization with other drivetrain components like differential gearbox, final drive, wheel axle, mechanical and electrical accessories, power convertors and torque couplings. Sensitivity analysis of different drivetrain vehicle models with different energy storage systems for a particular management control strategies and drive cycles can also be done.

Bibliography

[1] Max., A, 2004. Government policy and development of electric vehicles in Japan. Department of Environmental and Energy System Studies, Lund University, Gerdagatan 13, SE-223 62 Lund, Sweden. Energy Policy 34 (2006) 433-443.

[2] Larminie, J. and Lowry, J. 2003. Electric Vehicle Technology Explained. John Wiley & Sons publisher.

[3] Gifford, P., Adams, J., Corrigan, D., and Venkatesan, S. 1998. Development of advanced nickel/metal hydride batteries for electric and hybrid vehicles. Journal of Power Sources 80:157-163

[4] Chau, K.T., and Wong, Y,S. 2001. Overview of power management in hybrid electric vehicles. Energy Conversion and Management 43:1953-1968.

[5] German, J.M., 2004. Hybrid Electric Vehicles. Encyclopedia of Energy, Volume 3.

[6] Nelson, R.F. 2000. Power requirement for batteries in hybrid electric vehicles. Journal of Power Sources 91:2-26.

[7] Curtin, R., Shrago, Y., and Mikkelsen, J. 2009. "Plug-in Hybrid Electric Vehicles." Report submitted by University of Michigan.

[8] A Plug-in Hybrid Electric Vehicle. The Energy Independence and Security Act of 2007. On the WWW at http://en.wikipedia.org/wiki/Plug-in_hybrid visited on April 26, 2010.

[9] Plug-in Electric Hybrid Vehicles. Adopted by the IEEE-USA Board of Directors, 15 June, 2007. Position Statement by the Institute of Electrical and Electronics Engineers, Inc. – United States of America.

[10] Toyota Prius. Source: On WWW at http://www.hybrids.cc/toyota/toyota-prius-vehicles-history-of-toyota-prius-hybrid, visited on March 20, 2010.

[11] Toyota Prius, Source: On WWW at http://en.wikipedia.org/wiki/Toyota, visited on March 20, 2010.

[12] Toyota Prius Plug-in hybrid vehicle. Image source: WWW at http://www.thedailygreen.com/living- green/blogs/cars-transportation/green-cars-detroit-auto-show-46011608, visited on March 20, 2010.

[13] Bradely, T.H., and Quinn, C.W. 2010. Analysis of plug-in hybrid electric vehicle utility factors. Journal of Power Sources 195:5399 - 5408.

[14] Graham, R., Bradely, T.H., and Duvall, M. 2003. Development of plug-in hybrid electric light-duty and medium duty commercial vehicles. In: The 20th International electric vehicle symposium and exposition (EVS-20), Long Beach, CA, November 15-19, 2003.

[15] Liot, C., Fadel, M., Grandpierre, M., and Sans, M. 2005. Global Energy Management for Vehicle In Gerico Project. EVS 21, April 2005.

[16] Pesaran, A., Market, T., Tataria, H., and Howell, D. 2007. Battery Requirements for Plug-In Hybrid Electric Vehicles: Analysis and Rationale, 23rd. International Electric Vehicle Symposium and Exposition (EVS-23), Anaheim, California, December 2007.

[17] Kammen, D.M., Lemoine, D.M., Arons, S.M., Hummel, H. 2008. Evaluating the cost-effectiveness of greenhouse gas emission reductions from deploying plug-in hybrid electric vehicles. Energy and Resources Group, University of California. Plug-in hybrid Summit, Washington, DC, 2008.

[18] Samaras, C., Meisterling, K. 2008. Life cycle assessment of greenhouse gas emissions from plug-in hybrid vehicles: Implications for policy. Environmental Science and Technology 42: 3170-3176

[19] Silva, C., Ross, M., Farias, T. 2009. Evaluation of energy consumption, emissions and cost of plug-in hybrid vehicles. Energy Conversion and Management 50:1635–1643.

[20] T. Miller., 2006. Advances in NiMH and Li-Ion Batteries for Full Hybrids. Advances Automotive Batteries Conference, Baltimore, 2006.

[21] Christiaens S., Vaughan N., and Revereault P. 2005. Effect of Hybridization ratio and gear change strategy on fuel consumption. In: EAEC European automotive congress, Beograd, Serbia & Montenegro, June 2005.

[22] Wu, Ji., Emadi, A., Duoba, M. J., and Bohn, T. P. 2007. Plug-in hybrid electric vehicles: Testing, simulations, and analysis. Electric Power and Power Electronics Centre, IEEE Vehicle Power and Propulsive Conference 7803-9761-4: 469-476.

[23] Reynolds, C., and Kandlikar, M. 2007. How hybrid-electric vehicles are different from conventional vehicles: The effect of weight and power on fuel consumption. Environmental Research Letters 2: 014003 (8pp).

[24] Zervas, E., Lazarou, C., 2008. Influence of European passenger cars weight to exhaust CO2 emissions. Energy Policy 36:248–257.

[25] Quinn, C., Zimmerle, D., and Bradley, T.H., 2010. The effect of communication architecture on the availability, reliability, and economics of plug-in hybrid electric vehicle-to-grid ancillary services. Journal of Power Sources 195:1500-1509.

[26] Lukic, M. S., and Emadi, A. 2004. Effects of drivetrain hybridization on fuel economy and dynamic performance of parallel hybrid electric vehicles. IEEE Transactions on Vehicular Technology 53-2: 385-389.

[27] Bradley, T. H., Frank, A. 2009. Design, demonstration and sustainability impact assessments for plug-in hybrid electric vehicles. Renewable and Sustainable Energy Reviews 13:115-128.

[28] Vyas, A., Santini, D., Duoba, M., and Alexander, M. 2007. Plug-in hybrid electric vehicles: How does one determine their potential for reducing U.S. oil dependence? Argonne National Laboratory. 23rd International Electric Vehicle Symposium (EVS23), Anaheim, CA.

[29] Scott, M.J., Kintner-Meyer, M., Elliot, D.B., and Warwick, W.M. 2007. Impacts assessment of plug-in hybrid vehicles on electric utilities and regional U.S. power grids, Part 2: Economic assessment. Pacific Northwest National Laboratory.

[30] Shidore, N., Bohn, T., Duoba, M., Lohse-Busch, H., and Sharer, P. 2007. PHEV 'All electric range' and fuel economy in charge sustaining mode for low SOC operation of the JCS VL41M Li-ion battery using battery HIL. Argonne National Laboratory. 23rd International Electric Vehicle Symposium (EVS23), Anaheim, CA.

[31] Graham, R. 2001. Comparing the benefits and impacts of hybrid electric vehicle options. Electric Power Research Institute (EPRI), Palo, Alto, CA 1000349 Report.

[32] Duoba, M., Carlson, R., and Wu, Ji. 2007. Test procedures and benchmarking. Blended-type and EV-capable plug-in hybrid electric vehicles. Argonne National Laboratory. 23rd International Electric Vehicle Symposium (EVS23), Anaheim, CA.

[33] Markel, T., Brooker, A., Gonder, J., O'Keefe, M., Simpson, A., and Thornton, M. 2006. Plug-in hybrid vehicle analysis. National Renewable Energy Laboratory. Milestone Report NREL/MP-540-40609.

[34] Staunton, R. H., Ayers, C.W., Marilo, L.D., Chiasson, J.N., and Burress T.A. 2006. Evaluation of 2004 Toyota Prius hybrid electric drive system. Engineering Science and Technology Division. Oak Ridge National Laboratory ORNL/TM-2006/423.

[35] Ferdowsi, M. 2007. Plug-in hybrid vehicles - a vision for the future. Power Electronics and Motor Drives Laboratory 7803-9761-4: 457-462.

[36] Mendes, C.J., Stevens, M.B., Wilhelm, E.J., Fowler, M.W., and Fraser, R.A. 2007. Model-based design approaches for plug-in hybrid vehicle design. Plug-in Highway Network. PHEV 2007 Conference, Winnipeg, Manitoba, CA.

[37] Karbowski, D., Rousseau, A., Pagerit, S., and Sharer, P. 2006. Plug-in vehicle control strategy from global optimization to real-time application. Argonne National Laboratory. 22nd International Electric Vehicle Symposium (EVS22), Yokohama.

[38] Wang, L. 2005. Hybrid electric vehicle design based on a multi-objective optimization evolutionary algorithm. Walter J. Karplus Summer Research Grant Report.

[39] Karbowski, D., Haliburton, C., and Rousseau, A. 2007. Impact of component size on plug-in hybrid vehicle energy consumption using global optimization. Argonne National Laboratory. 23rd International Electric Vehicle Symposium (EVS23), Anaheim, CA.

[40] Argonne National Laboratory, PSAT (Powertrain System Analysis Toolkit), http://www.transportation.anl.gov/. Software for the modeling and simulation of vehicle drivertain configurations.

[41] Hubbard, A. G., and Toumi, Y. K. 1997. Proceedings of the American Control Conference, Albuquerque, New York.

[42] Tate, Edward D., and Boyd, Stephen P. 1998. Finding Ultimate Limits of Performance for Hybrid Electric Vehicles, Stanford University, Society of Automotive Engineers, Inc.

[43] Fontaras, G., Pistikopoulos, P., and Samaras, Z. 2008. Experimental evaluation of hybrid vehicle fuel economy and pollutant emissions over real-world simulation driving cycles, Laboratory of Applied Thermodynamics, Aristotle University Thessaloniki.

[44] Fellini, R., Michelena, N., Papalambros, P., and Sasena, M., 2007. Optimal Design of Automotive Hybrid Powertrain Systems, Department of Mechanical Engineering & Applied Mechanics, The University of Michigan, Ann Arbor, Michigan 48109, United States.

[45] Karden, E., Spijker, E., and Kok, D. 2003. In-vehicle Battery Management for High Volume Applications. VDI Conference Electronic Systems for Vehicles, Baden-Baden, September.

[46] Golbuff, S. 2006. Optimization of a plug-in hybrid electric vehicle. M.S. Thesis, School of Mechanical Engineering, Georgia Institute of Technology, Atlanta, GA. On the WWW at http://smartech.gatech.edu/handle/1853/11496, visited on Dec. 26, 2009.

[47] Cao, Q., Pagerit, S., Carlson, R., and Rousseau, A. 2007. PHEV Hymotion Prius model validation and control improvements. Argonne National Laboratory. 23rd International Electric Vehicle Symposium (EVS23), Anaheim, CA.

[48] Markel, T., and Simpson, A. 2006. Plug-in hybrid electric vehicle energy storage system design. National Renewable Energy Laboratory. Advanced Automotive Battery Conference NREL/CP-540-39614.

[49] Advanced Batteries for Electric-Drive Vehicles: A Technology and Cost-Effectiveness Assessment for Battery Electric Vehicles, Power Assist Hybrid Electric Vehicles, and Plug-in Hybrid Electric Vehicles. EPRI, Palo Alto, CA: 1009299.

[50] Shiau, C., Samaras, C., Hauffe, R., Hauffe, R., and Michalek, J. J. 2009. Impact of battery weight and charging patterns on the economic and environmental benefits of plug-in hybrid vehicles. Energy Policy, 37, February, pp. 2653-2663. See also URL http://www.elsevier.com/locate/enpol, visited on Dec. 10, 2009.

[51] Sharer, P., Rousseau, A., Nelson, P., and Pagerit, S. 2006. Vehicle simulation results for plug-in HEV battery requirements. Argonne National Laboratory. 23rd International Electric Vehicle Symposium (EVS23), Japan.

[52] Axsen, J., Burke, A., and Kurani, K. 2008. Batteries for plug-in hybrid electric vehicles (PHEVs): Goals and the state of technology. Institute of Transportation Studies University of California Davis, CA UCD-ITS-RR-08-14.

[53] Rousseau, A., Shidore, N., Carlson, R., and Freyermuth, V. 2007. Research on PHEV battery requirements and evaluation of early prototypes. Argonne National Laboratory. 7th Advanced Automotive Battery Conference.

[54] Duvall, M.S. 2005. Battery evaluation for plug-in hybrid electric vehicles. Electric Power Research Institute 7803-9280-9: 338-343.

[55] Nelson, P., Amine, K., and Rousseau, A. 2007. Advanced lithium-ion batteries for plug-in hybrid-electric vehicles. Argonne National Laboratory. 23rd International Electric Vehicle Symposium (EVS23), Anaheim, CA.

[56] Karden, E., Ploumen, S., Fricke, B., Miller, T., and Snyder, K. 2007. Energy storage devices for future hybrid electric vehicles. Journal of Power Sources 168: 2-11.

[57] Burke, A.F. 2007. Batteries and ultracapacitors for electric, hybrid, and fuel cell vehicles. Proceedings of the IEEE (95):806-820.

[58] Thomas, Sandy. 2009. Transportation options in a carbon-constrained world: Hybrids, plug-in hybrids, biofuels, fuel cell electric vehicles, and battery electric vehicles. International Journal of Hydrogen Energy 34:9279-9296.

[59] Amiri, M., Esfahanian, M., Hairi-Yazdic, M. R., and Esfahanian V. 2009. Minimization of power losses in hybrid electric vehicles in view of the prolonging of battery life. Journal of Power Sources 190:372-397.

[60] Rousseau, A., Shidore, N., Carlson, R., and Karbowski, D. 2007. Impact of battery characteristics on PHEV fuel economy. Argonne National Laboratory. 23rd International Electric Vehicle Symposium (EVS23), Anaheim, CA.

[61] Kelly, K.J., Mihalie, M., and Zolot, M. 2002. Battery usage and thermal performance of the Toyota Prius and Honda Insight during chassis dynamometer testing. XVII Annual Battery Conference on Applications and Advances. National Renewable Energy Laboratory 7803-7132-1: 247-252.

[62] Butler, L. K., Ehsani M., and Kamath P. 1999. A Matlab-Based Modelling and Simulation Package for Electric and Hybrid Electric Vehicle Design, IEEE Transactions on Vehicular Technology 48(6).

[63] Bowles, P., Peng, H., and Bang, X., 2000. Energy Management in a Parallel Hybrid Electric Vehicle With a Continuously Variable Transmission, Proceedings of the American Control Conference, Chicago, Illinois.

[64] Maynard, M., 2008. Toyota will offer a plug-in hybrid by 2010. The New York Times January 14, 2008.

[65] Wipke, K.B., and Cuddy, M.R. 1997. Analysis of the fuel economy benefit of drivetrain hybridization. National Renewable Energy Laboratory NREL/CP-540: 22309.

[66] Chau, K.T., and Wong,Y.S. 2001. Hybridization of energy sources in electric vehicles. Energy Conversion and Management 42: 1059-1069.

[67] Wipke, K., Markel, T., and Nelson, D. 2001. Optimizing energy management strategy and degree of hybridization for a hydrogen fuel cell SUV. Proceedings of the 18th Electric Vehicle Symposium, 18, Berlin.

[68] Katrasnik, T. 2007. Hybridization of powertrain and downsizing of the ICE – a way to reduce fuel consumption and pollutant emissions – Part 1. Energy Conversion and Management 48: 1411-1423.

[69] Zeraoulia, M., Benbouzid, M.E.H., and Diallo, D. 2006. Electric Motor Drive Selection Issues for HEV Propulsion Systems: A Comparative Study, IUT of Brest, University of Western Brittany Rue de Kergoat – BP 93169, 29231 Brest Cedex 3, France.

[70] Olszewski, M.,2005. Evaluation of 2004 Toyota Prius Hybrid Electric Drive System, Oak Ridge National Laboratory, U.S. Department of Energy FreedomCAR and Vehicle Technologies, EE-2G 1000 Independence Avenue, S.W. Washington, D.C. 20585-0121.

[71] Katrasnik, T. 2007. Hybridization of powertrain and downsizing of the ICE – analysis and parametric study – Part 2. Energy conversion and Management 48:1424-1434.

[72] Toyota Hybrid with Power System for the Toyota Prius. Source: http://slidefinder.net/t/toyota_hybrid_system/dave_hermance_general/1329087 and http://www.familycar.com/classroom/alternativepowersystems.htm , visited on March 20, 2010.

[73] Liu, J., Peng, H., and Filipi, Z. 2005. Modelling and Analysis of the Toyota Hybrid System, Proceedings of the 2005 IEEE/ASME International Conference on Advanced Intelligent Mechatronics Monterey, California, USA.

[74] Power Source Connection of a Prius Hybrid Synergy Drive System. Image source: On WWW at http://www.automobilesreview.com/auto-news/toyota-prius-hybrid-synergy-drive/12851/, visited on March 20, 2010.

[75] Kazuaki, S., Kazuaki., K., Kaoru., K., and Hata, Y. 2006. Development of Electric Motors for the TOYOTA Hybrid Vehicle PRIUS. Toyota Motor Corporation.

[76] Rousseau, A., Pagerit, S., and Gao, D.W. 2008. Plug-in hybrid electric vehicle control strategy parameter optimization. Argonne National Laboratory. 23rd International Electric Vehicle Symposium (EVS23), Anaheim, CA. Journal of Asian Electric Vehicles 6:1125-1133.

[77] Induction Permanent Magnet Electric motor comparison. Image source: On WWW at http://newenergyandfuel.com/http:/newenergyandfuel/com/2010/02/09/the-best-electric-vehicle-motor/, visited on March 20, 2010.

[78] GM electric motors for hybrids, EVs, in Baltimore. Image source: On WWW at http://www.sae.org/mags/aei/ENRG/7555, visited on March 20, 2010.

[79] Nickel Metal Hydride Battery. Image source: On WWW at http://www.hybridcars.com/hybrid-car-battery, visited on March 20, 2010

[80] Toyota Hybrid Engine. Image source: On WWW at http://exclusiveautocar.blogspot.com/2010/01/top-10-toyota-cars.html, visited on March 20, 2010.

[81] Federal Test Procedure Review Project: Preliminary Technical Report [Online]. Available: http://www.epa.gov/oms/regs/ld-hwy/ftp-rev/ftp-tech.pdf. visited on March 20, 2010.

[82] Tara, E., Shahidinejad, S., Filizadeh, S., and Bibeau, E. 2009. Battery Storage Sizing in a Retrofitted Plug-in Hybrid Electric Vehicle. IEEE. AUTO21 network of centers of excellence (Project no.DF302-DBS).

[83] EIA, 2008. Monthly Energy Review May 2008. U.S. Department of Energy. On the WWW at http://www.eia.doe.gov/emeu/aer/elect.html, visited on Dec. 22, 2009.

[84] EPRI, 2007. Environmental assessment of plug-in hybrid electric vehicles. Volume 1: Nationwide greenhouse gas emissions. Electric Power Research Institute, Palo Alto, CA. On the WWW at http://pubs.acs.org/doi/full/10.1021/es702178s, visited on Dec. 24, 2009.

[85] IPCC, 2001. Climate Change 2001.The Scientific Basis: Contribution of Working Group I to the Third Assessment Report of the Intergovernmental Panel on Climate Change, Cambridge University Press, New York. See also URL http://www.abc.edu, visited on Dec. 26, 2009.

[86] Shan, S., and Wang, G.G. 2005. An efficient Pareto set identification approach for multiobjective optimization on black-box functions. Journal of Mechanical Design, Vol. 127:866-874.

[87] Schaumann, E.J., Balling, R.J. and Day, K. 1998. Genetic algorithms with multiple objectives. 7th AIAA/USAF/NASA/ISSMO Symposium on Multidisciplinary Analysis and Optimization, St. Louis, MO, AIAA Vol. 3:2114-2123.

[88] Khokhar, Z.O., Vahabzadeh, H., Ziai, A., Wang, G.G., and Menon, C. 2010. On the performance of the Pareto Set Pursuing (PSP) method for mixed-variable multi-objective design optimization. ASME Transactions, Journal of Mechanical Design. March 2010

Appendix A

Selection of battery, motor and engine for drive cycles simulation

Table A-1. Selection of battery for US EPA-UDDS drive cycle

Battery No.	Battery Type
1	Saft Li-ion battery, Capacity = 6Ah, Cell number = 75
2	NiCd Saft STM5-100 6-V battery, Capacity = 102Ah, Cell number = 125
3	NiMH battery, Capacity = 11Ah, Cell number = 240
4	Ovonic NiMH battery, Capacity = 28Ah, Cell number = 300
5	Ovonic P127 NiMH battery, Capacity = 45Ah, Cell number = 300
6	NiMH Panasonic battery used in the MY01 US Prius, Capacity = 6.5Ah, Cell number = 168
7	NiMH Panasonic battery used in Japan Prius, Capacity = 6.5Ah, Cell number = 240
8	NiMH Panasonic battery used in the MY01 Japan Prius, Capacity = 6.5Ah, Cell number = 240
9	Ovonic M108 NiMH battery, Capacity = 60Ah, Cell number = 300
10	Ovonic NiMH battery, Capacity = 90Ah, Cell number = 300
11	NiMH battery, Capacity = 93Ah, Cell number = 275
12	NiZn Evercell battery, Capacity = 22Ah, Cell number = 196
13	GNB 12-EVB-1180 valve-regulated lead acid battery, Capacity = 104Ah, Cell number = 150
14	Hawker Genesis lead acid battery, Capacity = 12Ah, Cell number = 150
15	Hawker Odyssey sealed lead acid battery, Capacity = 6Ah, Cell number = 72
16	Optima valve-regulated spiral-wound lead acid battery, Capacity = 18Ah, Cell number = 150
17	Hawker Genesis 12V26Ah10EP sealed valve-regulated lead acid battery, Capacity = 25Ah, Cell number = 150
18	Hawker Genesis 12V26Ah10EP sealed valve-regulated lead acid (VRLA) battery, Capacity = 26Ah, Cell number = 27
19	Johnson Controls lead acid battery, Capacity = 28Ah, Cell number = 150
20	Horizon lead acid battery, Capacity = 91Ah, Cell number = 150

Table A-2. Selection of motor for US EPA-UDDS drive cycle

Motor No.	Motor Type
1	MY04 Toyota Prius Mobility, Continuous power = 25kW, Peak power = 50kW
2	Honda Insight, Continuous power = 10kW, Peak power = 10kW
3	MY04 Toyota Prius, Continuous power = 15kW, Peak power = 30kW
4	MY05 Ford Escape Hybrid MG2, Continuous power = 17kW, Peak power = 33kW
5	Auxilec Thomson, Continuous Power = 32kW, Peak power = 45kW
6	MY05 Ford Escape Hybrid MG1, Continuous power = 33kW, Peak power = 65kW
7	Toyota Camry MG2, Continuos power = 35kW, Peak power = 70kW
8	UQM PowerPhase75 (Unique Mobility), Continuous power = 36kW, Peak power = 75kW
9	Honda, Continuous power = 49kW, Peak power = 49kW
10	UQM Power Phase100, Continuous power = 55kW, Peak power = 100kW
11	Toyota Camry MG1, Continuous power = 55kW, Peak power = 105kW
12	Permanent magnet electric motor with Continuous power = 58kW, Peak power = 58kW
13	Honda Accord, Continuous power = 7kW, Peak power = 14kW
14	MY99 Toyota Prius, Continuous power = 7kW, Peak power = 15kW

Table A-3. Selection of engine for US EPA-UDDS drive cycle

Engine No.	Engine Type
1	1.497L 57kW MY04 USPrius gasoline engine
2	Geo 1.0L 41kW gasoline engine
3	Honda Insight 1.0L VTEC-E gasoline engine
4	1.5L 43kW Japan Prius gasoline engine
5	1.5L 52kW MY01US Prius gasoline engine
6	1.6L 85kW Civic gasoline engine
7	1.8L 90kW Corolla VVTi gasoline engine
8	1.8L 99kW Ford gasoline engine
9	2.3L 99kW MY05 Ford Escape Hybrid gasoline engine
10	3L 115kW Taurus gasoline engine
11	3L 150kW Honda Accord VTEC gasoline engine
12	3L 150kW Taurus gasoline engine
13	3.8L 132kW Caravan gasoline engine
14	4L 120kW Explorer gasoline engine
15	4L 160kW Explorer SOHC gasoline engine
16	4.8L 201kW Silverado gasoline engine

Table A-4. Selection of battery for Winnipeg weekday drive cycle

Battery No.	Battery Type
1	NiMH Panasonic battery used in the MY01 Japan Prius, Capacity = 6.5Ah, Cell number = 240
2	NiMH battery, Capacity = 11Ah, Cell number = 240
3	Hawker Genesis 12V26Ah10EP sealed valve-regulated lead acid battery, Capacity = 25Ah, Cell number = 150
4	Hawker Genesis 12V26Ah10EP sealed valve-regulated lead acid (VRLA) battery, Capacity = 26Ah, Cell number = 27
5	Johnson Controls lead acid battery, Capacity = 28Ah, Cell number = 150
6	Hawker Genesis lead acid battery, Capacity = 12Ah, Cell number = 150
7	NiMH Panasonic battery used in Japan Prius, Capacity = 6.5Ah, Cell number = 240
8	Hawker Odyssey sealed lead acid battery, Capacity = 6Ah, Cell number = 72
9	Optima valve-regulated spiral-wound lead acid battery, Capacity = 18Ah, Cell number = 150
10	NiZn Evercell battery, Capacity = 22Ah, Cell number = 196
11	Horizon lead acid battery, Capacity = 91Ah, Cell number = 150
12	GNB 12-EVB-1180 valve-regulated lead acid battery, Capacity = 104Ah, Cell number = 150
13	NiCd Saft STM5-100 6-V battery, Capacity = 102Ah, Cell number = 125
14	NiMH Panasonic battery used in the MY01 US Prius, Capacity = 6.5Ah, Cell number = 168
15	Ovonic NiMH battery, Capacity = 28Ah, Cell number = 300
16	Saft Li-ion battery, Capacity = 6Ah, Cell number = 75
17	NiMH battery, Capacity = 93Ah, Cell number = 275
18	Ovonic M108 NiMH battery, Capacity = 60Ah, Cell number = 300
19	Ovonic P127 NiMH battery, Capacity = 45Ah, Cell number = 300
20	Ovonic NiMH battery, Capacity = 90Ah, Cell number = 300

Table A-5. Selection of motor for Winnipeg weekday drive cycle

Motor No.	Motor Type
1	Honda Insight, Continuous power = 10kW, Peak power = 10kW
2	MY99 Toyota Prius, Continuous power = 7kW, Peak power = 15kW
3	Honda Accord, Continuous power = 7kW, Peak power = 14kW
4	MY04 Toyota Prius, Continuous power = 15kW, Peak power = 30kW
5	MY05 Ford Escape Hybrid MG2, Continuous power = 17kW, Peak power = 33kW
6	Auxilec Thomson, Continuous Power = 32kW, Peak power = 45kW
7	Honda, Continuous power = 49kW, Peak power = 49kW
8	MY04 Toyota Prius Mobility, Continuous power = 25kW, Peak power = 50kW
9	Permanent magnet electric motor with Continuous power = 58kW, Peak power = 58kW
10	MY05 Ford Escape Hybrid MG1, Continuous power = 33kW, Peak power = 65kW
11	Toyota Camry MG2, Continuos power = 35kW, Peak power = 70kW
12	UQM PowerPhase75 (Unique Mobility), Continuous power = 36kW, Peak power = 75kW
13	UQM Power Phase100, Continuous power = 55kW, Peak power = 100kW
14	Toyota Camry MG1, Continuous power = 55kW, Peak power = 105kW

Table A-6. Selection of engine for Winnipeg weekday drive cycle

Engine No.	Engine Type
1	Geo 1.0L 41kW gasoline engine
2	1.5L 43kW Japan Prius gasoline engine
3	Honda Insight 1.0L VTEC-E gasoline engine
4	1.5L 52kW MY01US Prius gasoline engine
5	1.497L 57kW MY04 USPrius gasoline engine
6	1.6L 85kW Civic gasoline engine
7	1.8L 90kW Corolla VVTi gasoline engine
8	2.3L 99kW MY05 Ford Escape Hybrid gasoline engine
9	1.8L 99kW Ford gasoline engine
10	3L 115kW Taurus gasoline engine
11	4L 120kW Explorer gasoline engine
12	3.8L 132kW Caravan gasoline engine
13	3L 150kW Honda Accord VTEC gasoline engine
14	3L 150kW Taurus gasoline engine
15	4L 160kW Explorer SOHC gasoline engine
16	4.8L 201kW Silverado gasoline engine

Appendix B

Hybridization and Multi-Objective Optimization results of PHEV20

Table B-1. Simulation results for different combinations of batteries, motors, and engines using US-EPA UDDS drive cycle

Iteration No.	Sampling Point	Convergence Criteria	Mean Fitness	Battery No.	Motor No.	Engine No.	Number of modules in a battery	Motor Power (kW)	Engine Power (kW)	Battery Capacity (kWh)
1	1	1.015		17	13	3	24	68.13	68.81	7.20
	2			19	9	2	24	73.83	73.61	8.06
	3			6	8	16	33	143.11	65.74	1.54
	4			20	3	16	8	73.57	72.07	8.74
	5			20	7	13	9	87.75	43.78	9.83
	6			3	6	15	11	143.11	65.74	3.49
	7			16	14	11	37	149.27	91.61	7.99
	8			1	12	15	120	66.33	47.53	9.12
	9			14	11	12	81	153.48	94.43	11.66
	10			8	10	3	53	67.00	76.50	2.48
2	11	1.015	1.29	19	3	12	29	82.75	59.81	9.74
3	12	1.015	2.00	2	1	3	4	74.00	69.00	2.45
	13			20	2	5	9	79.00	60.38	9.83
4	14	1.015	2.00	1	14	9	120	94.00	56.25	9.12
5	15	1.015	2.00	1	10	4	101	67.00	69.38	7.67
6	16	1.015	2.00	1	12	4	113	63.00	66.38	8.59
7	17	1.015	1.65	18	13	4	22	67.00	66.38	6.86
8	18	1.015	1.58	1	1	8	106	59.00	69.38	8.05
9	19	1.015	1.51	16	10	8	36	76.00	63.00	7.78
	20			17	4	7	25	356.53	96.45	7.50
10	21	1.015	1.07	20	6	4	6	150.13	44.63	6.55
11	22	1.015	1.44	18	3	2	26	77.00	61.88	8.11
12	23	1.015	1.06	20	12	7	6	83.00	55.50	6.55
13	24	1.015	1.09	19	11	8	33	137.81	71.58	11.09
14	25	1.015	1.06	20	4	3	7	268.69	99.05	7.64
15	26	1.015	1.11	20	6	8	7	112.50	67.13	7.64
16	27	1.015	1.25	1	9	2	101	63.00	66.38	7.67
17	28	1.015	1.18	20	13	2	6	88.00	45.00	6.55
18	29	1.015	1.19	20	1	4	6	76.00	66.00	6.55
19	30	1.015	1.28	1	14	1	123	91.00	55.88	9.35
20	31	1.015	1.05	1	1	3	101	57.20	65.63	7.67

Iteration No.	Sampling Point	Convergence Criteria	Mean Fitness	Battery No.	Motor No.	Engine No.	Number of modules in a battery	Motor Power (kW)	Engine Power (kW)	Battery Capacity (kWh)
21	32	1.015	1.75	14	3	15	67	80.00	60.00	9.65
22	33	1.015	2.00	1	1	10	106	58.94	74.17	8.05
23	34	1.015	2.00	19	6	13	26	99.00	54.38	8.74
24	35	1.015	2.00	17	14	16	24	156.50	67.13	7.20
25	36	1.015	2.00	1	13	14	101	60.00	69.00	7.67
	37			1	12	12	120	64.12	62.07	9.12
26	38	1.015	2.00	15	4	15	40	185.23	47.09	7.68
27	39	1.015	2.00	3	13	15	9	80.00	63.00	2.85
28	40	1.015	2.00	8	1	9	51	80.00	63.00	2.39
	41			1	4	1	110	165.88	48.26	8.36
29	42	1.015	2.00	20	6	16	6	124.50	67.13	6.55
	43			20	4	2	7	249.56	83.02	7.64
30	44	1.015	1.72	1	2	8	139	74.00	72.63	10.56
31	45	1.015	2.00	2	13	16	4	80.00	63.00	2.45
32	46	1.015	2.00	10	6	15	7	100.00	54.00	9.07
33	47	1.015	2.00	8	3	11	55	74.00	69.00	2.57
	48			1	8	10	110	88.00	57.00	8.36
34	49	1.015	1.66	2	11	6	3	76.00	75.00	1.84
	50			2	13	14	4	76.00	57.00	2.45
35	51	1.015	1.97	15	1	2	37	64.00	69.00	7.10
	52			7	1	7	41	76.00	69.00	1.77
36	53	1.015	1.72	7	6	11	51	78.00	69.00	2.20
	54			11	8	5	6	88.00	57.00	7.37
37	55	1.015	1.57	20	1	3	6	88.00	48.00	6.55
	56			15	1	16	40	65.50	65.06	7.68
	57			10	1	3	5	83.00	55.50	6.48
38	58	1.015	1.32	20	9	16	8	70.13	57.61	8.74
	59			1	3	2	110	67.00	66.38	8.36
	60			20	9	8	7	82.00	54.00	7.64
	61			7	12	1	41	80.00	60.00	1.77
39	62	1.015	1.15	1	14	12	117	91.38	63.09	8.89
	63			20	14	5	6	104.00	54.75	6.55
40	64	1.015	1.46	8	2	6	55	72.00	75.00	2.57
	65			18	6	1	23	142.00	51.56	7.18
	66			12	5	11	33	78.00	69.00	8.99

Iteration No.	Sampling Point	Convergence Criteria	Mean Fitness	Battery No.	Motor No.	Engine No.	Number of modules in a battery	Motor Power (kW)	Engine Power (kW)	Battery Capacity (kWh)
41	68	1.015	1.13	10	14	2	7	100.50	63.75	9.07
	69			16	13	13	35	66.00	66.75	7.56
	70			20	14	8	6	106.00	73.50	6.55
42	71	1.015	1.38	18	5	15	30	88.00	57.00	9.36
43	72	1.015	1.54	1	6	1	101	86.00	54.00	7.67
	73			16	1	1	35	65.00	67.13	7.56
	74			19	9	3	25	74.75	61.31	8.40
	75			1	5	2	115	71.00	64.88	8.74
44	76	1.015	1.10	6	14	14	31	84.00	57.00	1.45
	77			12	13	15	27	80.00	63.00	7.35
	78			6	10	15	31	80.00	63.00	1.45
	79			17	12	15	27	72.50	62.81	8.10
45	80	1.015	1.04	12	1	5	27	80.00	60.00	7.35
	81			5	14	8	14	130.00	79.50	9.07
	82			1	8	6	106	94.00	56.25	8.05
	83			3	8	7	9	114.00	79.50	2.85
	84			4	8	6	41	99.72	63.12	8.27
	85			15	2	2	52	84.00	57.00	9.98
46	86	1.015	1.04	5	3	16	15	67.00	64.88	9.72
47	87	1.015	1.08	1	7	9	130	78.00	60.75	9.88
	88			19	10	5	23	77.00	64.13	7.73
	89			5	14	4	14	100.00	54.00	9.07
	90			15	12	16	47	72.00	64.50	9.02
48	91	1.015	1.06	17	1	9	25	68.00	64.50	7.50
	92			3	12	5	9	80.00	60.00	2.85
	93			2	6	2	4	80.00	63.00	2.45
	94			11	6	3	5	103.00	69.75	6.14
	95			10	7	6	6	92.00	72.00	7.78
	96			6	8	1	31	92.00	57.00	1.45
49	97	1.015	1.04	12	6	12	27	120.00	75.00	7.35
	98			18	10	11	24	84.00	57.00	7.49
	99			19	10	13	25	76.00	60.00	8.40
	100			10	4	1	5	287.00	58.31	6.48
	101			17	1	10	25	67.00	66.38	7.50
	102			8	5	1	51	84.00	60.00	2.39
50	103	1.015	1.06	18	14	16	23	145.69	63.66	7.18
	104			15	13	16	40	67.94	76.30	7.68

Iteration No.	Sampling Point	Convergence Criteria	Mean Fitness	Battery No.	Motor No.	Engine No.	Number of modules in a battery	Motor Power (kW)	Engine Power (kW)	Battery Capacity (kWh)
51	105	1.015	1.05	19	4	1	25	278.81	10.00	8.40
	106			20	12	1	6	76.00	66.00	6.55
	107			5	6	2	11	110.88	67.22	7.13
	108			3	10	1	9	80.00	60.00	2.85
	109			8	4	2	51	176.13	72.28	2.39
52	110	1.015	1.16	19	14	15	25	110.00	53.63	8.40
	111			20	13	1	6	80.00	60.00	6.55
	112			19	14	3	26	104.50	66.75	8.74
	113			20	12	3	6	86.00	54.00	6.55
	114			19	8	4	25	122.00	8.63	8.40
53	115	1.015	1.08	6	1	16	31	80.00	63.00	1.45
	116			4	1	16	43	60.55	70.55	8.67
	117			1	13	15	106	59.98	66.99	8.05
	118			15	2	15	53	84.00	60.00	10.18
	119			20	2	11	9	82.00	60.75	9.83
54	120	1.015	1.15	10	13	16	5	82.00	54.00	6.48
	121			19	10	16	26	78.75	59.81	8.74
	122			3	14	1	9	92.00	57.00	2.85
	123			1	6	7	101	86.00	64.50	7.67
	124			17	4	15	25	274.82	66.26	7.50
	125			5	5	8	15	78.00	58.50	9.72
55	126	1.015	1.15	20	14	16	6	117.00	62.25	6.55
	127			2	5	15	4	80.00	63.00	2.45
56	128	1.015	1.14	7	6	5	51	80.00	60.00	2.20
	129			8	3	6	55	72.00	75.00	2.57
	130			1	7	10	134	76.00	63.00	10.18
	131			2	12	6	4	50.00	77.63	2.45
	132			4	10	12	41	70.38	60.73	8.27
57	133	1.015	1.16	20	1	2	6	87.00	45.00	6.55
	134			4	1	13	41	59.00	67.88	8.27
	135			4	1	6	39	62.25	63.19	7.86
	136			15	7	16	56	92.00	55.50	10.75
	137			16	1	3	35	66.13	55.36	7.56
	138			16	5	13	47	82.75	61.13	10.15
	139			5	2	7	16	74.00	58.50	10.37

Table B-2. Hybridization and multi-objective optimization results for US-EPA UDDS drive cycle

Iteration No.	Sampling Point	Hybridization Factor	Electric Efficiency in CD-mode (miles/kWh)	Fuel Efficiency in CS-mode (miles/gallon)	Fuel Economy (miles/gallon)	Operating Cost ($/mile)	Operation GHG Emission (kg/mile)
1	1	0.5	5.36	115.54	115.54	0.024	0.149
	2	0.5	5.47	82.58	82.58	0.024	0.150
	3	0.69	1.49	63.72	63.72	0.080	0.516
	4	0.51	4.61	96.93	96.93	0.028	0.173
	5	0.67	4.43	89.25	89.25	0.029	0.181
	6	0.69	5.29	71.67	71.67	0.026	0.157
	7	0.62	3.68	70.19	70.19	0.035	0.219
	8	0.58	5.14	100.43	100.43	0.025	0.156
	9	0.62	3.94	76.79	76.79	0.033	0.204
	10	0.47	5.28	76.50	76.50	0.025	0.156
2	11	0.58	4.62	88.29	88.29	0.028	0.174
3	12	0.52	5.64	65.05	65.05	0.025	0.150
	13	0.57	3.41	97.60	97.60	0.036	0.230
4	14	0.63	3.77	94.79	94.79	0.033	0.209
5	15	0.49	5.88	113.39	113.39	0.022	0.137
6	16	0.49	5.41	108.34	108.34	0.024	0.148
7	17	0.5	5.37	105.09	105.09	0.024	0.150
8	18	0.46	5.79	117.39	117.39	0.022	0.138
9	19	0.55	5.33	107.54	107.54	0.024	0.150
	20	0.79	4.47	77.28	77.28	0.029	0.182
10	21	0.77	5.66	119.16	119.16	0.022	0.141
11	22	0.55	4.80	85.50	85.50	0.027	0.169
12	23	0.6	5.12	89.72	89.72	0.025	0.158
13	24	0.66	4.32	96.87	96.87	0.029	0.184
14	25	0.73	4.89	107.86	107.86	0.026	0.163
15	26	0.63	5.45	115.86	115.86	0.023	0.147
16	27	0.49	5.84	90.71	90.71	0.023	0.140
17	28	0.66	5.74	96.63	96.63	0.023	0.142
18	29	0.54	5.59	109.73	109.73	0.023	0.144
19	30	0.62	3.86	98.52	98.52	0.032	0.204
20	31	0.47	5.96	129.31	129.31	0.021	0.134
21	32	0.57	4.38	89.66	89.66	0.029	0.183
22	33	0.44	5.72	96.56	96.56	0.023	0.142
23	34	0.65	5.27	87.18	87.18	0.025	0.155
24	35	0.7	3.48	66.45	66.45	0.037	0.231

Iteration No.	Sampling Point	Hybridization Factor	Electric Efficiency in CD-mode (miles/kWh)	Fuel Efficiency in CS-mode (miles/gallon)	Fuel Economy (miles/gallon)	Operating Cost ($/mile)	Operation GHG Emission (kg/mile)
25	36	0.47	5.63	93.40	93.40	0.023	0.145
	37	0.51	5.17	94.41	94.41	0.025	0.156
26	38	0.8	4.66	99.73	99.73	0.027	0.171
27	39	0.56	5.73	56.34	56.34	0.025	0.151
28	40	0.56	6.15	65.73	65.73	0.023	0.139
	41	0.77	4.99	121.48	121.48	0.025	0.159
29	42	0.65	5.12	97.32	97.32	0.025	0.157
	43	0.75	4.91	79.71	79.71	0.027	0.166
30	44	0.5	3.34	100.62	100.62	0.037	0.234
31	45	0.56	5.85	48.86	48.86	0.026	0.151
32	46	0.65	5.32	114.40	114.40	0.024	0.150
33	47	0.52	5.67	52.73	52.73	0.026	0.153
	48	0.61	5.50	100.56	100.56	0.024	0.147
34	49	0.5	5.21	43.65	43.65	0.029	0.170
	50	0.57	6.03	45.90	45.90	0.025	0.149
35	51	0.48	5.68	88.09	88.09	0.023	0.144
	52	0.52	4.22	72.03	72.03	0.031	0.193
36	53	0.53	6.73	65.36	65.36	0.022	0.129
	54	0.61	4.87	112.38	112.38	0.026	0.163
37	55	0.65	5.59	124.82	124.82	0.023	0.143
	56	0.5	5.56	102.05	102.05	0.023	0.145
	57	0.6	5.77	127.56	127.56	0.022	0.138
38	58	0.55	4.96	100.21	100.21	0.026	0.162
	59	0.5	5.45	91.55	91.55	0.024	0.149
	60	0.6	5.31	114.37	114.37	0.024	0.150
	61	0.57	3.81	73.62	73.62	0.034	0.211
39	62	0.59	3.70	79.13	79.13	0.034	0.216
	63	0.66	3.88	87.53	87.53	0.032	0.205
40	64	0.49	4.21	44.51	44.51	0.034	0.203
	65	0.73	5.27	109.80	109.80	0.024	0.152
	66	0.53	3.74	89.09	89.09	0.034	0.212
	67	0.52	2.72	64.14	64.14	0.046	0.292
41	68	0.61	4.03	79.64	79.64	0.032	0.199
	69	0.5	5.20	84.76	84.76	0.025	0.157
	70	0.59	3.80	85.37	85.37	0.033	0.209
42	71	0.61	4.06	89.33	89.33	0.031	0.196

Iteration No.	Sampling Point	Hybridization Factor	Electric Efficiency in CD-mode (miles/kWh)	Fuel Efficiency in CS-mode (miles/gallon)	Fuel Economy (miles/gallon)	Operating Cost ($/mile)	Operation GHG Emission (kg/mile)
43	72	0.61	6.02	122.73	122.73	0.021	0.133
	73	0.49	5.46	108.33	108.33	0.023	0.147
	74	0.55	5.43	116.21	116.21	0.023	0.147
	75	0.52	5.25	91.78	91.78	0.025	0.154
44	76	0.6	2.66	52.22	52.22	0.048	0.302
	77	0.56	4.28	84.73	84.73	0.030	0.188
	78	0.56	3.22	69.14	69.14	0.039	0.248
	79	0.54	4.57	84.82	84.82	0.028	0.176
45	80	0.57	4.44	98.87	98.87	0.028	0.179
	81	0.62	3.88	89.72	89.72	0.032	0.204
	82	0.63	5.63	107.49	107.49	0.023	0.143
	83	0.59	5.07	55.73	55.73	0.028	0.168
	84	0.61	5.38	105.80	105.80	0.024	0.149
	85	0.6	3.26	76.06	76.06	0.039	0.243
46	86	0.51	4.66	105.63	105.63	0.027	0.171
47	87	0.56	4.74	111.58	111.58	0.026	0.167
	88	0.55	5.59	106.85	106.85	0.023	0.144
	89	0.65	3.99	99.31	99.31	0.031	0.198
	90	0.53	4.81	87.65	87.65	0.027	0.168
48	91	0.51	5.09	101.95	101.95	0.025	0.158
	92	0.57	5.03	59.58	59.58	0.028	0.168
	93	0.56	5.68	46.09	46.09	0.027	0.157
	94	0.6	5.11	116.99	116.99	0.025	0.156
	95	0.56	4.63	99.94	99.94	0.027	0.172
	96	0.62	3.45	79.84	79.84	0.036	0.230
49	97	0.62	4.17	81.99	81.99	0.031	0.192
	98	0.6	4.95	97.74	97.74	0.026	0.162
	99	0.56	5.38	86.02	86.02	0.024	0.152
	100	0.83	5.02	107.27	107.27	0.025	0.159
	101	0.5	5.06	88.58	88.58	0.026	0.160
	102	0.58	6.15	70.50	70.50	0.023	0.138
50	103	0.7	3.48	67.71	67.71	0.037	0.231
	104	0.47	5.39	98.63	98.63	0.024	0.150
51	105	0.97	4.70	182.68	182.68	0.026	0.164
	106	0.54	5.20	101.31	101.31	0.025	0.155
	107	0.62	5.60	92.33	92.33	0.023	0.146
	108	0.57	5.61	64.52	64.52	0.025	0.151
	109	0.71	5.58	60.56	60.56	0.025	0.153

Iteration No.	Sampling Point	Hybridization Factor	Electric Efficiency in CD-mode (miles/kWh)	Fuel Efficiency in CS-mode (miles/gallon)	Fuel Economy (miles/gallon)	Operating Cost ($/mile)	Operation GHG Emission (kg/mile)
52	110	0.67	3.65	74.22	74.22	0.035	0.219
	111	0.57	5.61	112.38	112.38	0.023	0.143
	112	0.61	3.82	92.75	92.75	0.033	0.207
	113	0.61	5.24	111.74	111.74	0.024	0.153
	114	0.93	5.39	193.20	193.20	0.022	0.144
53	115	0.56	3.27	65.51	65.51	0.039	0.245
	116	0.46	5.25	102.13	102.13	0.024	0.153
	117	0.47	5.46	104.07	104.07	0.024	0.147
	118	0.58	3.02	79.24	79.24	0.041	0.261
	119	0.57	3.22	88.20	88.20	0.038	0.244
54	120	0.6	5.22	98.71	98.71	0.025	0.154
	121	0.57	5.26	94.13	94.13	0.025	0.154
	122	0.62	4.13	56.88	56.88	0.033	0.201
	123	0.57	5.88	105.38	105.38	0.022	0.138
	124	0.81	4.28	84.01	84.01	0.030	0.188
	125	0.57	4.82	121.31	121.31	0.026	0.164
55	126	0.65	3.65	72.68	72.68	0.035	0.220
	127	0.56	5.48	52.36	52.36	0.027	0.158
56	128	0.57	7.05	67.21	67.21	0.021	0.123
	129	0.49	5.82	50.93	50.93	0.025	0.151
	130	0.55	4.70	96.85	96.85	0.027	0.170
	131	0.39	5.07	51.16	51.16	0.028	0.170
	132	0.54	5.35	100.00	100.00	0.024	0.151
57	133	0.66	5.61	97.77	97.77	0.023	0.145
	134	0.47	5.41	92.80	92.80	0.024	0.150
	135	0.5	5.61	107.68	107.68	0.023	0.143
	136	0.62	4.05	90.36	90.36	0.031	0.197
	137	0.54	5.51	121.38	121.38	0.023	0.145
	138	0.58	4.19	81.58	81.58	0.031	0.192
	139	0.56	3.47	91.98	91.98	0.036	0.227

Table B-3. Pareto Design Points (PDP) results for US-EPA UDDS drive cycle

Iteration No.	Number of Sampling Points in Iteration	No.of PDPs	Co-ordinates of PDPs			Function Value of PDPs		
			Battery No.	Motor No.	Engine No.	Fuel Economy (mpg)	Operation Cost ($/mile)	GHG Emissions (kg/mile)
1	10	0						
2	1	1	17	13	3	115.54	0.024	0.149
3	2	1	17	13	3	115.54	0.024	0.149
4	1	1	17	13	3	115.54	0.024	0.149
5	1	2	17	13	3	115.54	0.024	0.149
			1	10	4	113.39	0.022	0.137
6	1	2	1	10	4	113.39	0.022	0.137
			17	13	3	115.54	0.024	0.149
7	1	2	1	10	4	113.39	0.022	0.137
			17	13	3	115.54	0.024	0.149
8	1	2	1	1	8	117.39	0.022	0.138
			1	10	4	113.39	0.022	0.137
9	2	2	1	1	8	117.39	0.022	0.138
			1	10	4	113.39	0.022	0.137
10	1	3	1	1	8	117.39	0.022	0.138
			1	10	4	113.39	0.022	0.137
			20	6	4	119.16	0.022	0.141
11	1	3	1	1	8	117.39	0.022	0.138
			20	6	4	119.16	0.022	0.141
			1	10	4	113.39	0.022	0.137
12	1	3	1	1	8	117.39	0.022	0.138
			1	10	4	113.39	0.022	0.137
			20	6	4	119.16	0.022	0.141
13	1	3	20	6	4	119.16	0.022	0.141
			1	1	8	117.39	0.022	0.138
			1	10	4	113.39	0.022	0.137
14	1	3	20	6	4	119.16	0.022	0.141
			1	1	8	117.39	0.022	0.138
			1	10	4	113.39	0.022	0.137
15	1	3	20	6	4	119.16	0.022	0.141
			1	1	8	117.39	0.022	0.138
			1	10	4	113.39	0.022	0.137
16	1	3	1	10	4	113.39	0.022	0.137
			1	1	8	117.39	0.022	0.138
			20	6	4	119.16	0.022	0.141

Iteration No.	Number of Sampling Points in Iteration	No.of PDPs	Co-ordinates of PDPs			Function Value of PDPs		
			Battery No.	Motor No.	Engine No.	Fuel Economy (mpg)	Operation Cost ($/mile)	GHG Emissions (kg/mile)
17			1	10	4	113.39	0.022	0.137
			1	1	8	117.39	0.022	0.138
			20	6	4	119.16	0.022	0.141
18	1	3	1	1	8	117.39	0.022	0.138
			1	10	4	113.39	0.022	0.137
			20	6	4	119.16	0.022	0.141
19	1	3	20	6	4	119.16	0.022	0.141
			1	1	8	117.39	0.022	0.138
			1	10	4	113.39	0.022	0.137
20	1	1	1	1	3	129.31	0.021	0.134
21	1	1	1	1	3	129.31	0.021	0.134
22	1	1	1	1	3	129.31	0.021	0.134
23	1	1	1	1	3	129.31	0.021	0.134
24	1	1	1	1	3	129.31	0.021	0.134
25	2	1	1	1	3	129.31	0.021	0.134
26	1	1	1	1	3	129.31	0.021	0.134
27	1	1	1	1	3	129.31	0.021	0.134
28	2	1	1	1	3	129.31	0.021	0.134
29	2	1	1	1	3	129.31	0.021	0.134
30	1	1	1	1	3	129.31	0.021	0.134
31	1	1	1	1	3	129.31	0.021	0.134
32	1	1	1	1	3	129.31	0.021	0.134
33	2	1	1	1	3	129.31	0.021	0.134
34	2	1	1	1	3	129.31	0.021	0.134
35	2	1	1	1	3	129.31	0.021	0.134
36	2	2	1	1	3	129.31	0.021	0.134
			7	6	11	65.36	0.022	0.129
37	3	2	1	1	3	129.31	0.021	0.134
			7	6	11	65.36	0.022	0.129
38	4	2	1	1	3	129.31	0.021	0.134
			7	6	11	65.36	0.022	0.129
39	2	2	1	1	3	129.31	0.021	0.134
			7	6	11	65.36	0.022	0.129
40	4	2	1	1	3	129.31	0.021	0.134
			7	6	11	65.36	0.022	0.129
41	3	2	1	1	3	129.31	0.021	0.134
			7	6	11	65.36	0.022	0.129

Iteration No.	Number of Sampling Points in Iteration	No.of PDPs	Co-ordinates of PDPs			Function Value of PDPs		
			Battery No.	Motor No.	Engine No.	Fuel Economy (mpg)	Operation Cost ($/mile)	GHG Emissions (kg/mile)
42	1	2	1	1	3	129.31	0.021	0.134
			7	6	11	65.36	0.022	0.129
43	4	3	7	6	11	65.36	0.022	0.129
			1	1	3	129.31	0.021	0.134
			1	6	1	122.73	0.021	0.133
44	4	3	1	1	3	129.31	0.021	0.134
			7	6	11	65.36	0.022	0.129
			1	6	1	122.73	0.021	0.133
45	6	3	1	1	3	129.31	0.021	0.134
			7	6	11	65.36	0.022	0.129
			1	6	1	122.73	0.021	0.133
46	1	3	7	6	11	65.36	0.022	0.129
			1	1	3	129.31	0.021	0.134
			1	6	1	122.73	0.021	0.133
47	4	3	1	1	3	129.31	0.021	0.134
			7	6	11	65.36	0.022	0.129
			1	6	1	122.73	0.021	0.133
48	6	3	1	1	3	129.31	0.021	0.134
			7	6	11	65.36	0.022	0.129
			1	6	1	122.73	0.021	0.133
49	6	3	1	1	3	129.31	0.021	0.134
			7	6	11	65.36	0.022	0.129
			1	6	1	122.73	0.021	0.133
50	2	3	1	1	3	129.31	0.021	0.134
			7	6	11	65.36	0.022	0.129
			1	6	1	122.73	0.021	0.133
51	5	4	19	4	1	182.68	0.026	0.164
			7	6	11	65.36	0.022	0.129
			1	1	3	129.31	0.021	0.134
			1	6	1	122.73	0.021	0.133
52	5	4	19	8	4	193.20	0.022	0.144
			1	1	3	129.31	0.021	0.134
			7	6	11	65.36	0.022	0.129
			1	6	1	122.73	0.021	0.133
53	5	4	19	8	4	193.20	0.022	0.144
			1	1	3	129.31	0.021	0.134
			7	6	11	65.36	0.022	0.129
			1	6	1	122.73	0.021	0.133

Iteration No.	Number of Sampling Points in Iteration	No.of PDPs	Co-ordinates of PDPs			Function Value of PDPs		
			Battery No.	Motor No.	Engine No.	Fuel Economy (mpg)	Operation Cost ($/mile)	GHG Emissions (kg/mile)
54	6	4	19	8	4	193.20	0.022	0.144
			7	6	11	65.36	0.022	0.129
			1	1	3	129.31	0.021	0.134
			1	6	1	122.73	0.021	0.133
55	2	4	19	8	4	193.20	0.022	0.144
			7	6	11	65.36	0.022	0.129
			1	1	3	129.31	0.021	0.134
			1	6	1	122.73	0.021	0.133
56	5	4	19	8	4	193.20	0.022	0.144
			7	6	5	67.21	0.021	0.123
			1	1	3	129.31	0.021	0.134
			1	6	1	122.73	0.021	0.133
57	7	4	19	8	4	193.20	0.022	0.144
			7	6	5	67.21	0.021	0.123
			1	1	3	129.31	0.021	0.134
			1	6	1	122.73	0.021	0.133

Table B-4. Simulation results for different combinations of batteries, motors, and engines using Winnipeg weekday drive cycle

Iteration No.	Sampling Point	Convergence Criteria	Mean Fitness	Battery No.	Motor No.	Engine No.	Number of modules in a battery	Motor Power (kW)	Engine Power (kW)	Battery Capacity (kWh)
1	1	1.015		17	13	3	7	80.00	66.00	8.59
	2	1.015		19	9	2	16	63.50	69.19	10.37
	3	1.015		6	8	16	80	73.00	62.63	11.52
	4	1.015		20	3	16	6	90.66	45.54	7.78
	5	1.015		20	7	13	8	85.50	34.50	10.37
	6	1.015		3	6	15	37	90.00	61.50	11.10
	7	1.015		16	14	11	158	114.00	48.00	12.01
	8	1.015		1	12	15	51	80.00	63.00	2.39
	9	1.015		14	11	12	31	92.00	57.00	1.45
	10	1.015		8	10	3	47	99.56	62.86	9.02
2	11	1.015	1.04	20	14	1	7	149.00	48.94	9.07
3	12	1.015	1.40	1	4	1	51	80.00	63.00	2.39
4	13	1.015	1.29	1	14	4	51	96.00	55.50	2.39
5	14	1.015	1.26	20	6	4	8	70.56	64.97	10.37
6	15	1.015	1.23	17	7	2	7	84.00	60.00	8.59
7	16	1.015	1.25	1	13	16	51	80.00	63.00	2.39
	17			18	8	1	11	88.60	28.10	9.50
	18			20	10	2	7	92.00	55.50	9.07
8	19	1.015	1.17	20	6	1	8	68.00	64.50	10.37
9	20	1.015	1.37	2	10	16	9	153.88	76.22	2.85
10	21	1.015	1.50	1	14	1	51	231.52	62.29	2.39
11	22	1.015	1.59	20	5	3	7	201.19	79.17	9.07
	23			20	1	2	8	70.00	65.25	10.37
	24			17	7	15	7	80.00	63.00	8.59
12	25	1.015	1.12	5	1	13	33	92.00	55.50	11.09
	26			18	1	14	13	73.75	63.56	11.23
	27			1	2	16	51	80.00	63.00	2.39
	28			20	6	16	9	70.00	65.25	11.66
13	29	1.015	1.24	1	6	1	51	80.00	63.00	2.39
14	30	1.015	1.38	20	8	3	7	100.00	33.00	9.07
	31			16	13	13	130	69.88	63.26	9.88
	32			3	3	3	26	70.38	60.73	7.80
	33			17	3	3	6	76.00	66.00	7.37

Iteration No.	Sampling Point	Convergence Criteria	Mean Fitness	Battery No.	Motor No.	Engine No.	Number of modules in a battery	Motor Power (kW)	Engine Power (kW)	Battery Capacity (kWh)
15	34	1.015	1.28	6	1	16	72	90.00	57.75	10.37
	35			6	11	13	94	102.00	53.25	13.54
	36			6	4	6	75	86.25	60.94	10.80
	37			4	4	13	32	84.00	60.00	9.98
	38			13	2	13	3	68.00	71.25	1.84
16	39	1.015	1.21	1	12	13	51	123.25	70.31	2.39
	40			9	13	1	41	76.00	60.00	8.86
	41			7	5	11	51	95.00	55.69	2.20
17	42	1.015	1.35	18	14	2	13	157.36	30.60	11.23
	43			20	14	16	10	110.50	64.88	12.96
	44			20	7	16	7	86.50	40.50	9.07
	45			20	4	2	8	66.00	66.75	10.37
18	46	1.015	1.15	3	14	1	34	153.84	49.35	10.20
	47			2	1	16	9	84.00	63.00	2.85
	48			2	1	10	9	84.00	60.00	2.85
	49			2	14	3	9	329.56	71.02	2.85
	50			2	12	13	9	226.00	79.50	2.85
19	51	1.015	1.24	3	8	1	29	69.00	65.63	8.70
20	52	1.015	1.36	20	12	11	8	91.00	55.50	10.37
	53			19	14	3	17	114.26	67.10	11.02
	54			11	10	1	8	108.25	54.23	8.74
	55			20	13	16	8	65.00	67.13	10.37
21	56	1.015	1.28	1	8	2	51	80.00	60.00	2.39
	57			11	1	1	9	78.00	60.75	9.83
	58			7	4	2	41	84.00	60.00	1.77
	59			2	10	3	9	143.00	93.75	2.85
	60			12	9	2	9	71.00	64.13	11.23
22	61	1.015	1.28	11	13	3	8	72.00	64.50	8.74
	62			17	9	3	7	76.00	66.00	8.59
	63			14	9	3	31	76.00	66.00	1.45
23	64	1.015	1.20	16	14	16	174	120.00	51.75	13.22
	65			11	14	8	10	134.25	71.06	10.92
	66			20	1	14	8	85.00	51.00	10.37
	67			9	12	6	47	124.00	50.25	10.15
24	68	1.015	1.41	19	10	16	16	96.00	55.50	10.37
	69			19	13	6	15	70.25	62.44	9.72
	70			19	5	6	14	203.40	79.52	9.07
	71			19	8	9	15	105.00	25.50	9.72

Iteration No.	Sampling Point	Convergence Criteria	Mean Fitness	Battery No.	Motor No.	Engine No.	Number of modules in a battery	Motor Power (kW)	Engine Power (kW)	Battery Capacity (kWh)
25	72	1.015	1.23	12	1	1	9	84.00	60.00	11.23
	73			19	7	2	15	65.00	67.13	9.72
	74			20	13	4	6	66.53	71.29	7.78
	75			18	4	1	12	68.06	56.39	10.37
26	76	1.015	1.10	20	13	14	8	65.69	64.08	10.37
	77			19	11	9	17	79.00	60.38	11.02
	78			9	14	16	62	140.30	68.37	13.39
	79			16	13	12	130	68.00	66.00	9.88
27	80	1.015	1.10	3	3	7	26	69.75	63.56	7.80
	81			15	1	6	54	79.00	61.13	10.89
	82			4	6	10	34	87.00	57.38	10.61
28	83	1.015	1.11	2	9	3	9	80.00	66.00	2.85
29	84	1.015	1.26	20	14	6	9	120.35	64.35	11.66
	85			20	13	9	6	86.00	54.00	7.78
	86			19	10	2	15	92.00	55.50	9.72
30	87	1.015	1.16	11	11	1	9	84.00	57.00	9.83
	88			2	12	2	9	217.00	57.66	2.85
	89			5	11	7	34	95.63	63.66	11.42
31	90	1.015	1.12	17	1	14	7	88.00	69.00	8.59
	91			19	3	14	14	101.00	34.50	9.07
	92			18	2	4	11	108.00	54.00	9.50
	93			17	12	15	7	98.00	63.00	8.59
32	94	1.015	1.10	9	9	15	55	77.00	61.13	11.88
	95			20	6	3	8	76.00	51.00	10.37
	96			11	11	13	10	88.00	57.00	10.92
	97			11	6	2	9	80.00	63.00	9.83
	98			15	2	2	48	106.00	42.00	9.68
	99			7	6	6	41	76.00	75.00	1.77
33	100	1.015	1.07	17	4	15	8	84.00	60.00	9.82
34	101	1.015	1.15	18	10	10	10	100.00	54.00	8.64
	102			18	12	5	10	114.00	52.13	8.64
	103			19	13	10	15	67.00	66.38	9.72
	104			17	8	12	7	80.00	60.00	8.59
	105			18	8	9	11	98.50	32.25	11.23
35	106	1.015	1.16	16	11	1	147	77.00	61.13	9.72
	107			18	8	2	11	59.13	69.05	7.78
	108			10	12	8	35	104.50	63.75	10.37
	109			18	4	7	12	71.00	57.00	10.37
36	110	1.015	1.13	11	14	13	10	129.96	70.16	11.02
	111			11	14	14	10	130.23	68.40	13.39

Iteration No.	Sampling Point	Convergence Criteria	Mean Fitness	Battery No.	Motor No.	Engine No.	Number of modules in a battery	Motor Power (kW)	Engine Power (kW)	Battery Capacity (kWh)
37	112	1.015	1.13	8	2	13	45	106.00	53.25	8.64
	113			20	13	12	8	64.00	69.00	10.37
	114			18	4	9	12	71.72	57.12	10.37
	115			17	3	15	6	76.00	63.00	7.37
	116			19	8	4	15	59.00	67.88	9.72
38	117	1.015	1.12	3	13	11	30	79.00	60.38	9.00
	118			12	13	8	8	77.00	61.13	9.98
	119			3	10	4	31	116.16	68.60	9.30
	120			1	2	15	51	80.00	63.00	2.39
	121			9	11	10	62	96.00	52.50	13.39
39	122	1.015	1.12	3	8	15	31	70.00	63.75	9.30
	123			12	5	15	8	295.97	73.10	9.98
	124			6	10	8	72	136.00	48.75	10.37
	125			10	3	7	31	72.00	67.50	8.44
	126			9	10	13	47	105.50	65.63	10.15
	127			8	11	1	59	92.00	55.50	11.33
40	128	1.015	1.15	16	14	14	174	118.58	69.93	13.22
	129			5	2	16	27	108.00	54.00	9.07
	130			13	13	13	3	68.00	71.25	1.84
	131			13	12	11	4	84.00	57.00	2.45
	132			20	10	16	8	92.00	58.50	10.37
41	133	1.015	1.11	17	5	7	6	194.00	67.50	7.37
	134			15	5	13	46	173.65	73.87	9.27
	135			12	8	9	8	89.53	45.84	9.98
	136			20	12	16	7	108.00	54.00	9.07
42	137	1.015	1.18	11	13	1	8	72.00	64.50	8.74
	138			1	10	16	51	88.50	67.13	2.39
	139			10	14	16	41	286.22	65.74	11.16

Table B-5. Hybridization and multi-objective optimization results for Winnipeg weekday drive cycle

Iteration No.	Sampling Point	Hybridization Factor	Electric Efficiency in CD-mode (miles/kWh)	Fuel Efficiency in CS-mode (miles/gallon)	Fuel Economy (miles/gallon)	Operating Cost ($/mile)	Operation GHG Emission (kg/mile)
1	1	0.55	4.08	95.81	95.81	0.031	0.194
	2	0.48	4.49	89.19	89.19	0.029	0.179
	3	0.54	3.97	69.11	69.11	0.033	0.204
	4	0.67	4.63	78.41	78.41	0.028	0.176
	5	0.71	4.14	96.61	96.61	0.030	0.192
	6	0.59	3.55	66.67	66.67	0.036	0.227
	7	0.7	4.04	76.49	76.49	0.032	0.199
	8	0.56	5.76	51.49	51.49	0.026	0.152
	9	0.62	2.04	47.90	47.90	0.062	0.390
	10	0.61	4.76	89.93	89.93	0.027	0.169
2	11	0.75	4.18	78.31	78.31	0.031	0.193
3	12	0.56	5.77	49.33	49.33	0.026	0.153
4	13	0.63	5.51	51.87	51.87	0.026	0.158
5	14	0.52	4.12	92.22	92.22	0.031	0.193
6	15	0.58	4.17	89.28	89.28	0.030	0.191
7	16	0.56	6.38	51.86	51.86	0.024	0.139
	17	0.76	4.91	88.20	88.20	0.026	0.165
	18	0.62	4.98	99.68	99.68	0.026	0.161
8	19	0.51	4.17	76.78	76.78	0.031	0.193
9	20	0.67	5.27	43.82	43.82	0.028	0.168
10	21	0.79	5.53	47.34	47.34	0.027	0.160
11	22	0.72	4.71	95.60	95.60	0.027	0.170
	23	0.52	3.55	84.46	84.46	0.035	0.223
	24	0.56	3.80	76.08	76.08	0.034	0.211
12	25	0.62	3.22	66.26	66.26	0.040	0.249
	26	0.54	3.28	69.42	69.42	0.039	0.244
	27	0.56	4.58	41.14	41.14	0.032	0.191
	28	0.52	3.65	83.44	83.44	0.035	0.218
13	29	0.56	6.31	48.71	48.71	0.024	0.142
14	30	0.75	4.97	108.54	108.54	0.025	0.160
	31	0.52	4.81	85.52	85.52	0.027	0.168
	32	0.54	4.88	87.95	87.95	0.027	0.166
	33	0.54	4.74	90.72	90.72	0.027	0.170

Iteration No.	Sampling Point	Hybridization Factor	Electric Efficiency in CD-mode (miles/kWh)	Fuel Efficiency in CS-mode (miles/gallon)	Fuel Economy (miles/gallon)	Operating Cost ($/mile)	Operation GHG Emission (kg/mile)
15	34	0.61	2.99	60.48	60.48	0.043	0.268
	35	0.66	3.43	71.26	71.26	0.037	0.233
	36	0.59	4.01	70.66	70.66	0.032	0.202
	37	0.58	4.01	73.46	73.46	0.032	0.202
	38	0.49	4.91	37.78	37.78	0.031	0.183
16	39	0.64	5.78	54.31	54.31	0.025	0.151
	40	0.56	4.74	68.68	68.68	0.028	0.174
	41	0.63	5.91	47.72	47.72	0.026	0.151
17	42	0.84	4.10	104.48	104.48	0.030	0.193
	43	0.63	3.61	82.38	82.38	0.035	0.220
	44	0.68	4.18	84.07	84.07	0.031	0.192
	45	0.5	4.44	96.47	96.47	0.028	0.180
18	46	0.76	3.82	66.59	66.59	0.034	0.212
	47	0.57	3.23	37.31	37.31	0.043	0.262
	48	0.58	3.30	39.67	39.67	0.042	0.255
	49	0.82	4.46	55.56	55.56	0.031	0.188
	50	0.74	4.85	45.01	45.01	0.030	0.180
19	51	0.51	4.67	66.97	66.97	0.029	0.177
20	52	0.62	4.16	80.35	80.35	0.031	0.193
	53	0.63	4.08	96.91	96.91	0.031	0.194
	54	0.67	4.94	75.26	75.26	0.027	0.166
	55	0.49	4.12	85.21	85.21	0.031	0.194
21	56	0.57	6.24	60.50	60.50	0.023	0.139
	57	0.56	3.47	64.73	64.73	0.037	0.233
	58	0.58	3.39	65.32	65.32	0.038	0.237
	59	0.6	5.41	57.03	57.03	0.026	0.158
	60	0.53	4.23	84.20	84.20	0.030	0.190
22	61	0.53	4.90	95.93	95.93	0.026	0.164
	62	0.54	3.82	89.91	89.91	0.033	0.207
	63	0.54	2.58	66.54	66.54	0.048	0.306
23	64	0.7	3.76	79.52	79.52	0.034	0.212
	65	0.65	3.86	78.95	78.95	0.033	0.207
	66	0.63	3.36	70.98	70.98	0.038	0.238
	67	0.71	4.15	74.02	74.02	0.031	0.195
24	68	0.63	4.41	83.10	83.10	0.029	0.183
	69	0.53	4.74	85.33	85.33	0.027	0.171
	70	0.72	4.56	77.39	77.39	0.029	0.178
	71	0.8	4.74	109.96	109.96	0.027	0.167

Iteration No.	Sampling Point	Hybridization Factor	Electric Efficiency in CD-mode (miles/kWh)	Fuel Efficiency in CS-mode (miles/gallon)	Fuel Economy (miles/gallon)	Operating Cost ($/mile)	Operation GHG Emission (kg/mile)
25	72	0.58	3.34	64.59	64.59	0.038	0.241
	73	0.49	4.74	92.02	92.02	0.027	0.169
	74	0.48	4.68	89.51	89.51	0.027	0.172
	75	0.55	4.54	78.37	78.37	0.029	0.179
26	76	0.51	4.24	83.42	83.42	0.030	0.189
	77	0.57	3.91	91.11	91.11	0.032	0.203
	78	0.67	3.33	66.31	66.31	0.038	0.241
	79	0.51	4.84	72.00	72.00	0.028	0.170
27	80	0.52	4.73	71.79	71.79	0.028	0.173
	81	0.56	3.42	71.16	71.16	0.037	0.234
	82	0.6	3.68	66.62	66.62	0.035	0.219
28	83	0.55	4.80	54.61	54.61	0.029	0.177
29	84	0.65	3.89	84.37	84.37	0.033	0.205
	85	0.61	4.45	94.02	94.02	0.029	0.180
	86	0.62	4.89	98.11	98.11	0.026	0.164
30	87	0.6	4.23	70.87	70.87	0.031	0.193
	88	0.79	4.95	51.79	51.79	0.029	0.173
	89	0.6	3.65	67.66	67.66	0.035	0.221
31	90	0.56	3.27	62.14	62.14	0.039	0.246
	91	0.75	4.84	81.84	81.84	0.027	0.168
	92	0.67	3.82	74.38	74.38	0.034	0.211
	93	0.61	3.78	76.28	76.28	0.034	0.212
32	94	0.56	4.03	67.02	67.02	0.033	0.202
	95	0.6	4.14	104.80	104.80	0.030	0.191
	96	0.61	3.79	78.53	78.53	0.034	0.211
	97	0.56	4.28	86.25	86.25	0.030	0.187
	98	0.72	3.82	80.17	80.17	0.033	0.209
	99	0.5	2.74	56.90	56.90	0.046	0.292
33	100	0.58	3.87	78.43	78.43	0.033	0.207
34	101	0.65	4.60	80.66	80.66	0.028	0.176
	102	0.69	4.58	92.32	92.32	0.028	0.175
	103	0.5	4.67	79.61	79.61	0.028	0.174
	104	0.57	3.97	69.22	69.22	0.033	0.204
	105	0.75	4.72	103.92	103.92	0.027	0.169
35	106	0.56	4.29	73.81	73.81	0.030	0.189
	107	0.46	4.89	93.86	93.86	0.026	0.165
	108	0.62	3.69	76.51	76.51	0.034	0.217
	109	0.55	4.39	82.67	82.67	0.029	0.183

Iteration No.	Sampling Point	Hybridization Factor	Electric Efficiency in CD-mode (miles/kWh)	Fuel Efficiency in CS-mode (miles/gallon)	Fuel Economy (miles/gallon)	Operating Cost ($/mile)	Operation GHG Emission (kg/mile)
36	110	0.65	3.68	75.23	75.23	0.035	0.217
	111	0.66	3.68	70.07	70.07	0.035	0.219
37	112	0.67	3.52	64.63	64.63	0.037	0.229
	113	0.48	4.28	75.60	75.60	0.030	0.189
	114	0.56	4.38	94.34	94.34	0.029	0.182
	115	0.55	4.30	72.58	72.58	0.030	0.189
	116	0.47	4.87	92.85	92.85	0.026	0.165
38	117	0.57	4.44	67.69	67.69	0.030	0.185
	118	0.56	4.40	85.77	85.77	0.029	0.183
	119	0.63	4.33	67.55	67.55	0.031	0.189
	120	0.56	4.64	42.93	42.93	0.032	0.188
	121	0.65	3.66	67.07	67.07	0.035	0.221
39	122	0.52	4.30	70.74	70.74	0.031	0.190
	123	0.8	4.16	68.09	68.09	0.032	0.196
	124	0.74	4.25	83.54	83.54	0.030	0.189
	125	0.52	4.08	68.09	68.09	0.032	0.200
	126	0.62	4.20	74.32	74.32	0.031	0.193
	127	0.62	3.91	67.12	67.12	0.033	0.208
40	128	0.63	3.87	74.54	74.54	0.033	0.208
	129	0.67	3.55	58.29	58.29	0.037	0.230
	130	0.49	5.58	42.87	42.87	0.027	0.161
	131	0.6	5.31	40.70	40.70	0.029	0.169
	132	0.61	4.17	86.06	86.06	0.031	0.192
41	133	0.74	4.17	70.40	70.40	0.031	0.195
	134	0.7	4.36	77.28	77.28	0.030	0.186
	135	0.66	4.41	92.97	92.97	0.029	0.181
	136	0.67	4.13	81.90	81.90	0.031	0.195
42	137	0.53	4.92	72.87	72.87	0.027	0.167
	138	0.57	6.32	52.56	52.56	0.024	0.140
	139	0.81	2.99	65.73	65.73	0.042	0.267

Table B-6. Pareto Design Points (PDP) results for Winnipeg weekday drive cycle

Iteration No.	Number of Sampling points in iteration	No. of PDPs	Co-ordinates of PDPs			Function Value of PDPs		
			Battery No.	Motor No.	Engine No.	Fuel Economy (mpg)	Operation Cost ($/mile)	GHG Emissions (kg/mile)
1	10							
2	1	3	8	10	3	89.93	0.027	0.169
			1	12	15	51.49	0.026	0.152
			20	7	13	96.61	0.030	0.192
3	1	3	8	10	3	89.93	0.027	0.169
			20	7	13	96.61	0.030	0.192
			1	12	15	51.49	0.026	0.152
4	1	4	8	10	3	89.93	0.027	0.169
			1	12	15	51.49	0.026	0.152
			20	7	13	96.61	0.030	0.192
			1	14	4	51.87	0.026	0.158
5	1	4	8	10	3	89.93	0.027	0.169
			1	12	15	51.49	0.026	0.152
			20	7	13	96.61	0.030	0.192
			1	14	4	51.87	0.026	0.158
6	1	4	8	10	3	89.93	0.027	0.169
			1	12	15	51.49	0.026	0.152
			20	7	13	96.61	0.030	0.192
			1	14	4	51.87	0.026	0.158
7	3	3	1	13	16	51.86	0.024	0.139
			20	10	2	99.68	0.026	0.161
			1	14	4	51.87	0.026	0.158
8	1	3	20	10	2	99.68	0.026	0.161
			1	13	16	51.86	0.024	0.139
			1	14	4	51.87	0.026	0.158
9	1	3	20	10	2	99.68	0.026	0.161
			1	13	16	51.86	0.024	0.139
			1	14	4	51.87	0.026	0.158
10	1	3	20	10	2	99.68	0.026	0.161
			1	13	16	51.86	0.024	0.139
			1	14	4	51.87	0.026	0.158
11	3	3	1	13	16	51.86	0.024	0.139
			20	10	2	99.68	0.026	0.161
			1	14	4	51.87	0.026	0.158

Iteration No.	Number of Sampling points in iteration	No. of PDPs	Co-ordinates of PDPs			Function Value of PDPs		
			Battery No.	Motor No.	Battery No.	Fuel Economy (mpg)	Operation Cost ($/mile)	GHG Emissions (kg/mile)
12	4	3	20	10	2	99.68	0.026	0.161
			1	13	16	51.86	0.024	0.139
			1	14	4	51.87	0.026	0.158
13	1	3	20	10	2	99.68	0.026	0.161
			1	13	16	51.86	0.024	0.139
			1	14	4	51.87	0.026	0.158
14	4	3	1	13	16	51.86	0.024	0.139
			20	8	3	108.54	0.025	0.160
			1	14	4	51.87	0.026	0.158
15	5	3	20	8	3	108.54	0.025	0.160
			1	13	16	51.86	0.024	0.139
			1	14	4	51.87	0.026	0.158
16	3	3	20	8	3	108.54	0.025	0.160
			1	13	16	51.86	0.024	0.139
			1	12	13	54.31	0.025	0.151
17	4	3	20	8	3	108.54	0.025	0.160
			1	13	16	51.86	0.024	0.139
			1	12	13	54.31	0.025	0.151
18	5	3	20	8	3	108.54	0.025	0.160
			1	13	16	51.86	0.024	0.139
			1	12	13	54.31	0.025	0.151
19	1	3	20	8	3	108.54	0.025	0.160
			1	13	16	51.86	0.024	0.139
			1	12	13	54.31	0.025	0.151
20	4	3	20	8	3	108.54	0.025	0.160
			1	13	16	51.86	0.024	0.139
			1	12	13	54.31	0.025	0.151
21	5	2	20	8	3	108.54	0.025	0.160
			1	8	2	60.50	0.023	0.139
22	3	2	20	8	3	108.54	0.025	0.160
			1	8	2	60.50	0.023	0.139
23	4	2	20	8	3	108.54	0.025	0.160
			1	8	2	60.50	0.023	0.139
24	4	3	1	8	2	60.50	0.023	0.139
			20	8	3	108.54	0.025	0.160
			19	8	9	109.96	0.027	0.167
25	4	3	1	8	2	60.50	0.023	0.139
			20	8	3	108.54	0.025	0.160
			19	8	9	109.96	0.027	0.167

Iteration No.	Number of Sampling points in iteration	No. of PDPs	Co-ordinates of PDPs			Function Value of PDPs		
			Battery No.	Motor No.	Battery No.	Fuel Economy (mpg)	Operation Cost ($/mile)	GHG Emissions (kg/mile)
26	4	3	1	8	2	60.50	0.023	0.139
			20	8	3	108.54	0.025	0.160
			19	8	9	109.96	0.027	0.167
27	3	3	1	8	2	60.50	0.023	0.139
			20	8	3	108.54	0.025	0.160
			19	8	9	109.96	0.027	0.167
28	1	3	1	8	2	60.50	0.023	0.139
			20	8	3	108.54	0.025	0.160
			19	8	9	109.96	0.027	0.167
29	3	3	1	8	2	60.50	0.023	0.139
			20	8	3	108.54	0.025	0.160
			19	8	9	109.96	0.027	0.167
30	3	3	1	8	2	60.50	0.023	0.139
			20	8	3	108.54	0.025	0.160
			19	8	9	109.96	0.027	0.167
31	4	3	1	8	2	60.50	0.023	0.139
			20	8	3	108.54	0.025	0.160
			19	8	9	109.96	0.027	0.167
32	6	3	1	8	2	60.50	0.023	0.139
			20	8	3	108.54	0.025	0.160
			19	8	9	109.96	0.027	0.167
33	1	3	1	8	2	60.50	0.023	0.139
			20	8	3	108.54	0.025	0.160
			19	8	9	109.96	0.027	0.167
34	5	3	1	8	2	60.50	0.023	0.139
			20	8	3	108.54	0.025	0.160
			19	8	9	109.96	0.027	0.167
35	4	3	1	8	2	60.50	0.023	0.139
			20	8	3	108.54	0.025	0.160
			19	8	9	109.96	0.027	0.167
36	2	3	1	8	2	60.50	0.023	0.139
			20	8	3	108.54	0.025	0.160
			19	8	9	109.96	0.027	0.167
37	5	3	1	8	2	60.50	0.023	0.139
			20	8	3	108.54	0.025	0.160
			19	8	9	109.96	0.027	0.167
38	5	3	1	8	2	60.50	0.023	0.139
			20	8	3	108.54	0.025	0.160
			19	8	9	109.96	0.027	0.167

Iteration No.	Number of Sampling points in iteration	No. of PDPs	Co-ordinates of PDPs			Function Value of PDPs		
			Battery No.	Motor No.	Battery No.	Fuel Economy (mpg)	Operation Cost ($/mile)	GHG Emissions (kg/mile)
39	6	3	1	8	2	60.50	0.023	0.139
			20	8	3	108.54	0.025	0.160
			19	8	9	109.96	0.027	0.167
40	5	3	1	8	2	60.50	0.023	0.139
			20	8	3	108.54	0.025	0.160
			19	8	9	109.96	0.027	0.167
41	4	3	1	8	2	60.50	0.023	0.139
			20	8	3	108.54	0.025	0.160
			19	8	9	109.96	0.027	0.167
42	3	3	1	8	2	60.50	0.023	0.139
			20	8	3	108.54	0.025	0.160
			19	8	9	109.96	0.027	0.167